

# Report on Dirty Paper Coding Estimation with multidimensional lattices

Pedro Comesaña-Alfaro and Fernando Pérez-González

September 10, 2018

## 1 Notation

Let us denote by  $\mathbf{x}$  the host signal,  $\mathbf{y}$  the watermarked signal,  $\mathbf{d}$  the dither vector,  $\mathbf{n}$  the AWGN introduced by the channel,  $\mathbf{z}$  the received signal (all of them taking values in  $\mathbb{R}^n$ ) and  $t_0$  the true real scaling factor.

The watermark embedding can be written as

$$\mathbf{y} = (1 - \alpha)\mathbf{x} + \alpha [Q_\Lambda(\mathbf{x} - \mathbf{d}) + \mathbf{d}] = (1 - \alpha)\mathbf{x} + \alpha [\mathbf{x} - (\mathbf{x} - \mathbf{d}) \bmod \Lambda],$$

and the attack undergone by the watermarked signal as

$$\mathbf{z} = t_0\mathbf{y} + \mathbf{n}.$$

The corresponding random vectors will be denoted by bold capital letters, with  $\mathbf{X} \sim \mathcal{N}(\mathbf{0}, \sigma_X^2 \mathbf{I}_{n \times n})$ ,  $\mathbf{D} \sim \mathcal{U}(\mathcal{V}(\Lambda))$ ,  $\mathbf{N} \sim \mathcal{N}(\mathbf{0}, \sigma_N^2 \mathbf{I}_{n \times n})$ ,  $\sigma_N^2 > 0$ , and  $\mathbf{I}_{n \times n}$  the  $n \times n$  identity matrix.

Our target will be to estimate  $t_0$  from the received signal  $\mathbf{z}$  and the knowledge about the parameters of the system (i.e.,  $\alpha$ ,  $\mathbf{d}$ ,  $\Lambda$ ,  $\sigma_X^2$ , and  $\sigma_N^2$ ) available at the decoder.

Throughout this report when we mention the *scalar quantizer* case we will mean that the lattice  $\Lambda = \Delta\mathbb{Z}^n$  is used. Similarly, when we say that a *low-dimensional lattice quantizer* is used, we will mean that the used lattice  $\Lambda$  can be written as  $\Lambda = \Lambda' \times \Lambda' \cdots \times \Lambda'$ , i.e., the considered lattice is the Cartesian product of a low-dimensional lattice  $\Lambda'$ . Finally, if we denote by  $A$  the  $n \times n$  generating matrix of  $\Lambda$ ,  $A$  will verify that for the lattice it generates the ratio between covering radius and packing radius is minimal among the lattices generated by the matrix class  $\{\text{diag}(\mathbf{v}) \cdot A : \mathbf{v} \in \mathbb{R}^n\}$ , where  $\text{diag}(\mathbf{v})$  denotes the diagonal matrix with elements those of  $\mathbf{v}$ . This last condition tries to avoid cases as  $\Lambda = \mathbb{Z} \times 10\mathbb{Z}$ , where the large difference of the quantization region sizes in different directions makes that the results developed in this report may not be applied.

## 2 Hypotheses

In this report we will consider the following hypotheses:

- Hypothesis 1:  $\sigma_X^2 \gg \sigma_\Lambda^2$ ,
- Hypothesis 2:  $(1 - \alpha)^2 t_0^2 \sigma_\Lambda^2 \ll \sigma_N^2$ ,
- Hypothesis 3:  $(1 - \alpha)^2 t_0^2 \sigma_\Lambda^2 + \sigma_N^2 \ll t_0^2 \sigma_\Lambda^2$ ,

implying

- Hypothesis 1:  $\text{HLR} \triangleq \alpha^2 \text{DWR} \rightarrow \infty$ ,
- Hypothesis 2:  $\text{SCR} \triangleq \frac{(1 - \alpha)^2}{\alpha^2} \text{WNR} t_0^2 \rightarrow 0$ ,
- Hypothesis 3:  $\text{TNLR} \triangleq (1 - \alpha)^2 + \frac{\alpha^2}{\text{WNR} t_0^2} \rightarrow 0$ ,

where HLR stands for *Host to Lattice Ratio*, SCR for *Self-noise to Channel-noise Ratio*, and TNLR for *Total-Noise to Lattice Ratio*.

Summarizing, the first hypothesis requires the variance of the host to be much larger than the quantization lattice second moment per dimension, the second one that the channel noise must be dominant over the self-noise (used in order to ensure that the total noise is approximately Gaussian when low-dimensional lattices are used), and the third one establishes that the variance of the total noise must be much smaller than the quantization lattice second moment per dimension (defining in that sense a high-SNR scenario).

All of these hypotheses, as well as  $n \rightarrow \infty$ , will be required for the low-dimensional lattice case analysis.

Nevertheless, whenever the number of dimensions goes to infinity and lattices with fundamental Voronoi region approaching a hypersphere are considered (hereafter, *high-dimensional good lattices*):

- **Hypothesis 2** can be dropped, as in that case a random vector uniformly distributed over that fundamental Voronoi region will be asymptotically Gaussian [5].
- **Hypothesis 3** can be relaxed, just requiring

$$(1 - \alpha)^2 t_0^2 \sigma_\Lambda^2 + \sigma_N^2 < t_0^2 \sigma_\Lambda^2,$$

or, equivalently,

$$\text{TNLR} < 1.$$

Be aware that the last condition can be verified for any  $\frac{\sigma_W^2}{\sigma_N^2}$ , as one could play with  $\alpha$ ; specifically, TNLR can be checked to be smaller than 1 whenever

$$\alpha < \frac{2\sigma_W^2 t_0^2}{\sigma_N^2 + \sigma_W^2 t_0^2}.$$

Nevertheless, a very small value of  $\alpha$  implies that **Hypothesis 1** is more difficult to be hold.

### 3 Target function definition

In order to obtain the estimate  $\hat{t}$  of the scaling factor, we use the Maximum Likelihood (ML) criterion, which seeks the most likely value of  $t$  given a vector of observations  $\mathbf{z}$  when there is not *a priori* knowledge about the distribution of the scaling factor, i.e.,

$$\hat{t}(\mathbf{z}) \triangleq \underset{t}{\operatorname{argmax}} \log \left( f_{\mathbf{Z}|T, \mathbf{K}}(\mathbf{z}|t, \mathbf{d}) \right) = \underset{t}{\operatorname{argmin}} -2 \log \left( f_{\mathbf{Z}|T, \mathbf{K}}(\mathbf{z}|t, \mathbf{d}) \right).$$

The hypotheses introduced above will be used to find a mathematically tractable approximation to  $f_{\mathbf{Z}|T, \mathbf{K}}(\mathbf{z}|t, \mathbf{d})$ . The followed approach will be based on the study of that probability density function (pdf) as

$$f_{\mathbf{Z}|T, \mathbf{K}}(\mathbf{z}|t, \mathbf{d}) = \sum_{\lambda \in \Lambda} p_{I|\mathbf{K}}(\lambda|\mathbf{d}) f_{\mathbf{Z}|T, \mathbf{K}, I}(\mathbf{z}|t, \mathbf{d}, \lambda), \quad (1)$$

where  $p_{I|\mathbf{K}}(\lambda|\mathbf{d})$  denotes the probability of the event that a sample of the host signal  $\mathbf{X}$  belongs to the Voronoi region of lattice point  $\lambda$  given that the dither takes value  $\mathbf{d}$ ; be aware that due to its definition,  $p_{I|\mathbf{K}}(\lambda|\mathbf{d})$  does not depend on  $t$ . Indeed, it is straightforward to see that

$$p_{I|\mathbf{K}}(\lambda|\mathbf{d}) = \int_{\lambda + \mathbf{d} + \mathcal{V}(\Lambda)} \frac{e^{-\frac{\|\mathbf{x}\|^2}{2\sigma_X^2}}}{(2\pi\sigma_X^2)^{n/2}} d\mathbf{x}.$$

Whenever the HLR goes to infinity (i.e., under **Hypothesis 1**) one can approximate the previous probability mass function (pmf) by

$$p_{I|\mathbf{K}}(\lambda|\mathbf{d}) \approx \frac{|\mathcal{V}(\Lambda)| e^{-\frac{\|\lambda + \mathbf{d}\|^2}{2\sigma_X^2}}}{(2\pi\sigma_X^2)^{n/2}},$$

where  $|\mathcal{V}(\Lambda)|$  denotes the volume of the fundamental Voronoi region of  $\Lambda$ .

Also when the HLR goes to infinity we can approximate the self-noise to be uniformly distributed within a scaled version of the fundamental Voronoi region (and consequently independent of  $\lambda$ ), yielding the following approximation

$$f_{\mathbf{Z}|T, \mathbf{K}}(\mathbf{z}|t, \mathbf{d}) \approx \sum_{\lambda \in \Lambda} \frac{p_{I|\mathbf{K}}(\lambda|\mathbf{d})}{[t(1-\alpha)]^n |\mathcal{V}(\Lambda)|} \int_{(1-\alpha)\mathcal{V}(\Lambda)} \frac{e^{-\frac{\|\mathbf{z}/t - \lambda - \mathbf{d} + \tau\|^2}{2\sigma_N^2/t^2}}}{(2\pi\sigma_N^2/t^2)^{n/2}} d\tau. \quad (2)$$

Since  $\text{SCR} \rightarrow 0$  (i.e., **Hypothesis 2**) in the scalar quantizer case or low-dimensional lattice quantizer case, and based on the results in [5] for the high-dimensional good lattice quantizer case, in (2) one can approximate the integral of the Gaussian in the scaled version of the fundamental Voronoi region of the lattice by a Gaussian distribution with variance the addition of the variances of the self-noise and the channel noise. Using this approximation, the pdf of  $\mathbf{Z}$  given  $t$ , that the centroid  $\lambda$  was transmitted, and the dither  $\mathbf{d}$ , can be written like

$$f_{\mathbf{Z}|T, \mathbf{K}, I}(\mathbf{z}|t, \mathbf{d}, \lambda) \approx \frac{e^{-\frac{\|\mathbf{z} - t\lambda - t\mathbf{d}\|^2}{2(\sigma_N^2 + (1-\alpha)^2 t^2 \sigma_\Lambda^2)}}}{(2\pi(\sigma_N^2 + (1-\alpha)^2 t^2 \sigma_\Lambda^2))^{n/2}}. \quad (3)$$

Taking into account the last expression, and  $\text{TNLR} \rightarrow 0$  (i.e., **Hypothesis 3**) for the low-dimensional lattice quantizer case, or  $\text{TNLR} < 1$  in the high-dimensional good lattice quantizer case, one can estimate, with a success probability asymptotically (with the  $\text{TNLR}$  in the first case, and with the number of dimensions in the second one) close to 1, the lattice point  $\lambda$  that was used at the embedder as  $\lambda = Q_\Lambda(\mathbf{z}/t - \mathbf{d})$ . Therefore (3) can be rewritten as

$$f_{\mathbf{Z}|T, \mathbf{K}, I}(\mathbf{z}|t, \mathbf{d}, \lambda) \approx \frac{e^{-\frac{\|\mathbf{z}-t\lambda-t\mathbf{d}\|^2}{2(\sigma_N^2+(1-\alpha)^2t^2\sigma_\Lambda^2)}}}{(2\pi(\sigma_N^2+(1-\alpha)^2t^2\sigma_\Lambda^2))^{n/2}} \delta\left(\lambda - Q_\Lambda\left(\frac{\mathbf{z}}{t} - \mathbf{d}\right)\right),$$

and

$$\begin{aligned} f_{\mathbf{Z}|T, \mathbf{K}}(\mathbf{z}|t, \mathbf{d}) &\approx \sum_{\lambda \in \Lambda} \frac{|\mathcal{V}(\Lambda)| e^{-\frac{\|\lambda+\mathbf{d}\|^2}{2\sigma_X^2}}}{(2\pi\sigma_X^2)^{n/2}} \frac{e^{-\frac{\|\mathbf{z}-t\lambda-t\mathbf{d}\|^2}{2(\sigma_N^2+(1-\alpha)^2t^2\sigma_\Lambda^2)}}}{(2\pi(\sigma_N^2+(1-\alpha)^2t^2\sigma_\Lambda^2))^{n/2}} \delta\left(\lambda - Q_\Lambda\left(\frac{\mathbf{z}}{t} - \mathbf{d}\right)\right) \\ &\approx \frac{|\mathcal{V}(\Lambda)| e^{-\frac{\|\mathbf{z}\|^2}{2\sigma_X^2t^2}}}{(2\pi\sigma_X^2)^{n/2}} \frac{e^{-\frac{\|(\mathbf{z}-t\mathbf{d})\text{mod}(t\Lambda)\|^2}{2(\sigma_N^2+(1-\alpha)^2t^2\sigma_\Lambda^2)}}}{(2\pi(\sigma_N^2+(1-\alpha)^2t^2\sigma_\Lambda^2))^{n/2}}, \end{aligned} \quad (4)$$

where in the last approximation we have taken into account in the first Gaussian function that  $\text{HLR} \rightarrow \infty$ , this condition jointly with  $n \rightarrow \infty$  in order to the terms in both exponentials to be independent, and  $\text{TNLR} < 1$  jointly with  $n \rightarrow \infty$  in order to  $\mathbf{z} - t\lambda - t\mathbf{d}$  to be in  $\mathcal{V}(t\Lambda)$ . Therefore,

$$\begin{aligned} -2 \log\left(f_{\mathbf{Z}|T, \mathbf{K}}(\mathbf{z}|t, \mathbf{d})\right) + K &\approx \\ L(t, \mathbf{z}) \triangleq \frac{\|(\mathbf{z}-t\mathbf{d})\text{mod}(t\Lambda)\|^2}{\sigma_N^2+(1-\alpha)^2t^2\sigma_\Lambda^2} + n \log\left(2\pi(\sigma_N^2+(1-\alpha)^2t^2\sigma_\Lambda^2)\right) + \frac{\|\mathbf{z}\|^2}{\sigma_X^2t^2}, \end{aligned} \quad (5)$$

and

$$\hat{t}(\mathbf{z}) \approx \underset{t}{\text{argmin}} L(t, \mathbf{z}).$$

Be aware that for the sake of notational simplicity  $K$  stands for  $\frac{|\mathcal{V}(\Lambda)|}{(2\pi\sigma_X^2)^{n/2}}$ ; as it does not depend on  $t$ , the solution to the previous optimization problem will not be modified.

For the scalar quantizer case, i.e.,  $\Lambda = \Delta\mathbb{Z}^n$ , from (4) it is straightforward to write

$$f_{\mathbf{Z}|T, \mathbf{K}}(\mathbf{z}|t, \mathbf{d}) \approx \frac{\Delta^n e^{-\frac{\|\mathbf{z}\|^2}{2\sigma_X^2t^2}}}{(2\pi\sigma_X^2)^{n/2}} \frac{e^{-\frac{\|(\mathbf{z}-t\mathbf{d})\text{mod}(t\Delta)\|^2}{2(\sigma_N^2+(1-\alpha)^2\Delta^2t^2/12)}}}{\left[2\pi(\sigma_N^2+(1-\alpha)^2\Delta^2t^2/12)\right]^{n/2}}, \quad (6)$$

so

$$L(t, \mathbf{z}) = \frac{\|(\mathbf{z}-t\mathbf{d})\text{mod}(t\Delta)\|^2}{\sigma_N^2+(1-\alpha)^2\Delta^2t^2/12} + n \log\left(2\pi(\sigma_N^2+(1-\alpha)^2\Delta^2t^2/12)\right) + \frac{\|\mathbf{z}\|^2}{\sigma_X^2t^2} \quad (7)$$

In order to study (5) we will first take into consideration its first term. Applying basic properties of the modulo operation, one can write

$$\begin{aligned}
(\mathbf{z} - t\mathbf{d}) \bmod(t\Lambda) &= \left[ t_0 \left( (1 - \alpha)\mathbf{x} + \alpha \left[ \mathbf{x} - (\mathbf{x} - \mathbf{d}) \bmod\Lambda \right] \right) + \mathbf{n} - t\mathbf{d} \right] \bmod(t\Lambda) \\
&= \left[ t_0 \left( \mathbf{x} - \alpha \left[ (\mathbf{x} - \mathbf{d}) \bmod\Lambda \right] \right) + \mathbf{n} - t\mathbf{d} \right] \bmod(t\Lambda) \\
&= \left[ (t_0 - t)\mathbf{x} - (t_0 - t)\alpha \left[ (\mathbf{x} - \mathbf{d}) \bmod\Lambda \right] + \mathbf{n} \right. \\
&\quad \left. + t \left( \mathbf{x} - \mathbf{d} - \alpha \left[ (\mathbf{x} - \mathbf{d}) \bmod\Lambda \right] \right) \right] \bmod(t\Lambda) \\
&= \left[ (t_0 - t)\mathbf{x} - (t_0 - t)\alpha \left[ (\mathbf{x} - \mathbf{d}) \bmod\Lambda \right] + \mathbf{n} \right. \\
&\quad \left. + t \left( (\mathbf{x} - \mathbf{d}) \bmod\Lambda - \alpha \left[ (\mathbf{x} - \mathbf{d}) \bmod\Lambda \right] \right) \right] \bmod(t\Lambda) \\
&= \left[ (t_0 - t)\mathbf{x} - (t_0 - t)\alpha \left[ (\mathbf{x} - \mathbf{d}) \bmod\Lambda \right] + \mathbf{n} \right. \\
&\quad \left. + t(1 - \alpha) \left( (\mathbf{x} - \mathbf{d}) \bmod\Lambda \right) \right] \bmod(t\Lambda) \\
&= \left[ (t_0 - t)\mathbf{x} + (t - \alpha t_0) \left[ (\mathbf{x} - \mathbf{d}) \bmod\Lambda \right] + \mathbf{n} \right] \bmod(t\Lambda).
\end{aligned}$$

### 3.1 Derivation of $f_{L(t, \mathbf{Z})|t=t_0}(x)$

In the particular case where  $t = t_0$ , it is clear that

$$(\mathbf{z} - t_0\mathbf{d}) \bmod(t_0\Lambda) = \left[ t_0(1 - \alpha) \left[ (\mathbf{x} - \mathbf{d}) \bmod\Lambda \right] + \mathbf{n} \right] \bmod(t_0\Lambda).$$

If the dimensionality of the problem  $n$  is large enough one could use the Central Limit Theorem (CLT), and approximate the pdf of  $L(t, \mathbf{Z})$  by a Gaussian with mean

$$E[L(t, \mathbf{Z})|t = t_0] = n + n \log \left( 2\pi \left[ \sigma_N^2 + (1 - \alpha)^2 t_0^2 \sigma_\Lambda^2 \right] \right) + \frac{n \left[ (\sigma_X^2 + \alpha^2 \sigma_\Lambda^2) t_0^2 + \sigma_N^2 \right]}{\sigma_X^2 t_0^2} \quad (8)$$

where we have used that both  $\text{HLR} \rightarrow \infty$ , and  $n \rightarrow \infty$  in order to consider the Euclidean norm of the quantization error in the first term to be independent of the Euclidean norm of the received signal; additionally, we have also consider  $\text{TNLR} \rightarrow 0$  for the low-dimensional lattice case, and  $\text{TNLR} < 1$  for the high-dimensional good lattice case, in order to neglect the modulo reduction in the first term.

These assumptions are also taken into account in the derivation of the vari-

ance, which in the scalar quantizer case can be written as

$$\text{Var}[L(t, \mathbf{Z})|t = t_0] = n \left[ \frac{\frac{(1-\alpha)^4 t_0^4 \Delta^4}{180} + 2\sigma_N^4 + \frac{(1-\alpha)^2 t_0^2 \Delta^2 \sigma_N^2}{3}}{(\sigma_N^2 + (1-\alpha)^2 \Delta^2 t^2/12)^2} + \frac{\frac{\alpha^4 t_0^4 \Delta^4}{180} + 2(t_0^2 \sigma_X^2 + \sigma_N^2)^2 + \frac{\alpha^2 t_0^2 \Delta^2 (t_0^2 \sigma_X^2 + \sigma_N^2)}{3}}{\sigma_X^4 t_0^4} \right], \quad (9)$$

while in the high-dimensional good lattice case is

$$\text{Var}[L(t, \mathbf{Z})|t = t_0] = n \left[ 2 + \frac{2(\sigma_X^2 t_0^2 + \alpha^2 t_0^2 \sigma_\Lambda^2 + \sigma_N^2)^2}{\sigma_X^4 t_0^4} \right]. \quad (10)$$

Alternatively, in the following scenarios:

- low-dimensional lattice quantizer,  $\text{HLR} \rightarrow \infty$ ,  $\text{SCR} \rightarrow 0$ ,  $\text{TNLR} \rightarrow 0$ , and  $n \rightarrow \infty$ , or
- high-dimensional good lattice quantizer,  $\text{HLR} \rightarrow \infty$  and  $\text{TNLR} < 1$ ,

the first term in (5) will asymptotically follow a  $\chi^2$  distribution with  $n$  degrees of freedom. Similarly, based on  $\text{HLR} \rightarrow \infty$ , and  $\text{TNLR} < 1$  the third term in (5) will also asymptotically follow a  $\chi^2$  distribution with  $n$  degrees of freedom. Again, based on  $\text{HLR} \rightarrow \infty$ , and  $n \rightarrow \infty$ , we will assume that the Euclidean norm of the quantization error considered in the first term is independent of the Euclidean norm of the received signal. Therefore, in the asymptotic case described by the considered hypotheses, when  $t = t_0$ , (5) can be seen as the addition of a deterministic term which depends on  $t$  and a  $\chi^2$  random variable with  $2n$  degrees of freedom.

Be aware that the Gaussian approximation derived from this  $\chi^2$  distribution is asymptotically equivalent to that introduced at the beginning of this section whenever the asymptotic framework (i.e.,  $\text{HLR} \rightarrow \infty$ ,  $\text{SCR} \rightarrow 0$ ,  $\text{TNLR} \rightarrow 0$ , and  $n \rightarrow \infty$ , for the low-dimensional lattice quantizer case, or  $\text{HLR} \rightarrow \infty$ , and  $\text{TNLR} < 1$  for the high-dimensional good lattice quantizer case) is applied to the mean and variance in (8) and (9) or (10), respectively.

### 3.2 Derivation of $f_{L(t, \mathbf{Z})|t \neq t_0}(x)$

On the other hand, whenever  $t$  is not close to  $t_0$  the vector in the numerator of the first term in (5) will be uniformly distributed in  $\mathcal{V}(t\Lambda)$ , whereas the last term will follow a scaled  $\chi^2$  distribution with  $n$  degrees of freedom. In a quantitative way, one can see that the quantization error considered in the first term of (5) is asymptotically uniform over the lattice fundamental Voronoi region whenever

$$\frac{(t_0 - t)^2 \sigma_X^2 + (t - \alpha t_0)^2 \sigma_\Lambda^2 + \sigma_N^2}{t^2 \sigma_\Lambda^2} \rightarrow \infty.$$

From  $\text{HLR} \rightarrow \infty$ , and  $\text{TNLR} < 1$  usually the dominant effect in the left-hand side will be  $(t_0 - t)^2 \sigma_X^2$  and the uniform approximation can be taken

into account in practice for  $(t_0 - t)^2 \sigma_X^2 \geq K_{\text{unif}} t^2 \sigma_\Lambda^2$ , with  $K_{\text{unif}}$  a positive real number.<sup>1</sup> Therefore, one will be able to use the uniform quantization error approximation whenever  $|t_0 - t| \geq \sqrt{\frac{K_{\text{unif}} t^2 \sigma_\Lambda^2}{\sigma_X^2}}$ , or equivalently

$$t \leq \frac{t_0}{1 + \sqrt{\frac{K_{\text{unif}} \sigma_\Lambda^2}{\sigma_X^2}}}, \text{ or } t \geq \frac{t_0}{1 - \sqrt{\frac{K_{\text{unif}} \sigma_\Lambda^2}{\sigma_X^2}}};$$

consequently, taking into account that  $\text{HLR} \rightarrow \infty$ , the size of the interval around  $t_0$  where the asymptotic uniform behavior can not be considered is rather small. Concerning the last term of (5), we will characterize it by a  $\chi^2$  distribution with  $n$  degrees of freedom and scaled by

$$\frac{(\sigma_X^2 + \alpha^2 \sigma_\Lambda^2) t_0^2 + \sigma_N^2}{\sigma_X^2 t^2}.$$

Taking into account the distribution of both the first and third terms and using again the assumption of both terms being independent (based on  $\text{HLR} \rightarrow \infty$ , and  $n \rightarrow \infty$ ), the distribution of (5) for values of  $t$  which are not close to  $t_0$  will be approximately the convolution of the pdf of the scaled square Euclidean norm of a random vector uniformly distributed on  $\mathcal{V}(\Lambda)$ , and a scaled  $\chi^2$  with  $n$  degrees of freedom. In order to simplify the resulting pdf, we will assume that  $n$  is large enough to the CLT be applied, yielding that whenever  $t$  is not close to  $t_0$  and a scalar quantizer is used, (5) will approximately follow a

$$\mathcal{N} \left( \frac{nt^2 \sigma_\Lambda^2}{\sigma_N^2 + (1 - \alpha)^2 t^2 \sigma_\Lambda^2} + n \log [2\pi (\sigma_N^2 + (1 - \alpha)^2 t^2 \sigma_\Lambda^2)] + \frac{n[(\sigma_X^2 + \alpha^2 \sigma_\Lambda^2) t_0^2 + \sigma_N^2]}{\sigma_X^2 t^2}, \right. \\ \left. \frac{n144t^4 \sigma_\Lambda^4 / 180}{(\sigma_N^2 + (1 - \alpha)^2 t^2 \sigma_\Lambda^2)^2} + \frac{2n [(\sigma_X^2 + \alpha^2 \sigma_\Lambda^2) t_0^2 + \sigma_N^2]^2}{\sigma_X^4 t^4} \right). \quad (11)$$

On the other hand, if we are in the high-dimensional good lattice quantizer scenario, then

$$\mathcal{N} \left( \frac{nt^2 \sigma_\Lambda^2}{\sigma_N^2 + (1 - \alpha)^2 t^2 \sigma_\Lambda^2} + n \log [2\pi (\sigma_N^2 + (1 - \alpha)^2 t^2 \sigma_\Lambda^2)] + \frac{n[(\sigma_X^2 + \alpha^2 \sigma_\Lambda^2) t_0^2 + \sigma_N^2]}{\sigma_X^2 t^2}, \right. \\ \left. \frac{2nt^4 \sigma_\Lambda^4}{(\sigma_N^2 + (1 - \alpha)^2 t^2 \sigma_\Lambda^2)^2} + \frac{2n [(\sigma_X^2 + \alpha^2 \sigma_\Lambda^2) t_0^2 + \sigma_N^2]^2}{\sigma_X^4 t^4} \right). \quad (12)$$

### 3.3 Study of the behavior of $L(t, \mathbf{z})$ under the asymptotical work hypotheses

As it was mentioned in Sect. 2, the analysis performed in this report for the low-dimensional lattice case is based on  $\text{HLR} \rightarrow \infty$ ,  $\text{SCR} \rightarrow 0$ ,  $\text{TNLR} \rightarrow 0$ ,

---

<sup>1</sup>In practice the uniform approximation is pretty accurate for  $K_{\text{unif}} \geq 5$  for the scalar quantizer case. In the high-dimensional good lattice quantizer case, it would be indeed enough that  $K_{\text{unif}} \geq 1$ .

and  $n \rightarrow \infty$ , while the high-dimensional good lattice case relies on  $\text{HLR} \rightarrow \infty$ ,  $\text{TNLR} < 1$ , and, of course,  $n \rightarrow \infty$ . In this section we will analyze the considered target function  $L(t, \mathbf{z})$  in terms of its limits with respect to those parameters, in order to check if the resulting limit function is well defined, i.e., if it does not depend on the order of the limits (as one would desire), or if it is indeed ill-defined. In order to avoid the problems due to  $L(t, \mathbf{z})$  diverging when  $n \rightarrow \infty$  (as it is proportional to this parameter), we will study  $L(t, \mathbf{z})/n$ , without loss of generality. Moreover, in order to avoid degenerated cases in our analysis, we will assume  $\sigma_X^2 > 0$ ,  $\sigma_\Lambda^2 > 0$ ,  $\sigma_N^2 > 0$ ,  $t_0 \neq 0$ , and  $t \neq 0$ . This will be proved to be a sufficient condition for showing the result we are interested in; in any case, practical cases are considered within this framework.

We will find useful to define  $L(t, \mathbf{z})$  in terms of the 4 considered limits. Therefore, we will make the following variable changes:

$$\begin{aligned}\sigma_X^2 &= \text{HLR}\sigma_\Lambda^2, \\ \sigma_N^2 &= t_0^2\sigma_\Lambda^2 [\text{TNLR} - (1 - \alpha)^2], \\ (1 - \alpha)^2 &= \frac{\text{SCR} \cdot \text{TNLR}}{1 + \text{SCR}},\end{aligned}$$

where due to its definition,  $\text{TNLR} \geq (1 - \alpha)^2$ . Thus, (5) can be rewritten as

$$\begin{aligned}\frac{L(t, \mathbf{z})}{n} &\triangleq \varphi_n(\text{HLR}, \text{SCR}, \text{TNLR}) = \frac{\|(\mathbf{z} - t\mathbf{d}) \bmod(t\Lambda)\|^2/n}{\sigma_\Lambda^2 \text{TNLR} \left[ \frac{t_0^2 + t^2 \text{SCR}}{\text{SCR} + 1} \right]} \\ &+ \log \left[ 2\pi \left( \sigma_\Lambda^2 \text{TNLR} \left[ \frac{t_0^2 + t^2 \text{SCR}}{\text{SCR} + 1} \right] \right) \right] \\ &+ \frac{\|\mathbf{z}\|^2/n}{\text{HLR}\sigma_\Lambda^2 t^2}.\end{aligned}$$

Due to the nature of the considered functions, the rightmost term of the previous equalities is obviously an analytic function with  $\text{HLR} > 0$  (i.e.,  $\sigma_X^2 > 0$ ), and it will be also analytic with  $\text{TNLR}$  and  $\text{SCR}$  as long as the denominator of the first term were positive; a sufficient condition for this to happen is that the involved variances ( $\sigma_\Lambda^2$ , and  $\sigma_N^2$ ) were positive, and the scaling factor values ( $t$ , and  $t_0$ ) were non-null. Thus, under those conditions,  $\varphi(\text{HLR}, \text{SCR}, \text{TNLR}) \triangleq \lim_{n \rightarrow \infty} \varphi_n(\text{HLR}, \text{SCR}, \text{TNLR})$  will be also an analytic function.

Therefore, under the previous conditions  $\frac{L(t, \mathbf{z})}{n}$  will uniformly converge [1] with  $n$  to an analytic function in  $(\text{HLR}, \text{SCR}, \text{TNLR}) \in (0, \infty) \times (0, \infty) \times ((1 - \alpha)^2, \infty)$ , implying that the order of the passages to the limit can be interchanged. This result is sufficient for proving that the limit target function is well-defined both for the high-dimensional good lattice case and the low-dimensional lattice one.

### 3.4 Derivation of the asymptotic value of $L(t, \mathbf{z})$ when the number of observations goes to infinity

First, we will focus on the case where  $t \approx t_0$ , quantified through the inequality  $(t_0 - t)^2 \sigma_X^2 + (t - \alpha t_0)^2 \alpha^2 \sigma_\Lambda^2 + \sigma_N^2 \ll t^2 \sigma_\Lambda^2$  (implying  $\text{TNLR} \rightarrow 0$ ) for the low-dimensional lattice quantizer case, and through its relaxed version  $(t_0 - t)^2 \sigma_X^2 +$



$(t - \alpha t_0)^2 \alpha^2 \sigma_\Lambda^2 + \sigma_N^2 < t^2 \sigma_\Lambda^2$  (implying  $\text{TNLR} < 1$ ) for the high-dimensional good lattice quantizer one. In that scenario

$$\begin{aligned} L(t, \mathbf{z}) &\approx n \frac{(t_0 - t)^2 \sigma_X^2 + (t - \alpha t_0)^2 \sigma_\Lambda^2 + \sigma_N^2}{\sigma_N^2 + (1 - \alpha)^2 t^2 \sigma_\Lambda^2} + n \log (2\pi (\sigma_N^2 + (1 - \alpha)^2 t^2 \sigma_\Lambda^2)) \\ &\quad + n \frac{(\sigma_X^2 + \alpha^2 \sigma_\Lambda^2) t_0^2 + \sigma_N^2}{\sigma_X^2 t^2} \\ &\approx 2n + \frac{n(t_0 - t)^2 \sigma_X^2}{\sigma_N^2 + (1 - \alpha)^2 t^2 \sigma_\Lambda^2} + n \log (2\pi (\sigma_N^2 + (1 - \alpha)^2 t^2 \sigma_\Lambda^2)), \end{aligned} \quad (13)$$

where we have used that  $\text{HLR} \rightarrow \infty$ ,  $\text{TNLR} \rightarrow 0$ , and  $n \rightarrow \infty$  for the low-dimensional lattice quantizer case, and that  $\text{HLR} \rightarrow \infty$ , and  $\text{TNLR} < 1$  for the high-dimensional good lattice quantizers.

On the other hand, if we study the case where  $t$  is not close to  $t_0$ , meaning  $(t_0 - t)^2 \sigma_X^2 + (t - \alpha t_0)^2 \alpha^2 \sigma_\Lambda^2 + \sigma_N^2 \gg t^2 \sigma_\Lambda^2$  for the low-dimensional lattice quantizer case and  $(t_0 - t)^2 \sigma_X^2 + (t - \alpha t_0)^2 \alpha^2 \sigma_\Lambda^2 + \sigma_N^2 > t^2 \sigma_\Lambda^2$  for the high-dimensional good lattice quantizers,  $L(t, \mathbf{z})$  can be approximated by

$$\begin{aligned} L(t, \mathbf{z}) &\approx n \frac{t^2 \sigma_\Lambda^2}{\sigma_N^2 + (1 - \alpha)^2 t^2 \sigma_\Lambda^2} + n \log (2\pi (\sigma_N^2 + (1 - \alpha)^2 t^2 \sigma_\Lambda^2)) \\ &\quad + n \frac{(\sigma_X^2 + \alpha^2 \sigma_\Lambda^2) t_0^2 + \sigma_N^2}{\sigma_X^2 t^2} \\ &\approx n \frac{t^2 \sigma_\Lambda^2}{\sigma_N^2 + (1 - \alpha)^2 t^2 \sigma_\Lambda^2} + n \log (2\pi (\sigma_N^2 + (1 - \alpha)^2 t^2 \sigma_\Lambda^2)) + n \frac{t_0^2}{t^2}; \end{aligned} \quad (14)$$

again, we have used that  $\text{HLR} \rightarrow \infty$ ,  $\text{TNLR} < 1$ , and  $n \rightarrow \infty$ .

## 4 Optimization

Due to the modulo operation in the first term of (5) the considered target function  $L(t, \mathbf{z})$  is not convex with  $t$ ; indeed, it will have a large number of non-differentiable points, corresponding to those values of  $t$  that move  $\mathbf{z}/t$  to a different Voronoi region of the original quantizer  $Q_\Lambda$ .

Taking into account these difficulties, we will use an initial estimation of the scaling factor  $t_0$ , denoted by  $t_1$ , to define a search interval where the solution to our problem can be guaranteed to lie on (if a deterministic approach is followed), or at least can be guaranteed to lie on with a given probability (if a probabilistic approach is followed); this search interval will be sampled finely enough to be reasonably sure that the global minimum of the target function (or a good approximation to it) will be found by the optimization algorithms to be introduced.

## 5 $t_1$ choices

### 5.1 $L(t, \mathbf{z})$ approximation

As a first strategy for defining  $t_1$ , we define an approximation to our target function which has a single minimum in  $t$ ; by doing so, one can ensure the convergence to the minimum of that approximating function, which is hoped to be close to  $t_0$ . Considering that for most of  $t$  values (i.e., those that are not close to  $t_0$ ) the uniform approximation of the quantization error can be assumed, our proposal to approximate the target function is

$$L_1(t, \mathbf{z}) \triangleq \frac{nt^2\sigma_\Lambda^2}{\sigma_N^2 + (1-\alpha)^2\sigma_\Lambda^2 t^2} + n \log(2\pi(\sigma_N^2 + (1-\alpha)^2\sigma_\Lambda^2 t^2)) + \frac{\|\mathbf{z}\|^2}{\sigma_X^2 t^2}.$$

It is just mechanical to check that the first derivative of  $L_1(t, \mathbf{z})$  with respect to  $t^2$  is

$$\frac{\partial L_1(t, \mathbf{z})}{\partial(t^2)} = \frac{n\sigma_\Lambda^2 \left[ \left(1 + (1-\alpha)^2\right) \sigma_N^2 + (1-\alpha)^4 \sigma_\Lambda^2 t^2 \right]}{\left[ \sigma_N^2 + (1-\alpha)^2 \sigma_\Lambda^2 t^2 \right]^2} - \frac{\|\mathbf{z}\|^2}{\sigma_X^2 t^4},$$

it is straightforward to see that one can write

$$\left( \frac{\partial L_1(t, \mathbf{z})}{\partial(t^2)} \right) \left[ \sigma_N^2 + (1-\alpha)^2 \sigma_\Lambda^2 t^2 \right]^2 \sigma_X^2 t^4 = a_0 + a_1 t^2 + a_2 t^4 + a_3 t^6, \quad (15)$$

where,

$$\begin{aligned} a_0 &= -\|\mathbf{z}\|^2 \sigma_N^4 \\ a_1 &= -2(1-\alpha)^2 \sigma_\Lambda^2 \sigma_N^2 \|\mathbf{z}\|^2 \\ a_2 &= \sigma_\Lambda^2 \left[ n \left(1 + (1-\alpha)^2\right) \sigma_N^2 \sigma_X^2 - (1-\alpha)^4 \sigma_\Lambda^2 \|\mathbf{z}\|^2 \right] \\ a_3 &= n(1-\alpha)^4 \sigma_\Lambda^4 \sigma_X^2. \end{aligned}$$

Therefore, considering that  $L_1(t, \mathbf{z}) \rightarrow \infty$  both when  $t \rightarrow 0$  and  $t \rightarrow \infty$ , and that according to Descartes' sign rule the number of real roots of (15) is at most one, it is evident that  $L_1(t, \mathbf{z})$  will have a single local (and consequently global) minimum for  $t > 0$ , proving that  $t_1 = \operatorname{argmin}_t L_1(\mathbf{z}, t)$  can be easily computed.

Interestingly, when  $n \rightarrow \infty$ , and for an arbitrary lattice, the left term in (15) goes to

$$\begin{aligned} &-n \left[ (\sigma_X^2 + \alpha^2 \sigma_\Lambda^2) t_0^2 + \sigma_N^2 \right] \left[ \sigma_N^2 + (1-\alpha)^2 \sigma_\Lambda^2 t^2 \right]^2 \\ &+ n \sigma_\Lambda^2 \sigma_X^2 t^4 \left[ (1 + (1-\alpha)^2) \sigma_N^2 + (1-\alpha)^4 \sigma_\Lambda^2 t^2 \right], \end{aligned}$$

which, assuming that  $\text{HLR} \rightarrow \infty$ ,  $\text{SCR} \rightarrow 0$ ,  $\text{TNLR} \rightarrow 0$ , and that  $t$  is not much larger than  $t_0$ ,<sup>2</sup> can be approximated by

$$n\sigma_N^2\sigma_X^2 \left[ -\sigma_N^2 t_0^2 + \left(1 + (1-\alpha)^2\right) \sigma_\Lambda^2 t^4 \right];$$

---

<sup>2</sup>This is the only place where  $\text{SCR} \rightarrow 0$ , and  $\text{TNLR} \rightarrow 0$  are used in order to prove a property of the high-dimensional good lattice case. Additionally, assumptions on the value of  $t$  are made. Nevertheless, the objective of considering these conditions is just to prove the non-consistent nature of the resulting estimator, no affecting to the calculation of  $t_1$ .

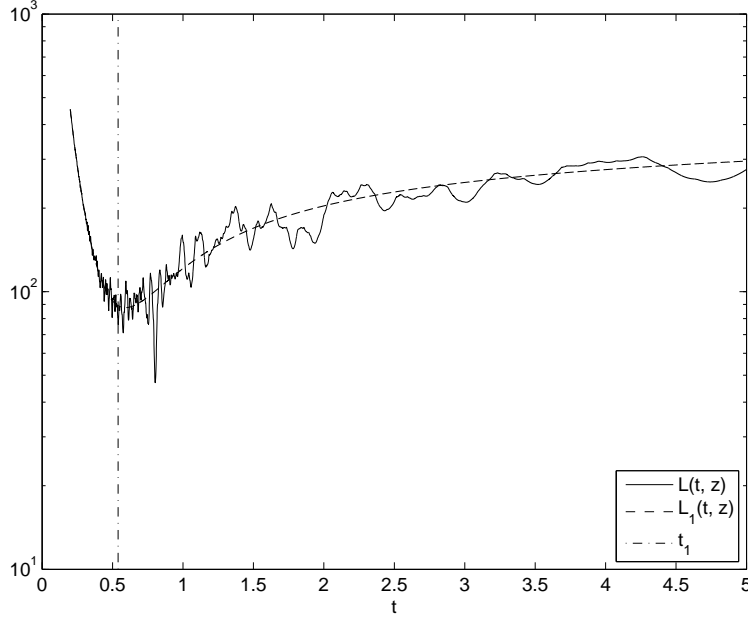


Figure 1: Comparison between  $L(t, \mathbf{z})$  and  $L_1(t, \mathbf{z})$ . The proposed value of  $t_1$  (dash-dot line) is not that exactly minimizing  $L_1(t, \mathbf{z})$ , but that in (16). HLR  $\approx 34.9765$  dB, SCR  $\approx -1.0618$  dB, TNLR  $\approx -3.5736$  dB,  $t_0 = 0.8$ ,  $\alpha = \alpha_{\text{Costa}} \approx 0.5608$ ,  $n = 40$ , scalar quantizer.

consequently, under the work hypotheses and when the dimensionality of the problem goes to infinity, the value of  $t$  minimizing  $L_1(t, \mathbf{z})$  can be approximated by

$$t_1 \triangleq \left( \frac{\sigma_N^2 t_0^2}{[1 + (1 - \alpha)^2] \sigma_\Lambda^2} \right)^{1/4}. \quad (16)$$

Obviously this value does not coincide with  $t_0$ , indicating that the obtained estimator is not consistent.

A graphical example of this approximation can be found in Fig. 1.

## 5.2 Variance-based estimators

The variance-based estimator for the i.i.d. Gaussian case takes the form

$$\hat{t}_{\text{var}}(\mathbf{z}) = \sqrt{\frac{\frac{\|\mathbf{z}\|^2}{n} - \sigma_N^2}{\sigma_X^2 + \alpha^2 \sigma_\Lambda^2}}. \quad (17)$$

Furthermore, its Cramer Rao-Bound (CRB) is

$$\frac{[(\sigma_X^2 + \alpha^2 \sigma_\Lambda^2) t_0^2 + \sigma_N^2]^2}{2n (\sigma_X^2 + \alpha^2 \sigma_\Lambda^2)^2 t_0^2}.$$

Nevertheless, one must take into account that the previous estimator is biased (so the CRB is wrongly used); in order to prove it, we will consider a simplified case, where  $n = 1$ ,  $\sigma_N^2 = 0$ ,  $\sigma_X^2 + \alpha^2\sigma_\Lambda^2 = 1$ , and  $t_0 = 1$ . In that scenario, it is obvious that

$$\mathbb{E}\{\hat{T}_{\text{var}}(\mathbf{Z})\} = \mathbb{E}\{|Z|\} = 2 \int_0^\infty \frac{\tau e^{-\frac{\tau^2}{2}}}{\sqrt{2\pi}} d\tau = \sqrt{\frac{2}{\pi}}.$$

On the other hand, the following estimator could be used

$$\hat{t}_{\text{var}}^2(\mathbf{z}) = \frac{\frac{\|\mathbf{z}\|^2}{n} - \sigma_N^2}{\sigma_X^2 + \alpha^2\sigma_\Lambda^2};$$

the latter is indeed an unbiased estimator of  $t_0^2$ , whose CRB is easily proved to be

$$\frac{2 [(\sigma_X^2 + \alpha^2\sigma_\Lambda^2) t_0^2 + \sigma_N^2]^2}{n (\sigma_X^2 + \alpha^2\sigma_\Lambda^2)^2}. \quad (18)$$

### 5.2.1 Studying the links between $\hat{T}_{\text{var}}(\mathbf{Z})$ and $\hat{T}_{\text{var}}^2(\mathbf{Z})$

In this section we will study the pdf of the square root of  $\hat{T}_{\text{var}}^2(\mathbf{Z})$ , derive its mean and variance, and analyze in which asymptotic cases the statistics of  $\hat{T}_{\text{var}}(\mathbf{Z})$  obtained following this methodology converge to those previously derived under the false premise that this estimator is unbiased.

Based on the assumption that the number of considered dimensions is very large, the pdf of  $\hat{T}_{\text{var}}^2(\mathbf{Z})$  given  $t_0$  can be approximated by  $\mathcal{N}\left(t_0^2, \frac{2[(\sigma_X^2 + \alpha^2\sigma_\Lambda^2)t_0^2 + \sigma_N^2]^2}{n(\sigma_X^2 + \alpha^2\sigma_\Lambda^2)^2}\right)$ . In general, if we have a random variable  $T^2$  with pdf  $\mathcal{N}(\mu, \sigma^2)$ , the mean of its square root  $T$  is

$$\begin{aligned} \mathbb{E}\{T\} &= \int_0^\infty \tau \left( \frac{2\tau e^{-\frac{(\tau^2 - \mu)^2}{2\sigma^2}}}{\sqrt{2\pi\sigma^2}} + j \frac{2\tau e^{-\frac{(\tau^2 + \mu)^2}{2\sigma^2}}}{\sqrt{2\pi\sigma^2}} \right) d\tau \\ &= \frac{(1+j)e^{-\frac{\mu^2}{2\sigma^2}}}{2^{3/4}\sqrt{\pi}\sigma^{1/2}} \left[ \sigma\Gamma\left(\frac{3}{4}\right) {}_1F_1\left(\frac{3}{4}; \frac{1}{2}; \frac{\mu^2}{2\sigma^2}\right) - j\sqrt{2}\mu\Gamma\left(\frac{5}{4}\right) {}_1F_1\left(\frac{5}{4}; \frac{3}{2}; \frac{\mu^2}{2\sigma^2}\right) \right], \end{aligned}$$

where  ${}_1F_1(\cdot; \cdot; \cdot)$  denotes the confluent hypergeometric function of the first kind. Similarly, the mean  $|T|^2$  can be obtained as

$$\begin{aligned} \mathbb{E}\{|T|^2\} &= \mathbb{E}\{|T^2|\} = \int_0^\infty \tau^2 \left( \frac{2\tau e^{-\frac{(\tau^2 - \mu)^2}{2\sigma^2}}}{\sqrt{2\pi\sigma^2}} + \frac{2\tau e^{-\frac{(\tau^2 + \mu)^2}{2\sigma^2}}}{\sqrt{2\pi\sigma^2}} \right) d\tau \\ &= e^{-\frac{\mu^2}{2\sigma^2}} \sqrt{\frac{2\sigma^2}{\pi}} + \mu \text{Erf}\left(\frac{\mu}{\sqrt{2\sigma^2}}\right). \end{aligned}$$

Replacing  $\mu$  and  $\sigma^2$  by  $t_0^2$  and (18), respectively, it is straightforward to obtain the mean and variance of  $T$ .

Nevertheless, it is also interesting to study the behavior of the considered random variable when the mean of  $T^2$  is much larger than its standard deviation, i.e.,  $\frac{\mu^2}{\sigma^2} \rightarrow \infty$ ; intuitively, one can see that in this case the effects of the tails of the Gaussian taking negative values can be dismissed. Indeed, it can be shown that

$$\lim_{\frac{\mu}{\sigma} \rightarrow \infty} \mathbb{E}\{T\} = \sqrt{\mu},$$

$$\lim_{\frac{\mu}{\sigma} \rightarrow \infty} \mathbb{E}\{|T^2|\} \frac{\mu^2}{\sigma^2} = \frac{\mu}{4}.$$

In this asymptotic case, if  $\mu$  and  $\sigma^2$  were replaced by  $t_0^2$  and (18), the mean and the (wrongly calculated) CRB for the estimator in (17) are obtained. This result seems to indicate that the estimator in (17) will be asymptotically unbiased, and therefore its CRB correctly calculated, just when the previously introduced condition on the ratio  $\frac{\mu}{\sigma}$  is verified. For finite non-null values of  $\sigma_X^2 + \alpha^2 \sigma_\Lambda^2$ ,  $\sigma_N^2$ , and  $t_0$  that condition holds, for example, when  $n \rightarrow \infty$ .

Furthermore, when  $n \rightarrow \infty$  both variance-based estimators asymptotically follow a Gaussian distribution.

### 5.2.2 Additional comments on $\hat{T}_{\text{var}}^2(\mathbf{Z})$ and $\hat{T}_{\text{var}}(\mathbf{Z})$

At the sight of the definition and theoretical characterization of  $\hat{T}_{\text{var}}^2(\mathbf{Z})$  and  $\hat{T}_{\text{var}}(\mathbf{Z})$  provided in the previous sections, it is obvious that the negative values of  $\hat{T}_{\text{var}}^2(\mathbf{Z})$  and imaginary of  $\hat{T}_{\text{var}}(\mathbf{Z})$  have non-null probability. The causes of this problem are basically two:

- The approximate nature of the proposed pdf. Given that we are assuming  $\|\mathbf{Z}\|^2$  to follow a Gaussian distribution, the probability of that random variable taking negative values will be non-null. This problem would be solved if the real pdf (the convolution of two scaled  $\chi^2$  distribution with  $n$  degrees of freedom) were considered. Nevertheless, the price to be paid is a significant increase in the complexity of the resulting pdf, which will make more hard to perform a theoretical analysis.
- Even if one considers the exact pdf of  $\|\mathbf{Z}\|^2$ , the probability of obtaining a negative value of  $\hat{T}_{\text{var}}^2(\mathbf{Z})$  or complex value of  $\hat{T}_{\text{var}}(\mathbf{Z})$  will be still non-null. This is explained by the fact that *a priori* information is not used at the derivation of the proposed estimators.

Therefore, if *a priori* information on the possible interval of  $t_0$  values were available, the ML optimization problem should be redefined in order to consider those constraints.<sup>3</sup> In our case, where the *a priori* information constrains  $t_0$  to be real, the ML problem might be defined as

$$\hat{t}_{\text{var}}^2(\mathbf{z}) = \underset{t^2 \geq 0}{\operatorname{argmax}} f_{\mathbf{Z}|T^2}(\mathbf{z}|t^2).$$

---

<sup>3</sup>Indeed, strictly speaking the resulting estimator is no longer ML, as *a priori* information is used; nevertheless, it is neither MAP, as the *a priori* knowledge does not inform on the pdf of  $T_0$ , but just on its domain.

In the case of i.i.d. Gaussian signals, as the derivative of the pdf with respect to  $t^2$  has a single local minimum, if that minimum were located at a negative value of  $t^2$  it is straightforward to see that the value of  $t^2$  maximizing  $f_{\mathbf{Z}|T^2}(\mathbf{z}|t^2)$  will be 0. Therefore, the estimators obtained by following the above criterion are

$$\hat{t}_{\text{var}}^2(\mathbf{z}) = \left[ \frac{\frac{\|\mathbf{z}\|^2}{n} - \sigma_N^2}{\sigma_X^2 + \alpha^2 \sigma_\Lambda^2} \right]^+, \quad (19)$$

or

$$\hat{t}_{\text{var}}(\mathbf{z}) = \sqrt{\left[ \frac{\frac{\|\mathbf{z}\|^2}{n} - \sigma_N^2}{\sigma_X^2 + \alpha^2 \sigma_\Lambda^2} \right]^+}. \quad (20)$$

Both of these estimators will be biased. Assuming a large number of dimensions in order to: 1) the original non-truncated estimators studied at the beginning of this section be Gaussian, and 2) for  $\hat{T}_{\text{var}}(\mathbf{Z})$  estimator, the condition derived at the end of Sect. 5.2.1 be hold, the pdfs of (19) and (20) are, respectively

$$f_{\hat{T}_{\text{var}}^2|T_0^2}(t^2|t_0^2) \approx \begin{cases} \frac{e^{-\frac{n(\sigma_X^2 + \alpha^2 \sigma_\Lambda^2)^2(t^2 - t_0^2)^2}{4[(\sigma_X^2 + \alpha^2 \sigma_\Lambda^2)t_0^2 + \sigma_N^2]^2}}}{\sqrt{\frac{4\pi[(\sigma_X^2 + \alpha^2 \sigma_\Lambda^2)t_0^2 + \sigma_N^2]^2}{n(\sigma_X^2 + \alpha^2 \sigma_\Lambda^2)^2}}} & \text{if } t^2 > 0 \\ Q\left(\frac{t_0^2}{\sqrt{\frac{2[(\sigma_X^2 + \alpha^2 \sigma_\Lambda^2)t_0^2 + \sigma_N^2]^2}{n(\sigma_X^2 + \alpha^2 \sigma_\Lambda^2)^2}}}\right) \delta(t^2) & \text{otherwise} \end{cases}, \quad (21)$$

and

$$f_{\hat{T}_{\text{var}}|T_0}(t|t_0) \approx \begin{cases} \frac{e^{-\frac{n(\sigma_X^2 + \alpha^2 \sigma_\Lambda^2)^2 t_0^2 (t - t_0)^2}{[(\sigma_X^2 + \alpha^2 \sigma_\Lambda^2)t_0^2 + \sigma_N^2]^2}}}{\sqrt{\frac{\pi[(\sigma_X^2 + \alpha^2 \sigma_\Lambda^2)t_0^2 + \sigma_N^2]^2}{n(\sigma_X^2 + \alpha^2 \sigma_\Lambda^2)^2 t_0^2}}} & \text{if } t \in \mathbb{R}^+ \\ Q\left(\frac{t_0}{\sqrt{\frac{[(\sigma_X^2 + \alpha^2 \sigma_\Lambda^2)t_0^2 + \sigma_N^2]^2}{2n(\sigma_X^2 + \alpha^2 \sigma_\Lambda^2)^2 t_0^2}}}\right) \delta(t) & \text{otherwise} \end{cases},$$

where  $Q(x)$  is defined as

$$Q(x) \triangleq \int_{-\infty}^x \frac{e^{-x^2/2}}{\sqrt{2\pi}}.$$

## 6 Search interval lower-bound

### 6.1 General discussion on the methodologies proposed for determining $t_{\text{lower}}$ and $t_{\text{upper}}$

The methodologies proposed in Sect. 6 and Sect. 7 for determining lower and upper-bounds to the search interval, can be coarsely classified into three categories:

- deterministic: Sects. 6.2, 7.1, and 7.2. These approaches ensure that  $\hat{t}(\mathbf{z})$  is contained in the derived search interval.
- probabilistic: Sects. 6.3, 7.3, and 7.4. These schemes are based on statistically characterizing the target function, and determine an interval of scaling factors such that if  $t_0$  were out of that interval, it would be very unlikely that the value of the target function at  $t_0$  were smaller than  $L(t_1, \mathbf{z})$ . Assuming the bias of  $\hat{t}(\mathbf{z})$  to be small, these methods could be seen as a relaxed version of the deterministic ones; as  $t_0$  is just ensured to be within the provided interval with a certain probability, the width of that interval can be reduced. Links in this direction will be established between the estimators proposed in Sects. 6.2, and 7.1, and those in Sects. 6.3, and 7.4; and between the estimators proposed in Sect. 7.2, and Sect. 7.3.
- derived from the variance-based estimator: Sects. 6.4 and 7.5. Although these approaches are also probabilistic, in this case it is not the target function, but the variance-based estimator which is statistically characterized in order to define an interval of scaling factors such that if  $t_0$  were out of that interval, it would be very unlikely that the current variance-based estimator were obtained.

## 6.2 Deterministic approach

Defining  $L_2(t, \mathbf{z})$  as

$$L_2(t, \mathbf{z}) \triangleq n \log \left( 2\pi \left( \sigma_N^2 + (1 - \alpha)^2 t^2 \sigma_\Lambda^2 \right) \right) + \frac{\|\mathbf{z}\|^2}{\sigma_X^2 t^2}, \quad (22)$$

and given that  $L(\hat{t}(\mathbf{z}), \mathbf{z}) \leq L(t_1, \mathbf{z})$  by definition, and that the first term of  $L(t, \mathbf{z})$  is non-negative, it is clear that  $\hat{t}(\mathbf{z})$  must verify

$$L_2(\hat{t}(\mathbf{z}), \mathbf{z}) \leq L(\hat{t}(\mathbf{z}), \mathbf{z}) \leq L(t_1, \mathbf{z}).$$

Furthermore, the first derivative of  $L_2(t, \mathbf{z})$  with respect to  $t^2$  is

$$\frac{\partial L_2(t, \mathbf{z})}{\partial (t^2)} = \frac{n(1 - \alpha)^2 \sigma_\Lambda^2}{\sigma_N^2 + (1 - \alpha)^2 t^2 \sigma_\Lambda^2} - \frac{\|\mathbf{z}\|^2}{\sigma_X^2 t^4},$$

which has 2 roots in  $t^2$ , one of them negative; the only positive one can be found at  $t_2^2$

$$t_2^2 = \frac{\|\mathbf{z}\|^2 + \|\mathbf{z}\| \sqrt{\|\mathbf{z}\|^2 + \frac{4n\sigma_N^2 \sigma_X^2}{(1 - \alpha)^2 \sigma_\Lambda^2}}}{2n\sigma_X^2};$$

additionally, since for  $t \rightarrow 0$ ,  $L_2(t, \mathbf{z}) \rightarrow \infty$ , we have that  $L_2(t, \mathbf{z})$  has a single minimum located at  $t_2$ . Therefore, a lower-bound to the search interval can be calculated as the largest  $t \leq t_2$  such that  $L_2(t, \mathbf{z})$  is larger than or equal to  $L(t_1, \mathbf{z})$ , i.e.,

$$t_{\text{lower}} = \underset{t: t \leq t_2, L_2(t, \mathbf{z}) \geq L(t_1, \mathbf{z})}{\operatorname{argmax}} t, \quad (23)$$

which due to the strictly monotonically decreasing nature of  $L_2(t, \mathbf{z})$  for  $t < t_2$  and that for  $t \rightarrow 0$ ,  $L_2(t, \mathbf{z}) \rightarrow \infty$ , will be well-defined. On the other hand  $L_2(t_2, \mathbf{z}) \leq L_2(t_1, \mathbf{z}) \leq L(t_1, \mathbf{z})$ , holding both equalities only if  $t_1 = t_2$  and if the quantization error in the first term of  $L(t_1, \mathbf{z})$  is null. Taking this into account, and due to the continuity of  $L_2(t, \mathbf{z})$ , is obvious that  $L_2(t_{\text{lower}}, \mathbf{z}) = L(t_1, \mathbf{z})$ , so we will focus on the study of the solutions for  $t \leq t_2$  to the equation

$$n \log (2\pi (\sigma_N^2 + (1 - \alpha)^2 t^2 \sigma_\Lambda^2)) + \frac{\|\mathbf{z}\|^2}{\sigma_X^2 t^2} = \frac{\|(\mathbf{z} - t_1 \mathbf{d}) \bmod (t_1 \Lambda)\|^2}{\sigma_N^2 + (1 - \alpha)^2 t_1^2 \sigma_\Lambda^2} + n \log (2\pi (\sigma_N^2 + (1 - \alpha)^2 t_1^2 \sigma_\Lambda^2)) + \frac{\|\mathbf{z}\|^2}{\sigma_X^2 t_1^2}. \quad (24)$$

Although to the best of authors' knowledge closed formulas for the solutions of this equation are not available, due to the monotonically decreasing nature of  $L_2(t, \mathbf{z})$  for  $t \leq t_2$ , and that  $L_2(t_2, \mathbf{z}) \leq L(t_1, \mathbf{z})$  the solution we are looking for is unique and can be found by simple search methods.

The upper-bound counterpart of this method can be found in Sect. 7.1.

### 6.2.1 Asymptotic value when the number of observations goes to infinity

In this case

$$L_2(t, \mathbf{z}) \approx n \log (2\pi (\sigma_N^2 + (1 - \alpha)^2 t^2 \sigma_\Lambda^2)) + n \frac{(\sigma_X^2 + \alpha^2 \sigma_\Lambda^2) t_0^2 + \sigma_N^2}{\sigma_X^2 t^2}, \quad (25)$$

and

$$t_2 \approx \sqrt{\frac{(\sigma_X^2 + \alpha^2 \sigma_\Lambda^2) t_0^2 + \sigma_N^2 + \sqrt{(\sigma_X^2 + \alpha^2 \sigma_\Lambda^2) t_0^2 + \sigma_N^2} \sqrt{(\sigma_X^2 + \alpha^2 \sigma_\Lambda^2) t_0^2 + \sigma_N^2 + \frac{4\sigma_N^2 \sigma_X^2}{(1 - \alpha)^2 \sigma_\Lambda^2}}}{2\sigma_X^2}} \quad (26)$$

which is obviously larger than or equal to  $t_0$ ; whenever  $\text{HLR} \rightarrow \infty$ , and  $\text{TNLR} < 1$ , the last expression can be approximated by

$$t_2 \approx \sqrt{\frac{t_0^2 + t_0 \sqrt{t_0^2 + \frac{4\sigma_N^2}{(1 - \alpha)^2 \sigma_\Lambda^2}}}{2}}. \quad (27)$$

Therefore, the remaining question to be answered is if  $t_{\text{lower}}$  will be smaller than or equal to  $t_0$ . In order to do so, we will first consider the case  $t_1 \approx t_0$ , so, considering (13) as the second term in (24), one obtains

$$n \log (2\pi (\sigma_N^2 + (1 - \alpha)^2 t^2 \sigma_\Lambda^2)) + n \frac{t_0^2}{t^2} = 2n + \frac{n(t_0 - t_1)^2 \sigma_X^2}{\sigma_N^2 + (1 - \alpha)^2 t_1^2 \sigma_\Lambda^2} + n \log (2\pi (\sigma_N^2 + (1 - \alpha)^2 t_1^2 \sigma_\Lambda^2)).$$

If  $t_0 \leq t_1$ , then it is obvious that the first term evaluated at  $t = t_0$  is smaller than the second one, implying that  $t_{\text{lower}} < t_0$ . On the other hand, if  $t_0 > t_1$ , then, given that both of them are smaller than or equal to  $t_2$ ,

$$L_2(t_0, \mathbf{z}) < L_2(t_1, \mathbf{z}) \leq L(t_1, \mathbf{z}), \quad (28)$$



proving that  $t_{\text{lower}} < t_0$ .

Finally, if  $t_1$  is not close to  $t_0$ , (14) will replace to the second term in (24), yielding

$$\begin{aligned} & n \log (2\pi (\sigma_N^2 + (1 - \alpha)^2 t^2 \sigma_\Lambda^2)) + n \frac{t_0^2}{t^2} = \\ & n \frac{t_1^2 \sigma_\Lambda^2}{\sigma_N^2 + (1 - \alpha)^2 t_1^2 \sigma_\Lambda^2} + n \log (2\pi (\sigma_N^2 + (1 - \alpha)^2 t_1^2 \sigma_\Lambda^2)) + n \frac{t_0^2}{t_1^2}. \end{aligned} \quad (29)$$

If  $t_0 \leq t_1$ , then  $\log (2\pi (\sigma_N^2 + (1 - \alpha)^2 t_0^2 \sigma_\Lambda^2)) \leq \log (2\pi (\sigma_N^2 + (1 - \alpha)^2 t_1^2 \sigma_\Lambda^2))$ ; additionally  $\frac{t^2 \sigma_\Lambda^2}{\sigma_N^2 + (1 - \alpha)^2 t^2 \sigma_\Lambda^2}$  is monotonically increasing with  $t$ , implying that

$$\frac{t_1^2 \sigma_\Lambda^2}{\sigma_N^2 + (1 - \alpha)^2 t_1^2 \sigma_\Lambda^2} \geq \frac{t_0^2 \sigma_\Lambda^2}{\sigma_N^2 + (1 - \alpha)^2 t_0^2 \sigma_\Lambda^2} > 1,$$

due to  $\text{TNLR} < 1$ . Therefore, at  $t = t_0$  the first term in (29) will be smaller than the second one, proving that  $t_{\text{lower}} < t_0$ . For the case  $t_0 > t_1$ , (28) can be applied.

### 6.3 Partially probabilistic approach

A close look at (5) allows us to see that the evaluation of both its second and third terms for different values of  $t$  is computationally cheap. Indeed, if we denote by  $M_t$  the number of values of  $t$  where the target function has to be evaluated, the associated computational cost will be  $O(n + M_t)$ . Nevertheless, this is not the case for the first term, where the computational cost is linearly increased with the product of the dimensionality of the problem and  $M_t$ , i.e.,  $O(n \cdot M_t)$ .

Taking this into account, it could make sense to characterize the target function by considering the computationally cheap second and third terms to be deterministic (taking advantage of the knowledge of  $\|\mathbf{z}\|^2$  available at the decoder), and the computationally expensive first term to be random, avoiding in this way the evaluation of the latter. Although the knowledge of  $\mathbf{z}$  at the decoder would allow to compute the exact value of the entire target function, this methodology statistically characterizes the output of the target function without explicitly computing its expensive first term, therefore providing a valuable tool for analyzing the target function output.

From a statistical point of view, one can justify the approach presented in this section by the asymptotic (when the number of observations goes to infinity and  $\text{HLR} \rightarrow \infty$ ) independence between  $\|\mathbf{Z}\|^2$ , and  $\|(\mathbf{Z} - t\mathbf{d})\text{mod}(t\Lambda)\|^2$ ; the approximate independence between these two terms has been already used in Sect. 3 for deriving  $f_{\mathbf{Z}|T, \mathbf{K}}(\mathbf{z}|t, \mathbf{d})$ .

Formally, we will characterize  $L(t, \mathbf{Z})$  as

$$L(t, \mathbf{Z}) = L_2(t, \mathbf{z}) + L_3(t, \mathbf{Z}),$$

where

$$L_3(t, \mathbf{Z}) = \frac{\|(\mathbf{Z} - t\mathbf{d})\text{mod}(t\Lambda)\|^2}{\sigma_N^2 + (1 - \alpha)^2 t^2 \sigma_\Lambda^2}.$$

Following this approach, it is straightforward to see that whenever  $\text{TNLR} < 1$ , the pdf of  $L_3(t, \mathbf{Z})$  for  $t = t_0$  would converge to  $f_{\chi_n^2}(x)$  when  $n \rightarrow \infty$  and good lattices are used, and will approximately follow that distribution when the last conditions do not hold (i.e., the low-dimensional lattice case), but  $\text{SCR} \rightarrow 0$  is verified; therefore,

$$\Pr(L(t, \mathbf{Z}) < L(t_1, \mathbf{z}) | t = t_0) = \int_{-\infty}^{L(t_1, \mathbf{z})} f_{\chi_n^2} \left( x - n \log \left[ 2\pi (\sigma_N^2 + (1 - \alpha)^2 t^2 \sigma_\Lambda^2) \right] - \frac{\|\mathbf{z}\|^2}{\sigma_X^2 t^2} \right) d\mathfrak{B}(0)$$

will not be monotonically decreasing with  $t$ , but will be null at  $t = 0$  and  $t \rightarrow \infty$ , and will have only one local maximum. This behavior is inherited from  $L_2(t, \mathbf{z})$ , defined at (22) and contained in the argument of  $f_{\chi_n^2}$  in (30). As it was proved in Sect. 6.2, the derivative of (22) with respect to  $t$  will be null for just a positive value of  $t$ , denoted by  $t_2$ . From this result, we can see that not only a lower-bound to the search interval can be found, calculated as the largest  $t \leq t_2$  such that the probability of  $L(t, \mathbf{Z})$  being smaller than  $L(t_1, \mathbf{z})$  for  $t = t_0$  is smaller than or equal to  $P_{e1}$ , i.e.,

$$t_{\text{lower}} = \underset{t: t \leq t_2, \Pr(L(t, \mathbf{Z}) < L(t_1, \mathbf{z}) | t = t_0) \leq P_{e1}}{\operatorname{argmax}} t,$$

but also an upper-bound to the mentioned interval, defined as

$$t_{\text{upper}} = \underset{t: t \geq t_2, \Pr(L(t, \mathbf{Z}) < L(t_1, \mathbf{z}) | t = t_0) \leq P_{e1}}{\operatorname{argmin}} t,$$

i.e., the smallest  $t \geq t_2$ , such that the probability of  $L(t, \mathbf{Z})$  being smaller than  $L(t_1, \mathbf{z})$  for  $t = t_0$  is smaller than or equal to  $P_{e1}$ .

As the analysis introduced in this section for the lower-bound is strongly related to the corresponding one for the upper-bound, we will jointly study both of them here, and Sect. 7.4 will just refer to the current section.

Whenever  $L(t_1, \mathbf{z}) - L_2(t_2, \mathbf{z}) \leq F_{\chi_n^2}^{-1}(P_{e1})$ , both the upper and lower-bound derived above will coincide and will be equal to  $t_2$ , i.e.,  $t_2$  is good enough for verifying the defined constraint, so the subsequent optimization using the search interval is not longer required. Indeed, in that case other points besides  $t_2$  might be feasible solutions to both the upper and lower-bounds definition problem; denoting those points by  $t_3$ , they are defined by  $L_2(t_3, \mathbf{z}) \geq L(t_1, \mathbf{z}) - F_{\chi_n^2}^{-1}(P_{e1})$ . In the extreme case where  $P_{e1} \rightarrow 0$ , the condition for the upper and lower-bound coinciding can be rewritten as

$$L_2(t_2, \mathbf{z}) \geq L(t_1, \mathbf{z}); \quad (31)$$

given that  $L(t_1, \mathbf{z}) \geq L_2(t_1, \mathbf{z})$ , with equality only if  $\|(\mathbf{z} - t\mathbf{d}) \bmod(t\Lambda)\|^2 = 0$ , and that  $L_2(t_1, \mathbf{z}) \geq L_2(t_2, \mathbf{z})$ , with equality only if  $t_1 = t_2$ , (31) will hold only when these two conditions are simultaneously verified.

Otherwise, the upper and lower-bound correspond to the two only solutions for  $t > 0$  to the equation

$$n \log \left[ 2\pi (\sigma_N^2 + (1 - \alpha)^2 t^2 \sigma_\Lambda^2) \right] + \frac{\|\mathbf{z}\|^2}{\sigma_X^2 t^2} + F_{\chi_n^2}^{-1}(P_{e1}) = L(t_1, \mathbf{z}). \quad (32)$$

It is worth pointing out the similarities between the last formula and (24); the only difference is the presence of  $F_{\chi_n^2}^{-1}(P_{e1})$  in (32), reflecting the relaxed nature of the lower-bound derived in this section (due to its probabilistic approach), in comparison with the deterministic strategy proposed in Sect. 6.2. Indeed, both formulas will be exactly the same whenever the probabilistic nature is removed from (32) by setting  $P_{e1} = 0$ .

To the best of the authors' knowledge closed formulas for the solutions to the previous equation are not available, although due to the discussed properties of  $L_2(t, \mathbf{z})$ , the numerical search of those solutions can be performed even using a dichotomy search algorithm.

Similarly to the analysis performed in Sect. 3.1, for values of  $n$  large enough one could use the CLT approximation for the pdf of  $L_3(t, \mathbf{Z})$ , obtaining a Gaussian distribution with mean

$$\mathbb{E}[L_3(t, \mathbf{Z})|t = t_0] = n,$$

and variance for the scalar quantizer case

$$\text{Var}[L_3(t, \mathbf{Z})|t = t_0] = n \left[ \frac{\frac{144(1-\alpha)^4 t^4 \sigma_\Lambda^4}{180} + 2\sigma_N^4 + 4(1-\alpha)^2 t^2 \sigma_\Lambda^2 \sigma_N^2}{(\sigma_N^2 + (1-\alpha)^2 t^2 \sigma_\Lambda^2)^2} \right],$$

while the variance for the high-dimensional good lattice quantizer case is

$$\text{Var}[L_3(t, \mathbf{Z})|t = t_0] = 2n;$$

replacing these mean and variance by the asymptotic values achieved by considering  $\text{SCR} \rightarrow 0$  in the scalar quantizer case and taking the exact values when the high-dimensional good lattice quantizer case is considered, (32) can be approximated by

$$n \log \left[ 2\pi (\sigma_N^2 + (1-\alpha)^2 t^2 \sigma_\Lambda^2) \right] + \frac{\|\mathbf{z}\|^2}{\sigma_X^2 t^2} + n - \sqrt{2n} Q^{-1}(P_{e1}) = L(t_1, \mathbf{z}).$$

In Fig. 2 we can see how the bounds derived by using the approach proposed in this section are a relaxed version of those obtained by using the deterministic method proposed in Sects. 6.2 and 7.1. Specifically, the larger  $P_{e1}$ , the smaller the obtained search interval.

### 6.3.1 Asymptotic values when the number of observations goes to infinity

Similarly to the previous section, here we will analyze the asymptotic behavior of the search interval bounds when the number of considered observations goes to infinity. In order to do that, we will consider the asymptotic values of  $L(t_1, \mathbf{z})$  when  $n \rightarrow \infty$ , both for  $t_1 \approx t_0$ , and when  $t_1$  is not close to  $t_0$  (both situations are quantitatively described in Sect. 3.4), given by (13) and (14), respectively.

Note that in this case (32) is still valid, but one must consider that  $F_{\chi_n^2}^{-1}(P_{e1})$  will go 0 if  $P_{e1} = 0$ , and will go to  $n$  if  $P_{e1} > 0$  (assuming  $P_{e1}$  to be independent of  $n$ ).

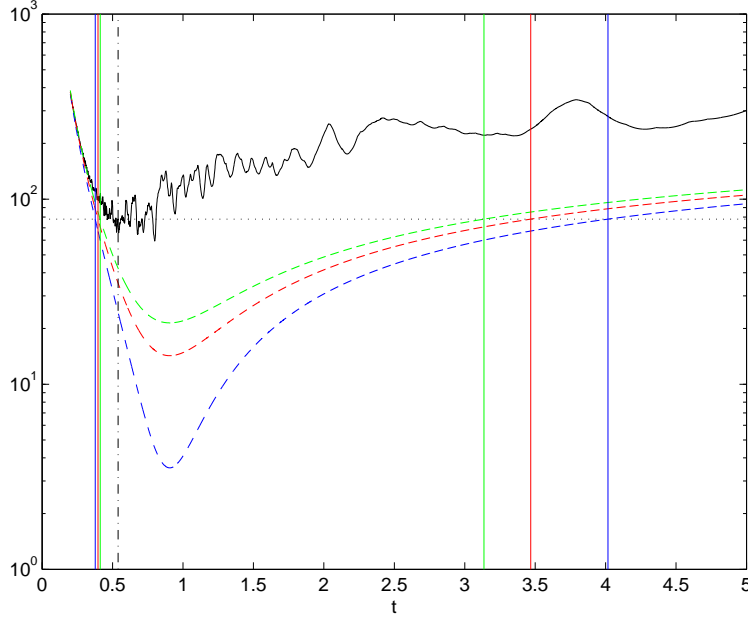


Figure 2: Comparison between  $L(t, \mathbf{z})$  (solid black line),  $L(t_1, \mathbf{z})$  (dotted black line),  $L_2(t, \mathbf{z})$  (dashed blue line), and the left term of (32) for  $P_{e1} = 10^{-6}$  (dashed red line), and  $P_{e1} = 10^{-3}$  (dashed green line). The corresponding search interval bounds are plotted by using vertical solid lines with the same color that the function used for computing them.  $t_1$  (vertical dash-dot black line) calculated by using (16). HLR  $\approx 34.9765$  dB, SCR  $\approx -1.0618$  dB, TNLN  $\approx -3.5736$  dB,  $t_0 = 0.8$ ,  $\alpha = \alpha_{\text{Costa}} \approx 0.5608$ ,  $n = 40$ , scalar quantizer.

If  $P_{e1} = 0$ , we have exactly the deterministic version of the problem already studied in Sect. 6.2.1 (the upper-bound will be studied in Sect. 7.1.1).

For  $P_{e1} > 0$ , we will separately study the cases  $t_1 \approx t_0$  and  $t_1$  not close to  $t_0$ .

- $t_1 \approx t_0$

Whenever  $t_1 \approx t_0$  the upper and lower-bounds to the search interval will be the solutions to

$$\frac{(t_0 - t_1)^2 \sigma_X^2}{\sigma_N^2 + (1 - \alpha)^2 t_1^2 \sigma_\Lambda^2} + 1 - \frac{t_0^2}{t^2} + \log \left( \frac{\sigma_N^2 + (1 - \alpha)^2 t_1^2 \sigma_\Lambda^2}{\sigma_N^2 + (1 - \alpha)^2 t^2 \sigma_\Lambda^2} \right) = 0. \quad (33)$$

Although a closed solution to the last equation does not exist, one wonders if  $t_0$  will be always contained in the interval defined by the solutions to that equation. In order to solve this question we will take into account that the left side of (33) goes to  $-\infty$  both when  $t \rightarrow 0$  and  $t \rightarrow \infty$ ; therefore, a necessary and sufficient condition for  $t_0$  to be included in the resulting search interval is that the result of evaluating (33) at  $t = t_0$ , i.e.,

$$\frac{(t_0 - t_1)^2 \sigma_X^2}{\sigma_N^2 + (1 - \alpha)^2 t_1^2 \sigma_\Lambda^2} + \log \left( \frac{\sigma_N^2 + (1 - \alpha)^2 t_1^2 \sigma_\Lambda^2}{\sigma_N^2 + (1 - \alpha)^2 t_0^2 \sigma_\Lambda^2} \right), \quad (34)$$

should be non-negative for the considered  $t_1$ . This is obviously the case for  $t_1 \geq t_0$ , confirming that in this scenario  $t_0$  is contained in the search interval; in particular, for  $t_1 = t_0$  (34) is null.

In order to study the case  $t_1 < t_0$  we will take into account that the derivative of (34) with respect to  $t_1$  is given by

$$\frac{2 \left[ -\sigma_N^2 \sigma_X^2 t_0 + \sigma_N^2 \left( (1-\alpha)^2 \sigma_\Lambda^2 + \sigma_X^2 \right) t_1 + (1-\alpha)^2 \sigma_\Lambda^2 t_1 \left( (1-\alpha)^2 \sigma_\Lambda^2 t_1^2 + \sigma_X^2 t_0 (t_1 - t_0) \right) \right]}{\left[ \sigma_N^2 + (1-\alpha)^2 t_1^2 \sigma_\Lambda^2 \right]^2}.$$

The numerator of the last formula can be written like  $a_0 + a_1 t_1 + a_2 t_1^2 + a_3 t_1^3$ , where

$$\begin{aligned} a_0 &= -2\sigma_N^2 \sigma_X^2 t_0, \\ a_1 &= 2 \left[ \sigma_N^2 \sigma_X^2 + (1-\alpha)^2 \sigma_\Lambda^2 (\sigma_N^2 - \sigma_X^2 t_0^2) \right], \\ a_2 &= 2(1-\alpha)^2 t_0 \sigma_\Lambda^2 \sigma_X^2, \\ a_3 &= 2(1-\alpha)^4 \sigma_\Lambda^4, \end{aligned}$$

proving, using Descartes' sign rule, that the derivative of (34) will be null for at most a positive  $t_1$ . Additionally if that derivative is evaluated at  $t_1 = t_0$ , the result is

$$\frac{2(1-\alpha)^2 \sigma_\Lambda^2 t_0}{\sigma_N^2 + (1-\alpha)^2 t_0^2 \sigma_\Lambda^2},$$

proving that there exists an interval, open in its upper-bound  $t_0$ , such that (34) is negative for the values of  $t_1$  contained in it. Consequently, the question to be answered is how large that interval is.

If one evaluates (34) at

$$t_1 = t_0 - \sqrt{\frac{\sigma_N^2 + (1-\alpha)^2 t_0^2 \sigma_\Lambda^2}{\sigma_X^2}}, \quad (35)$$

the result can be written like  $\log(x_1) + \frac{1}{x_1}$ , where

$$x_1 = \frac{\sigma_N^2 + (1-\alpha)^2 \sigma_\Lambda^2 \left( t_0 - \sqrt{\frac{\sigma_N^2 + (1-\alpha)^2 t_0^2 \sigma_\Lambda^2}{\sigma_X^2}} \right)^2}{\sigma_N^2 + (1-\alpha)^2 t_0^2 \sigma_\Lambda^2}.$$

Thus, given that  $x_1 \geq 0$ , the result in App. A proves that (34) evaluated at the right hand of (35) is non-negative. Furthermore, whenever  $\text{HLR} \rightarrow \infty$ , the right term in (35) asymptotically goes to  $t_0$ , proving that whenever  $\text{HLR} \rightarrow \infty$ , the interval where (34) takes negative values is asymptotically small.

Therefore, whenever  $\text{HLR} \rightarrow \infty$ ,  $t_0$  will be contained in or will be asymptotically close to the search interval, irrespectively of  $t_1$ .

Additionally, one can conclude that for  $t_1 = t_0$ , (33) will have a single solution corresponding to  $t = t_0$ .

Fig. 3 illustrates the conclusions derived for the case  $t_1 \approx t_0$ .

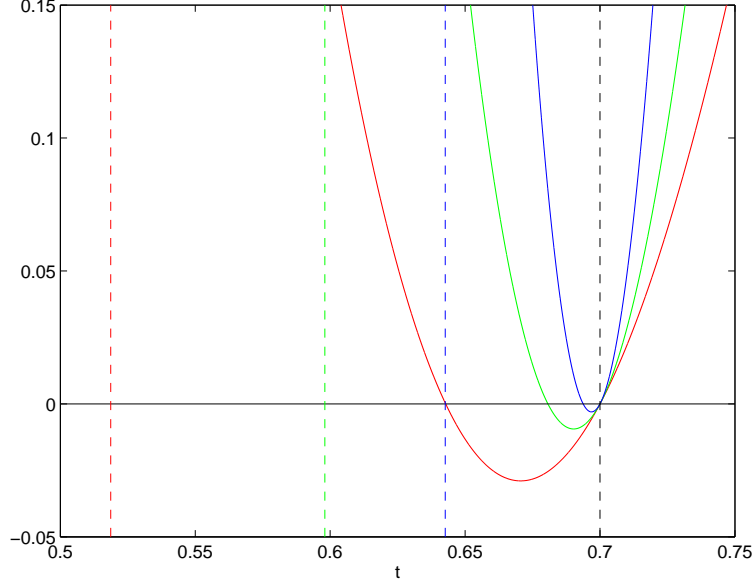


Figure 3: Comparison of (34) for different values of HLR (red 10 dB, green 15 dB, blue 20 dB).  $\text{SCR} \approx 3.0980$  dB,  $\text{TNLR} \approx -1.7319$  dB,  $t_0 = 0.7$ ,  $\alpha = \alpha_{\text{Costa}} \approx 0.3289$ . The vertical colored dashed lines stand for the values of  $t_1$  derived by using (35), illustrating that they converge to  $t_0$  (vertical black dashed line) as  $\text{HLR} \rightarrow \infty$ .

- $t_1$  not close to  $t_0$

On the other hand, for the case where  $t_1$  is not close to  $t_0$ , one will look for two solutions to

$$\frac{t_0^2}{t_1^2} - \frac{t_0^2}{t^2} - 1 + \frac{t_1^2 \sigma_\Lambda^2}{\sigma_N^2 + (1 - \alpha)^2 t_1^2 \sigma_\Lambda^2} + \log \left( \frac{\sigma_N^2 + (1 - \alpha)^2 t_1^2 \sigma_\Lambda^2}{\sigma_N^2 + (1 - \alpha)^2 t^2 \sigma_\Lambda^2} \right) = 0. \quad (36)$$

Similarly to the case  $t_1 \approx t_0$ , the left-hand side of the previous equation will go to  $-\infty$  as  $t \rightarrow 0$  and  $t \rightarrow \infty$ . Therefore, for  $t_0$  to be contained in the search interval, (36) evaluated at  $t = t_0$ , i.e.,

$$f(t_1, \sigma_\Lambda^2) \triangleq \frac{t_0^2}{t_1^2} - 2 + \frac{t_1^2 \sigma_\Lambda^2}{\sigma_N^2 + (1 - \alpha)^2 t_1^2 \sigma_\Lambda^2} + \log \left( \frac{\sigma_N^2 + (1 - \alpha)^2 t_1^2 \sigma_\Lambda^2}{\sigma_N^2 + (1 - \alpha)^2 t_0^2 \sigma_\Lambda^2} \right) \quad (37)$$

should be non-negative.

In order to prove that this is the case, we will find useful to define

$$\sigma_{\Lambda_0}^2 \triangleq \frac{\sigma_N^2}{t_0^2 [1 - (1 - \alpha)^2]},$$

where

$$t_0^2 \sigma_{\Lambda_0}^2 = \sigma_N^2 + (1 - \alpha)^2 t_0^2 \sigma_{\Lambda_0}^2,$$

i.e., the threshold of the **relaxed version of Hypothesis 3** (TNLR = 1) is achieved.

The proof is splitted in the next steps:

1. Prove that

$$\frac{\partial f(t_1, \sigma_{\Lambda_0}^2)}{\partial t_1} \begin{cases} = 0, & \text{if } t_1 = t_0 \\ \neq 0, & \text{otherwise} \end{cases},$$

and

$$\begin{aligned} f(t_0, \sigma_{\Lambda_0}^2) &= 0, \\ f(t_1, \sigma_{\Lambda_0}^2) &> 0, t_1 \neq t_0. \end{aligned}$$

**Proof**

$$f(t_1, \sigma_{\Lambda_0}^2) = \frac{t_0^2}{t_1^2} - 2 + \frac{t_1^2}{t_1^2 + \alpha(\alpha - 2)(t_1^2 - t_0^2)} + \log \left( \alpha(2 - \alpha) + \frac{(1 - \alpha)^2 t_1^2}{t_0^2} \right) \quad (38)$$

which is obviously null at  $t_1 = t_0$ . Additionally, the derivative of the last formula with respect to  $t_1$  is

$$\frac{-2(\alpha - 2)^2 \alpha^2 t_0^6 - 4(2 - \alpha)(1 - \alpha)^2 \alpha t_0^4 t_1^2 - 2[1 - 2(2 - \alpha)\alpha(2 - (2 - \alpha)\alpha)] t_0^2 t_1^4 + 2(1 - \alpha)^4 t_0^6}{t_1^3 (t_1^2 - (2 - \alpha)\alpha(t_1^2 - t_0^2))^2} \quad (39)$$

whose numerator can be written like  $a_0 + a_1 t_1^2 + a_2 t_1^4 + a_3 t_1^6$ , where

$$\begin{aligned} a_0 &= -2(\alpha - 2)^2 \alpha^2 t_0^6, \\ a_1 &= -4(2 - \alpha)(1 - \alpha)^2 \alpha t_0^4, \\ a_2 &= -2[1 - 2(2 - \alpha)\alpha(2 - (2 - \alpha)\alpha)] t_0^2, \text{ and} \\ a_3 &= 2(1 - \alpha)^4. \end{aligned}$$

Using Descartes' sign rule, it is evident that (39) will be null just for at most a positive  $t_1$ , which can be shown to be  $t_0$  just by replacing  $t_1$  by  $t_0$  in (39). Given that (38) goes to infinity when  $t_1 \rightarrow 0$  and  $t_1 \rightarrow \infty$ , Step 1 is proved.

Fig. 4 illustrates Step 1.

2. Let us define

$$\xi_1 \triangleq \sqrt{\frac{(1 - \alpha)^2 t_0^2}{1 + (1 - \alpha)^2}}.$$

For each  $t_1 \leq \xi_1$ , there exists a single  $\sigma_{t_1}^2 \geq 0$  such that

$$\left. \frac{\partial f(t_1, \sigma_{\Lambda}^2)}{\partial \sigma_{\Lambda}^2} \right|_{(t_1, \sigma_{t_1}^2)} = 0.$$

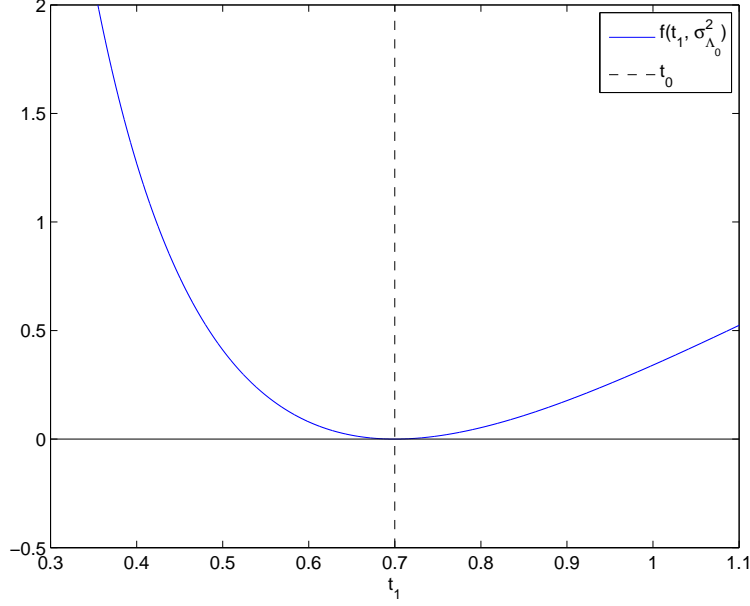


Figure 4:  $f(t_1, \sigma_{\Lambda_0}^2)$  as a function of  $t_1$ .  $\sigma_N^2 = 1$ ,  $\alpha = 0.5$ ,  $t_0 = 0.7$ .

Additionally, in that case

$$\left. \frac{\partial^2 f(t_1, \sigma_{\Lambda}^2)}{(\partial \sigma_{\Lambda}^2)^2} \right|_{(t_1, \sigma_{\Lambda}^2)} > 0.$$

If  $t_1 > \xi_1$ , then

$$\left. \frac{\partial f(t_1, \sigma_{\Lambda}^2)}{\partial \sigma_{\Lambda}^2} \right|_{(t_1, \sigma^2)} > 0, \text{ for any } \sigma^2 \geq 0.$$

**Proof**

$$\begin{aligned} \frac{\partial f(t_1, \sigma_{\Lambda}^2)}{\partial \sigma_{\Lambda}^2} &= \sigma_N^2 \left[ -(1-\alpha)^2 \sigma_N^2 t_0^2 + \left(1 + (1-\alpha)^2\right) \sigma_N^2 t_1^2 + (1-\alpha)^2 \sigma_{\Lambda}^2 t_1^2 \left( (2-\alpha)\alpha(t_0^2 - t_1^2) + t_1^2 \right) \right] \\ &\quad \left[ \left( \sigma_N^2 + (1-\alpha)^2 t_0^2 \sigma_{\Lambda}^2 \right) \left( \sigma_N^2 + (1-\alpha)^2 t_1^2 \sigma_{\Lambda}^2 \right) \right]^{-1}. \end{aligned}$$

It is easy to see that the last formula nullifies just when

$$\sigma_{\Lambda}^2 = \sigma_{t_1}^2 \triangleq \frac{\sigma_N^2 \left[ (1-\alpha)^2 t_0^2 - \left(1 + (1-\alpha)^2\right) t_1^2 \right]}{(1-\alpha)^2 t_1^2 \left( (2-\alpha)\alpha(t_0^2 - t_1^2) + t_1^2 \right)},$$

which is non-negative (therefore providing a valid variance value) if and only if  $t_1 \leq \xi_1$  (indeed,  $\sigma_{\xi_1}^2 = 0$ ); in any case,

$$\left. \frac{\partial^2 f(t_1, \sigma_{\Lambda}^2)}{(\partial \sigma_{\Lambda}^2)^2} \right|_{(t_1, \sigma_{t_1}^2)} = \frac{t_1^4 \left( 2\alpha(t_0^2 - t_1^2) + t_1^2 + \alpha^2(t_1^2 - t_0^2) \right)^4}{\sigma_N^4 (t_0^2 - t_1^2)^4},$$



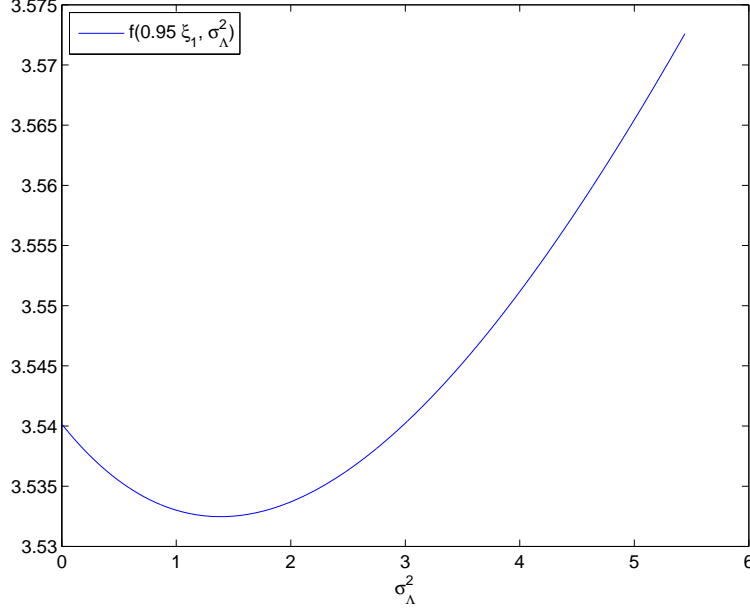


Figure 5:  $f(t_1, \sigma_\Lambda^2)$  as a function of  $\sigma_\Lambda^2$ .  $\sigma_N^2 = 1$ ,  $\alpha = 0.5$ ,  $t_0 = 0.7$ ,  $t_1 = 0.95\xi_1$ .

proving that for each  $t_1 \leq \xi_1$ , the curve  $f(t_1, \sigma_\Lambda^2)$  has a minimum at  $\sigma_\Lambda^2 = \sigma_{t_1}^2 \geq 0$ , and that for  $t_1 > \xi_1$ ,  $\left. \frac{\partial f(t_1, \sigma_\Lambda^2)}{\partial \sigma_\Lambda^2} \right|_{(t_1, \sigma^2)} > 0$ , for any  $\sigma^2 \geq 0$ .

Figs. 5, 6, and 7 illustrate Step 2 for the cases  $t_1 < \xi_1$ ,  $t_1 = \xi_1$  and  $t_1 > \xi_1$ , respectively.

3. Prove that

$$\frac{\partial (\sigma_{t_1}^2)}{\partial t_1} \leq 0, \quad \forall t_1 \in [0, t_0];$$

additionally  $\sigma_{t_1}^2|_{t_1=0} = \infty$ , and  $\sigma_{t_1}^2|_{t_1=\xi_1} = 0$ .

**Proof**

$$\frac{\partial (\sigma_{t_1}^2)}{\partial (t_1^2)} = \frac{\sigma_N^2 [(-2 + \alpha) \alpha (t_0^2 - t_1^2) - 2t_1^2] (t_0^2 - t_1^2)}{t_1^4 ((2 - \alpha) \alpha (t_0^2 - t_1^2) + t_1^2)^2}, \quad (40)$$

has 4 roots on  $t_1$ , located at  $\pm t_0$  and

$$\pm \sqrt{\frac{-(2 - \alpha) \alpha t_0^2}{1 + (1 - \alpha)^2}}.$$

Given that the last two are imaginary, the only real non-negative root is that located at  $t_0$ . Therefore, (40) will have the same sign for any  $t_1 \in [0, t_0]$ . Given that

$$\lim_{t_1 \rightarrow 0} \frac{\partial (\sigma_{t_1}^2)}{\partial (t_1^2)} = -\infty,$$

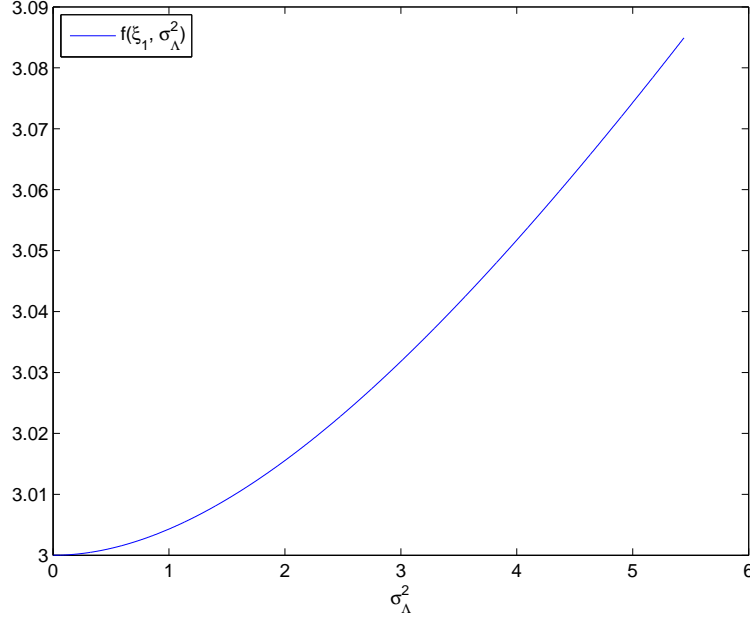


Figure 6:  $f(t_1, \sigma_\Lambda^2)$  as a function of  $\sigma_\Lambda^2$ .  $\sigma_N^2 = 1$ ,  $\alpha = 0.5$ ,  $t_0 = 0.7$ ,  $t_1 = \xi_1$ .

it is straightforward that

$$\frac{\partial (\sigma_{t_1}^2)}{\partial (t_1^2)} \leq 0, \quad \forall t_1 \in [0, t_0],$$

so

$$\frac{\partial (\sigma_{t_1}^2)}{\partial t_1} \leq 0, \quad \forall t_1 \in [0, t_0].$$

4. Due to Step 3, it is possible to uniquely define  $\xi_2 \triangleq \arg_{t_1: \sigma_{t_1}^2 = \sigma_{\Lambda_0}^2}$ .
5. Prove that  $\xi_2 \leq \xi_1 \leq t_0$ .

**Proof**

At the sight of the definition of  $\xi_1$  it is obvious that  $\xi_1 \leq t_0$ . On the other hand, based on the monotonically decreasing nature of  $\sigma_{t_1}^2$  with  $t_1$  proved at Step 3, and the fact that  $\sigma_{\xi_1}^2 = 0$  and  $\sigma_{\xi_2}^2 = \sigma_{\Lambda_0}^2$ , it is straightforward that  $\xi_2 \leq \xi_1$ .

Steps 3, 4, and 5 are illustrated in Fig. 8.

6. Prove that if  $t_1 \geq \xi_2$ , then

$$\left. \frac{\partial f(t_1, \sigma_\Lambda^2)}{\partial \sigma_\Lambda^2} \right|_{(t_1, \sigma^2)} \geq 0, \quad \text{for any } \sigma^2 \geq \sigma_{\Lambda_0}^2.$$

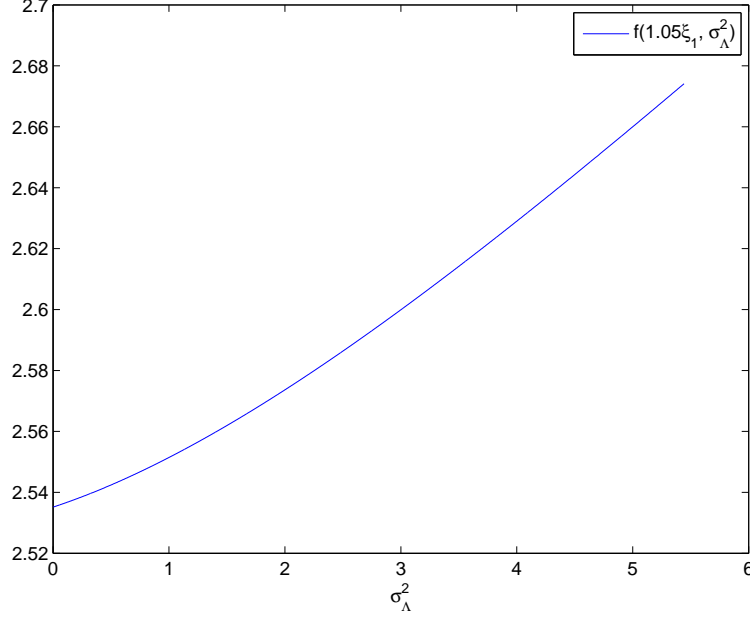


Figure 7:  $f(t_1, \sigma_\Lambda^2)$  as a function of  $\sigma_\Lambda^2$ .  $\sigma_N^2 = 1$ ,  $\alpha = 0.5$ ,  $t_0 = 0.7$ ,  $t_1 = 1.05\xi_1$ .

**Proof**

From Step 2, it is clear that the former statement is true for  $t_1 > \xi_1$ . From Steps 2, 3 and 4, for  $\xi_2 \leq t_1 \leq \xi_1$ ,  $\sigma_{t_1}^2 \in [0, \sigma_{\Lambda_0}^2]$ ; also from Step 2

$$\left. \frac{\partial^2 f(t_1, \sigma_\Lambda^2)}{(\partial \sigma_\Lambda^2)^2} \right|_{(t_1, \sigma_{t_1}^2)} > 0,$$

which jointly with the fact that for a particular  $t_1$  the derivative nullifies just at  $\sigma_{t_1}^2$  implies that for any  $t_1 \in [\xi_2, \xi_1]$ , then

$$\left. \frac{\partial f(t_1, \sigma_\Lambda^2)}{\partial \sigma_\Lambda^2} \right|_{(t_1, \sigma^2)} \geq 0, \text{ for any } \sigma^2 \geq \sigma_{\Lambda_0}^2.$$

7. Prove that

$$f(t_1, \sigma_\Lambda^2) \geq 0, \quad \forall t_1 \geq \xi_2, \forall \sigma_\Lambda^2 \geq \sigma_{\Lambda_0}^2.$$

**Proof**

This result comes from the combination of Step 1, as  $f(t_1, \sigma_{\Lambda_0}^2) \geq 0$ , and Step 6, as for all  $t_1 \geq \xi_2$

$$\left. \frac{\partial f(t_1, \sigma_\Lambda^2)}{\partial \sigma_\Lambda^2} \right|_{(t_1, \sigma^2)} \geq 0, \quad \forall \sigma^2 \geq \sigma_{\Lambda_0}^2.$$

8. Prove that

$$f(t_1, \sigma_\Lambda^2) \geq 0, \quad \forall t_1 \in [0, \xi_2], \forall \sigma_\Lambda^2 \geq 0.$$

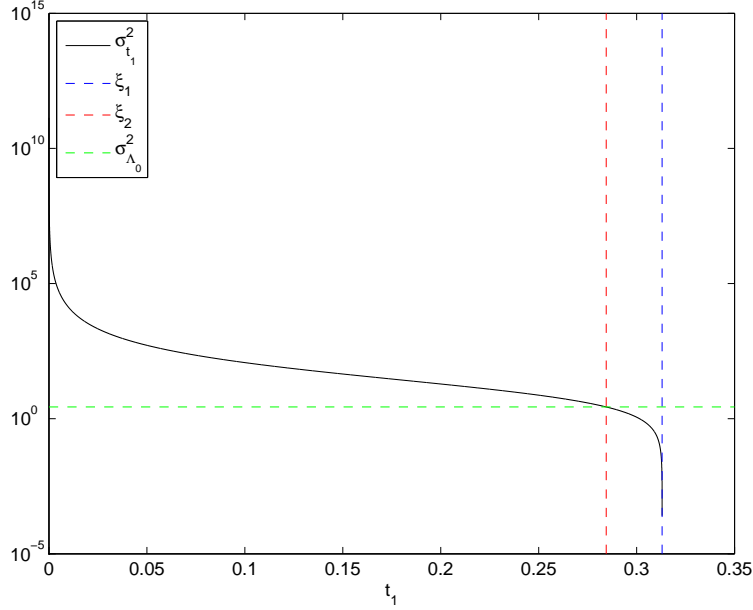


Figure 8:  $\sigma_{t_1}^2$  as a function of  $t_1$ .  $\sigma_N^2 = 1$ ,  $\alpha = 0.5$ ,  $t_0 = 0.7$ . Furthermore, one can check that  $\sigma_{t_1}^2|_{t_1=0} = \infty$ ,  $\sigma_{t_1}^2|_{t_1=\xi_1} = 0$ , and  $\sigma_{t_1}^2|_{t_1=\xi_2} = \sigma_{\Lambda_0}^2$ .

**Proof**

For all  $t_1 \leq \xi_1$  we have that  $\sigma_{t_1}^2 \geq 0$ , i.e., it is well defined as a variance. Therefore, in that scenario we can define

$$g(t_1) \triangleq f(t_1, \sigma_{t_1}^2),$$

verifying that

$$g(t_1) = \min_{\sigma^2 \geq 0} f(t_1, \sigma^2).$$

On the other hand, the derivative of  $g(t_1)$  with respect to  $t_1^2$  is

$$\frac{\partial g(t_1)}{\partial(t_1^2)} = \frac{-t_0^2}{(1-\alpha)^2(t_0^2 - t_1^2)^2} + \frac{1}{t_0^2 - t_1^2} - \frac{t_0^2}{t_1^4} + \frac{1}{t_1^2},$$

which is null just at

$$t_1 = \pm \sqrt{\frac{-(1-\alpha) \left( -3(1-\alpha) \pm \sqrt{(\alpha-3)(1+\alpha)} \right) t_0^2}{6 - 4(2-\alpha)\alpha}}.$$

Given that the 4 roots are complex, the derivative will take the same sign in all  $t_1 \geq 0$ . In particular,

$$\lim_{t_1 \rightarrow 0} \frac{\partial g(t_1)}{\partial(t_1^2)} = -\infty,$$

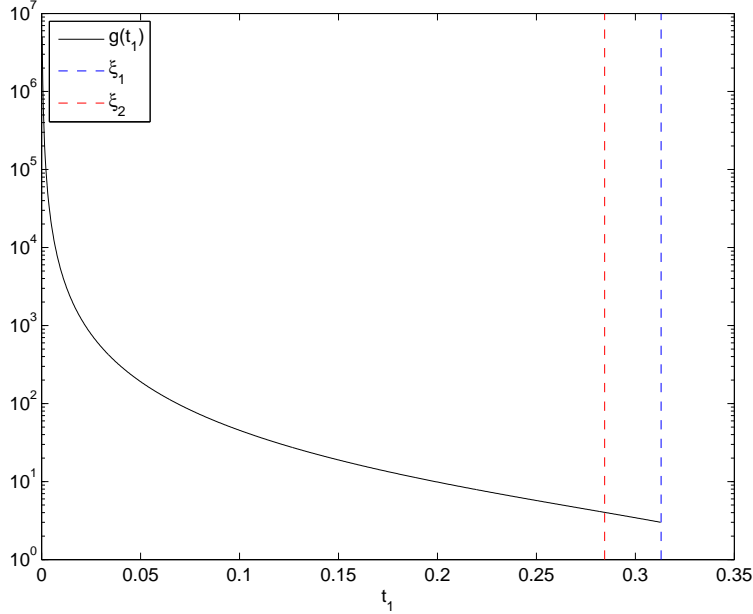


Figure 9:  $g(t_1)$ .  $\sigma_N^2 = 1$ ,  $\alpha = 0.5$ ,  $t_0 = 0.7$ .

proving that  $g(t_1)$  is monotonically decreasing with  $t_1$  in  $[0, \xi_1]$ . Finally, from the definition of  $g(\cdot)$ , the definition of  $\xi_2$ , and Step 7, one obtains that

$$g(\xi_2) = f(\xi_2, \sigma_{\xi_2}^2) = f(\xi_2, \sigma_{\Lambda_0}^2) \geq 0.$$

Step 8 is illustrated in Fig. 9.

#### 6.4 Search interval lower-bound calculated from the variance-based estimator

The previous strategies for defining the search interval lower-bound are based on characteristics of the target function  $L(t, \mathbf{z})$ , so they are valid for any initial estimator  $t_1$ . Nevertheless, a different approach for defining the search interval could be based on the statistical characterization of the variance-based estimator when this were used. In this section we will exploit some of the results derived in Sect. 5.2 for obtaining a lower-bound of the search interval. Given that throughout this report we are assuming the scaling factor to be real, we will use the estimators and pdfs derived in Sect. 5.2.2; additionally, as the probability of the upper tail of a Gaussian with mean and variance those of  $\hat{T}_{\text{var}}(\mathbf{Z})$  is not monotonically increasing with  $t_0$ ,  $\hat{T}_{\text{var}}^2(\mathbf{Z})$ , proposed in (19) and whose pdf was studied in (21), will be used.

Taking these considerations into account, one choice for defining  $t_{\text{lower}}$  could be

$$t_{\text{lower}} = \sqrt{\operatorname{argmax}_{t^2: t^2 \geq 0, \Pr(\hat{T}_{\text{var}}^2 = t_1^2 | t_0^2 \leq t^2) \leq P_{e1}} t^2},$$

i.e., the largest  $t$  such that the probability of obtaining the considered variance-based estimator when the real scaling factor is smaller than or equal to  $t$ , is smaller than or equal to  $P_{e1}$ . Nevertheless, given that the pdf we have access to is  $f_{\hat{T}^2_{\text{var}}|T_0^2}$ , no having knowledge about  $f_{\hat{T}^2_{\text{var}}}$  or  $f_{T_0}$ , the probability in the constraint of the last formula can not be evaluated and a different strategy must be followed. In that sense, we propose to use

$$t_{\text{lower}} = \sqrt{\operatorname{argmax}_{t^2: t^2 \geq 0, \forall (t')^2 \leq t^2, \Pr(\hat{T}^2_{\text{var}} \geq t_1^2 | t_0^2 = (t')^2) \leq P_{e1}} t^2}, \quad (41)$$

which is nothing but the largest  $t$  such that for every  $(t')^2 \leq t^2$ , if the square real scaling factor is  $(t')^2$ , then the probability of obtaining a variance-based estimator larger than or equal to  $t_1$ , is smaller than or equal to  $P_{e1}$ .

It is important to note that whenever  $P_{e1} < 0.5$ ,  $t_{\text{lower}} < t_1$ , so one might just consider the corresponding interval in the optimizations described in (41).

Based on (21), the probability in (41) can be calculated as

$$\Pr(\hat{T}^2_{\text{var}} \geq t_1^2 | t_0^2) \approx \int_{t_1^2}^{\infty} \frac{e^{-\frac{n(\sigma_X^2 + \alpha^2 \sigma_\Lambda^2)^2 (\tau - t_0^2)^2}{4[(\sigma_X^2 + \alpha^2 \sigma_\Lambda^2)t_0^2 + \sigma_N^2]^2}}}{\sqrt{\frac{4\pi[(\sigma_X^2 + \alpha^2 \sigma_\Lambda^2)t_0^2 + \sigma_N^2]^2}{n(\sigma_X^2 + \alpha^2 \sigma_\Lambda^2)^2}}} d\tau = Q\left(\frac{t_1^2 - t_0^2}{\sqrt{\frac{2[(\sigma_X^2 + \alpha^2 \sigma_\Lambda^2)t_0^2 + \sigma_N^2]^2}{n(\sigma_X^2 + \alpha^2 \sigma_\Lambda^2)^2}}}\right) \quad (42)$$

Given that  $Q(x)$  is monotonically decreasing with  $x$ , we will prove that its argument in (42) is also monotonically decreasing with  $t_0^2$  in order to show that (41) has, at most, a single solution. Indeed,

$$\frac{\partial}{\partial t_0^2} \left( \frac{t_1^2 - t_0^2}{\sqrt{\frac{2[(\sigma_X^2 + \alpha^2 \sigma_\Lambda^2)t_0^2 + \sigma_N^2]^2}{n(\sigma_X^2 + \alpha^2 \sigma_\Lambda^2)^2}}} \right) = \frac{-\sqrt{n}((\sigma_X^2 + \alpha^2 \sigma_\Lambda^2)t_1^2 + \sigma_N^2)\sigma_X^2}{\sqrt{2}((\sigma_X^2 + \alpha^2 \sigma_\Lambda^2)t_0^2 + \sigma_N^2)^2}.$$

Therefore, based on  $\Pr(\hat{T}^2_{\text{var}} \geq t_1^2 | t_0^2)$  being monotonically increasing with  $t_0^2$ , (41) is equivalent to

$$t_{\text{lower}} = \operatorname{argmax}_{t: \Pr(\hat{T}^2_{\text{var}} \geq t_1^2 | t_0^2 = t^2) \leq P_{e1}} t.$$

Note that the minimum value of  $P_{e1}$  one would expect to obtain is

$$Q\left(\sqrt{\frac{n}{2}} \frac{t_1^2(\sigma_X^2 + \alpha^2 \sigma_\Lambda^2)}{\sigma_N^2}\right), \quad (43)$$

as  $t_0^2 \geq 0$ . A smaller value can not be obtained by the followed approach due to the same reasons exposed at Sect. 5.2.2. Nevertheless, in order to achieve a trade-off between simplicity and accuracy we will pursue the current approximation. In any case, it is worth pointing out that whenever the number of dimensions is very large (as it was assumed at the derivation of the used

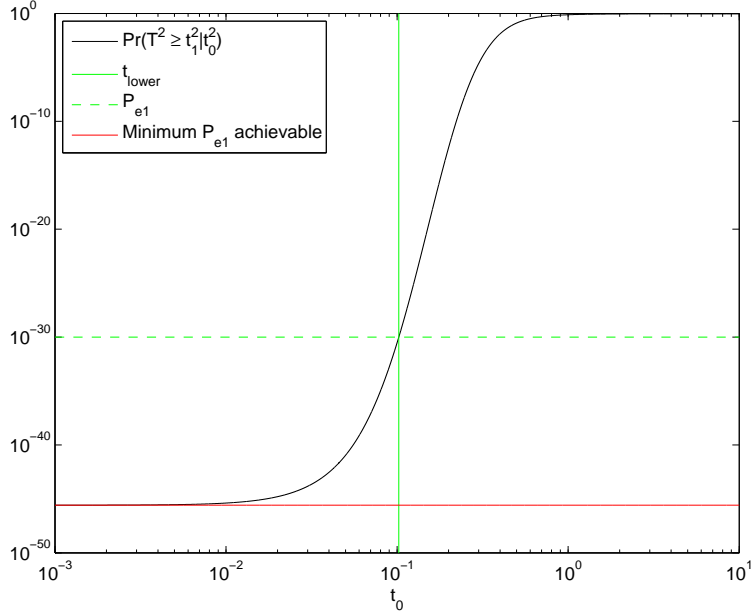


Figure 10:  $\Pr\left(\hat{T}_{\text{var}}^2 \geq t_1^2 | t_0^2\right)$ , (43), and  $t_{\text{lower}}$ . HLR = 10 dB, WNR = -3 dB,  $t_1 = 0.7$ ,  $\alpha = 0.5$ ,  $n = 4$ ,  $P_{e1} = 10^{-30}$ . In this case we use the WNR instead of the SCR and TNLR as the latter quantities depend on  $t_0$ , while the WNR does not depend on it.

approximation), HLR  $\rightarrow \infty$ , and TNLR  $< 1$ , the problem of (42) being lower-bounded by (43) can be dismissed, as the argument of (42) is proportional to  $\sqrt{n}$  and  $(\sigma_X^2 + \alpha^2 \sigma_\Lambda^2) / \sigma_N^2$ , so (43) goes to 0.

Denoting by  $\xi = Q^{-1}(P_{e1})$ , and assuming that  $P_{e1}$  is larger than or equal to (43), the mentioned unique solution is

$$t_{\text{lower}}^2 = \left[ \frac{2\xi^2 \sigma_N^2 + n(\sigma_X^2 + \alpha^2 \sigma_\Lambda^2)t_1^2 - \sqrt{2n}\xi[(\sigma_X^2 + \alpha^2 \sigma_\Lambda^2)t_1^2 + \sigma_N^2]}{(n - 2\xi^2)(\sigma_X^2 + \alpha^2 \sigma_\Lambda^2)} \right]^+.$$

The probability studied at (42), the lower-bound on it derived in (43), and the value of  $t_{\text{lower}}$  obtained in the last formula are illustrated in Fig. 10.

The upper-bound counterpart of this method can be found in Sect. 7.5.

## 7 Search interval upper-bound

### 7.1 Deterministic approach I

As it was proved in Sect. 6.2,  $L_2(t, \mathbf{z})$  first derivative with respect to  $t^2$  has a single positive root at  $t_2$ , corresponding to a global minimum. Consequently, an upper-bound to the search interval can be calculated similarly to (23), specifically as the smallest  $t \geq t_2$  such that the value of  $L_2(t, \mathbf{z})$  is larger than or equal

to  $L(t_1, \mathbf{z})$ , i.e.,

$$t_{\text{upper}} = \underset{t \geq t_2, L_2(t, \mathbf{z}) \geq L(t_1, \mathbf{z})}{\operatorname{argmin}} t, \quad (44)$$

which due to the strictly monotonically increasing nature of  $L_2(t, \mathbf{z})$  for  $t > t_2$ , and that for  $t \rightarrow \infty$ ,  $L_2(t, \mathbf{z}) \rightarrow \infty$ , will be well-defined. Similarly to Sect. 6.2,  $t_{\text{upper}}$  will verify  $L_2(t_{\text{upper}}, \mathbf{z}) = L(t_1, \mathbf{z})$ , although in this case we will focus on the study of the solutions for  $t \geq t_2$  to (24). Again, despite we think that closed formulas are not available, due to the monotonically increasing nature of  $L_2(t, \mathbf{z})$  in the range of interest, and that  $L_2(t_2, \mathbf{z}) \leq L(t_1, \mathbf{z})$  the solution can be found by simple search methods.

The lower-bound counterpart of this method can be found in Sect. 6.2.

### 7.1.1 Asymptotic value when the number of observations goes to infinity

Taking into account that (25), (26), and (27) are still verified, is trivial to note that  $t_{\text{upper}}$  will be larger than or equal to  $t_0$ , as this is smaller than or equal to  $t_2$ .

## 7.2 Deterministic approach II

For the upper-bound, simpler bounding functions can be used, allowing the closed calculation of  $t_{\text{upper}}$ ; this is the case, for example of

$$L_4(t, \mathbf{z}) \triangleq n \log \left( 2\pi \left( \sigma_N^2 + (1 - \alpha)^2 t^2 \sigma_\Lambda^2 \right) \right),$$

where we have removed the last term in  $L_2(t, \mathbf{z})$ , and which allows to introduce the following upper-bound to the search interval

$$t_{\text{upper}} = \sqrt{\frac{1}{(1 - \alpha)^2 \sigma_\Lambda^2} \left[ \frac{e^{\frac{L(t_1, \mathbf{z})}{n}}}{2\pi} - \sigma_N^2 \right]}. \quad (45)$$

Furthermore, when the number of observations goes to infinity and  $t_1 \approx t_0$ , one can use the approximation derived in Sect. 3.4; therefore, replacing (13) in (45), one obtains

$$t_{\text{upper}} \approx \sqrt{\frac{1}{(1 - \alpha)^2 \sigma_\Lambda^2} \left[ \left( \sigma_N^2 + (1 - \alpha)^2 t_1^2 \sigma_\Lambda^2 \right) e^{2 + \frac{(t_0 - t_1)^2 \sigma_X^2}{\sigma_N^2 + (1 - \alpha)^2 t_1^2 \sigma_\Lambda^2}} - \sigma_N^2 \right]} \geq t_1 e^{1 + \frac{(t_0 - t_1)^2 \sigma_X^2}{2[\sigma_N^2 + (1 - \alpha)^2 t_1^2 \sigma_\Lambda^2]}}; \quad (46)$$

as it was proved in App. B,  $t_1 e^{\frac{(t_0 - t_1)^2 \sigma_X^2}{2[\sigma_N^2 + (1 - \alpha)^2 t_1^2 \sigma_\Lambda^2]}} \geq t_0$  for any  $t_1 \geq t_0$ , and for any  $t_1 > 0$  smaller than or equal to a value that goes to  $t_0$  whenever  $\text{HLR} \rightarrow \infty$ , and  $\text{TNLR} < 1$ . Therefore, under those conditions  $t_{\text{upper}} \geq t_0$ .

Finally, note that a similar strategy, based on a simplified version of  $L_2(t, \mathbf{z})$ , can not be used for the derivation of a lower-bound, as one can not neglect



either of both terms in  $L_2(t, \mathbf{z})$ . Indeed, the second term is required in order to  $L_2(t, \mathbf{z}) \rightarrow \infty$  when  $t \rightarrow 0$ , and the first one should be also considered in order to be able to upper-bound  $L(t, \mathbf{z})$ , as it might be negative.

### 7.3 Probabilistic approach

Trying to reduce the search interval upper-bounds based on deterministic approaches proposed in the previous sections, we can use the previously introduced probabilistic modeling of  $L(t, \mathbf{Z})$  (valid under the conditions introduced in Sect. 3.1) for  $t = t_0$  in order to obtain a new, hopefully smaller, search interval upper-bound value by relaxing the former deterministic constraints to just be verified with a given high probability. Formally, we can calculate such a point as the smallest positive real scaling factor  $t$  such that for every  $t' > t$  the event of  $L(t', \mathbf{Z})$  being smaller than  $L(t_1, \mathbf{z})$  has a probability smaller than or equal to  $P_{e1}$ , i.e.,

$$t_{\text{upper}} = \underset{t: t \geq 0, \forall t' > t, \Pr(L(t', \mathbf{Z}) < L(t_1, \mathbf{z}) | t_0 = t') \leq P_{e1}}{\operatorname{argmin}} t. \quad (47)$$

Taking into account the probabilistic modeling of  $L(t, \mathbf{Z})$  for  $t = t_0$ , the considered probability can be calculated as

$$\Pr(L(t, \mathbf{Z}) < L(t_1, \mathbf{z}) | t = t_0) = \int_{-\infty}^{L(t_1, \mathbf{z})} f_{\chi_{2n}^2} \left( x - n \log \left[ 2\pi (\sigma_N^2 + (1 - \alpha)^2 t^2 \sigma_\Lambda^2) \right] \right) dx \quad (48)$$

with  $f_{\chi_{2n}^2}(x)$  the pdf of the  $\chi^2$  distribution with  $2n$  degrees of freedom; from the last equation it is obvious that this probability is monotonically decreasing (indeed approaching 0) with  $t$ . Therefore, the constraint in (47) will be always well defined (i.e., it will never define an empty set of feasible  $t$ 's for any particular  $P_{e1} > 0$  and  $L(t_1, \mathbf{z})$ ), although we will not be able to use it in order to define a lower-bound counterpart. Moreover, due to the monotonicity of  $\Pr(L(t, \mathbf{Z}) < L(t_1, \mathbf{z}) | t = t_0)$ , (47) is equivalent to

$$t_{\text{upper}} = \underset{t: t \geq 0, \Pr(L(t, \mathbf{Z}) < L(t_1, \mathbf{z}) | t_0 = t) \leq P_{e1}}{\operatorname{argmin}} t.$$

In Fig. 11 we can compare the upper-bound obtained by using the method proposed in this section, and the bounds obtained by using the deterministic method proposed in Sects. 6.2.1 and 7.1.1. As expected, the upper-bound derived in this section is larger than that obtained in Sect. 7.1.1, due to the different definition of  $L_2(t, \mathbf{z})$  and  $L_4(t, \mathbf{z})$ ; nevertheless, one must also take into account that the upper-bound derived from  $L_4(t, \mathbf{z})$  can be calculated by using a closed formula.

Furthermore, if we denote by  $F_{\chi_{2n}^2}(x)$  the distribution function of the  $\chi^2$  distribution with  $2n$  degrees of freedom, the mentioned constraint can be rewritten as

$$F_{\chi_{2n}^2} \left( L(t_1, \mathbf{z}) - n \log \left[ 2\pi (\sigma_N^2 + (1 - \alpha)^2 t^2 \sigma_\Lambda^2) \right] \right) \leq P_{e1},$$

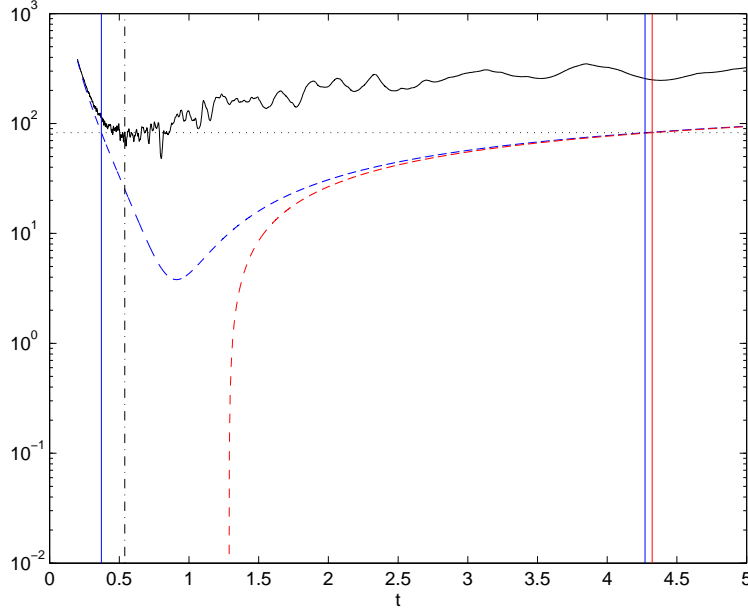


Figure 11: Comparison between  $L(t, \mathbf{z})$  (solid black line),  $L(t_1, \mathbf{z})$  (dotted black line),  $L_2(t, \mathbf{z})$  (dashed blue line), and  $L_4(t, \mathbf{z})$  (dashed red line). The corresponding search-interval bounds are plotted by using vertical solid lines with the same color that the function used for computing them.  $t_1$  (vertical dash-dot black line) calculated by using (16). HLR  $\approx 34.9765$  dB, SCR  $\approx -1.0618$  dB, TNLR  $\approx -3.5736$  dB,  $t_0 = 0.8$ ,  $\alpha = \alpha_{\text{Costa}} \approx 0.5608$ ,  $n = 40$ , scalar quantizer.

which due to the strictly monotonically increasing nature of  $F_{\chi^2_{2n}}(x)$ , and the strictly monotonically increasing nature of the argument of the log function with  $t$ , allows one to calculate  $t_{\text{upper}}$  as the only solution to

$$n \log \left[ 2\pi (\sigma_N^2 + (1 - \alpha)^2 t^2 \sigma_\Lambda^2) \right] + F_{\chi^2_{2n}}^{-1}(P_{e1}) = L(t_1, \mathbf{z}), \quad (49)$$

which can be shown to be

$$t_{\text{upper}} = \left[ \left( \frac{1}{(1 - \alpha)^2 \sigma_\Lambda^2} \left[ \frac{e^{\frac{L(t_1, \mathbf{z}) - F_{\chi^2_{2n}}^{-1}(P_{e1})}{n}}}{2\pi} - \sigma_N^2 \right] \right)^+ \right]^{1/2}. \quad (50)$$

Similarly, if one decides to use the CLT-based Gaussian approximation to the pdf of  $L(t, \mathbf{Z})$  given that  $t = t_0$  (introduced in Sect. 3.1, formulas (8), (9), and (10), assuming additionally that SCR  $\rightarrow 0$  for the scalar quantizer case), should consider that the mean and variance of that distribution are  $2n$  and  $4n$  respectively, so (50) would be replaced by

$$t_{\text{upper}} = \left[ \left( \frac{1}{(1 - \alpha)^2 \sigma_\Lambda^2} \left[ \frac{e^{\frac{L(t_1, \mathbf{Z}) - 2n + \sqrt{4n}Q^{-1}(P_{e1})}{n}}}{2\pi} - \sigma_N^2 \right] \right)^+ \right]^{1/2}. \quad (51)$$

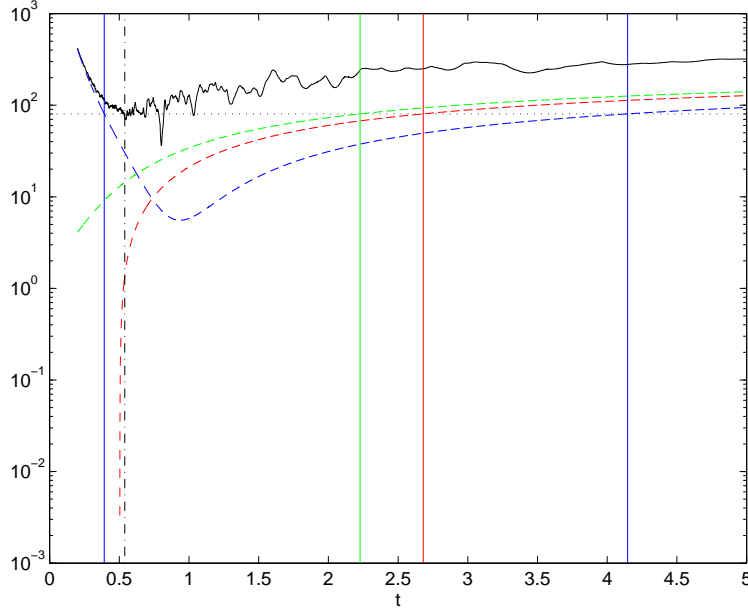


Figure 12: Comparison between  $L(t, \mathbf{z})$  (solid black line),  $L(t_1, \mathbf{z})$  (dotted black line),  $L_2(t, \mathbf{z})$  (dashed blue line), and the left term of (49) for  $P_{e1} = 10^{-6}$  (dashed red line), and  $P_{e1} = 10^{-3}$  (dashed green line). The corresponding search-interval bounds are plotted by using vertical solid lines with the same color that the function used for computing them.  $t_1$  (vertical dash-dot black line) calculated by using (16). HLR  $\approx 34.9765$  dB, SCR  $\approx -1.0618$  dB, TNLNR  $\approx -3.5736$  dB,  $t_0 = 0.8$ ,  $\alpha = \alpha_{\text{Costa}} \approx 0.5608$ ,  $n = 40$ , scalar quantizer.

In Fig. 12 we can compare the upper-bounds obtained by using the method proposed in this section, and the bounds obtained by using the deterministic method proposed in Sects. 6.2.1 and 7.1.1. Similarly to Fig. 2, the larger  $P_{e1}$ , the smaller the search interval upper-bound.

### 7.3.1 Asymptotic value when the number of observations goes to infinity

For the sake of completeness we will analyze the asymptotic value of  $t_{\text{upper}}$  as a function of  $t_1$  when  $n \rightarrow \infty$ ; this analysis will provide us with a theoretical insight of the search interval upper-bound (and therefore the computational cost) when a large number of observations are available at the decoder.

First, we will focus on the case where  $t_1 \approx t_0$ ; as it is shown in Sect. 3.4,

$$L(t_1, \mathbf{z}) \approx 2n + \frac{n(t_0 - t_1)^2 \sigma_X^2}{\sigma_N^2 + (1 - \alpha)^2 t_1^2 \sigma_\Lambda^2} + n \log (2\pi (\sigma_N^2 + (1 - \alpha)^2 t_1^2 \sigma_\Lambda^2)),$$

yielding

$$t_{\text{upper}} \approx \left( t_1^2 e^{\frac{\sigma_X^2 (t_0 - t_1)^2}{\sigma_N^2 + (1-\alpha)^2 t_1^2 \sigma_\Lambda^2}} + \frac{\sigma_N^2 \left( e^{\frac{\sigma_X^2 (t_0 - t_1)^2}{\sigma_N^2 + (1-\alpha)^2 t_1^2 \sigma_\Lambda^2}} - 1 \right)}{(1-\alpha)^2 \sigma_\Lambda^2} \right)^{1/2}.$$

At the sight of the last expression one can check that whenever  $t_1 \rightarrow t_0$ , then  $t_{\text{upper}} \rightarrow t_1$ , and consequently  $t_{\text{upper}} \rightarrow t_0$ . One interesting question to be answered is if  $t_{\text{upper}} \geq t_0$  irrespectively of  $t_1$ . A sufficient condition for that to happen is that

$$t_1^2 e^{\frac{\sigma_X^2 (t_0 - t_1)^2}{\sigma_N^2 + (1-\alpha)^2 t_1^2 \sigma_\Lambda^2}} \geq t_0^2,$$

which is discussed in App. B. It is interesting to point out the similarities between the left term of the last expression and the square of the last term of (46); in Sect. 7.2 a deterministic approach was proposed based on a lossy version of the objective function, in order to be able to obtain closed formulas for  $t_{\text{upper}}$ . Nevertheless, the penalty to be paid is also clear: when following that deterministic lossy approach the obtained upper-bound is nothing but the upper-bound derived in the current section multiplied by  $e$ , consequently increasing the size of the search interval.

On the other hand, if we study the case where  $t_1$  is not close to  $t_0$ ,  $L(t_1, \mathbf{z})$  is shown in Sect. 3.4 to be approximately

$$L(t_1, \mathbf{z}) \approx n \frac{t_1^2 \sigma_\Lambda^2}{\sigma_N^2 + (1-\alpha)^2 t_1^2 \sigma_\Lambda^2} + n \log (2\pi (\sigma_N^2 + (1-\alpha)^2 t_1^2 \sigma_\Lambda^2)) + n \frac{t_0^2}{t_1^2},$$

yielding

$$t_{\text{upper}} \approx \left( t_1^2 e^{\frac{t_0^2}{t_1^2} + \frac{t_1^2 \sigma_\Lambda^2}{\sigma_N^2 + (1-\alpha)^2 t_1^2 \sigma_\Lambda^2} - 2} + \frac{\sigma_N^2 \left( e^{\frac{t_0^2}{t_1^2} + \frac{t_1^2 \sigma_\Lambda^2}{\sigma_N^2 + (1-\alpha)^2 t_1^2 \sigma_\Lambda^2} - 2} - 1 \right)}{(1-\alpha)^2 \sigma_\Lambda^2} \right)^{1/2}.$$

In order to check if also in this case  $t_{\text{upper}} \geq t_0$  we will consider the sufficient condition

$$t_1^2 e^{\frac{t_0^2}{t_1^2}} \geq t_0^2,$$

or equivalently

$$\log \left( \frac{t_1^2}{t_0^2} \right) \geq -\frac{t_0^2}{t_1^2},$$

which is true for any value of  $t_1 > 0$ , since, as it is shown in App. A,  $\log(x) \geq -\frac{1}{x}$  for any  $x \geq 0$ .

## 7.4 Partially probabilistic approach

Please refer to Sect. 6.3.

## 7.5 Search interval upper-bound calculated from the variance-based estimator

In this section we will follow an approach similar to that proposed at Sect. 6.4 in order to obtain an upper-bound to the search interval when the variance-based estimator is used as  $t_1$ .

Similarly to (41), the upper-bound will be computed this time as the smallest  $t > 0$  such that for every  $(t')^2 \geq t^2$ , if the square real scaling factor is  $(t')^2$ , then the probability of obtaining a variance-based estimator smaller than or equal to  $t_1$ , is smaller than or equal to  $P_{e1}$ , i.e.,

$$t_{\text{upper}} = \sqrt{\underset{t^2: t^2 \geq 0, \forall (t')^2 \geq t^2, \Pr(\hat{T}^2_{\text{var}} \leq t_1^2 | t_0^2 = (t')^2) \leq P_{e1}}{\text{argmin}} t^2}. \quad (52)$$

Based on (21), the probability in (52) can be calculated as

$$\Pr(\hat{T}^2_{\text{var}} \leq t_1^2 | t_0^2) \approx Q\left(\frac{t_0^2}{\sqrt{\frac{2[(\sigma_X^2 + \alpha^2 \sigma_\Lambda^2)t_0^2 + \sigma_N^2]^2}{n(\sigma_X^2 + \alpha^2 \sigma_\Lambda^2)^2}}}\right) u(t_1^2) + \int_0^{t_1^2} \frac{e^{\frac{-n(\sigma_X^2 + \alpha^2 \sigma_\Lambda^2)^2(\tau - t_0^2)^2}{4[(\sigma_X^2 + \alpha^2 \sigma_\Lambda^2)t_0^2 + \sigma_N^2]^2}}}{\sqrt{\frac{4\pi[(\sigma_X^2 + \alpha^2 \sigma_\Lambda^2)t_0^2 + \sigma_N^2]^2}{n(\sigma_X^2 + \alpha^2 \sigma_\Lambda^2)^2}}} d\tau \quad (53)$$

where  $u(x)$  stands for the step function, defined as

$$u(x) \triangleq \begin{cases} 0, & \text{if } x < 0, \\ 1, & \text{otherwise} \end{cases}.$$

Taking into account that  $t_1^2 = \hat{t}^2_{\text{var}}(\mathbf{z})$  defined in (19) is non-negative, (53) can be rewritten as

$$\Pr(\hat{T}^2_{\text{var}} \leq t_1^2 | t_0^2) \approx \int_{-\infty}^{t_1^2} \frac{e^{\frac{-n(\sigma_X^2 + \alpha^2 \sigma_\Lambda^2)^2(\tau - t_0^2)^2}{4[(\sigma_X^2 + \alpha^2 \sigma_\Lambda^2)t_0^2 + \sigma_N^2]^2}}}{\sqrt{\frac{4\pi[(\sigma_X^2 + \alpha^2 \sigma_\Lambda^2)t_0^2 + \sigma_N^2]^2}{n(\sigma_X^2 + \alpha^2 \sigma_\Lambda^2)^2}}} d\tau = Q\left(\frac{t_0^2 - t_1^2}{\sqrt{\frac{2[(\sigma_X^2 + \alpha^2 \sigma_\Lambda^2)t_0^2 + \sigma_N^2]^2}{n(\sigma_X^2 + \alpha^2 \sigma_\Lambda^2)^2}}}\right) \quad (54)$$

Given that  $Q(x)$  is monotonically decreasing with  $x$ , we will prove that its argument in (54) is monotonically increasing with  $t_0^2$  in order to show that (52) has a single solution. Indeed,

$$\frac{\partial}{\partial t_0^2} \left( \frac{t_0^2 - t_1^2}{\sqrt{\frac{2[(\sigma_X^2 + \alpha^2 \sigma_\Lambda^2)t_0^2 + \sigma_N^2]^2}{n(\sigma_X^2 + \alpha^2 \sigma_\Lambda^2)^2}}} \right) = \frac{\sqrt{n}((\sigma_X^2 + \alpha^2 \sigma_\Lambda^2)t_1^2 + \sigma_N^2) \sigma_X^2}{\sqrt{2}((\sigma_X^2 + \alpha^2 \sigma_\Lambda^2)t_0^2 + \sigma_N^2)^2}.$$

Based on  $\Pr(\hat{T}^2_{\text{var}} \leq t_1^2 | t_0^2)$  being monotonically decreasing with  $t_0^2$ , (52) is equivalent to

$$t_{\text{upper}} = \underset{t: t \geq 0, \Pr(\hat{T}^2_{\text{var}} \leq t_1^2 | t_0^2 = t^2) \leq P_{e1}}{\text{argmin}} t.$$

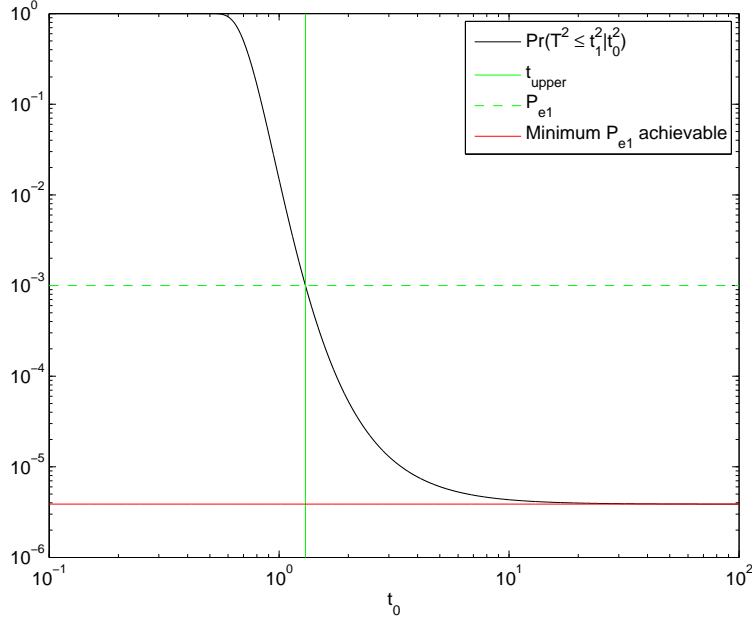


Figure 13:  $\Pr\left(\hat{T}_{\text{var}}^2 \leq t_1^2 t_0^2\right)$ , (43), and  $t_{\text{lower}}$ . HLR = 10 dB, WNR = -3 dB,  $t_1 = 0.7$ ,  $\alpha = 0.5$ ,  $n = 40$ ,  $P_{e1} = 10^{-3}$ . In this case we use the WNR instead of the SCR and TNLr the latter quantities depend on  $t_0$ , while the WNR does not depend on it.

Note that in this case the minimum value of  $P_{e1}$  one could expect to obtain is

$$Q\left(\sqrt{\frac{n}{2}}\right). \quad (55)$$

Similarly to the discussion in Sect. 6.4, the bound on (54) due to (55) can be dismissed when the number of considered dimensions is very large, as in that scenario (55) goes to 0.

Denoting by  $\xi = Q^{-1}(P_{e1})$ , and assuming that  $P_{e1} \geq Q(\sqrt{n/2})$ , the mentioned only solution is

$$t_{\text{upper}}^2 = \frac{2\xi^2 \sigma_N^2 + n(\sigma_X^2 + \alpha^2 \sigma_\Lambda^2) t_1^2 + \sqrt{2n} \xi [(\sigma_X^2 + \alpha^2 \sigma_\Lambda^2) t_1^2 + \sigma_N^2]}{(n - 2\xi^2)(\sigma_X^2 + \alpha^2 \sigma_\Lambda^2)}.$$

The probability studied at (54), the lower-bound on it derived derived in (55), and the value of  $t_{\text{upper}}$  obtained in the last formula are illustrated in Fig. 13.

## 7.6 Discussion on the importance of $t_1$ choice

Finally, it is worth to point out that although deterministic and probabilistic methods for the derivation of lower and upper-bounds can use any initial point

$t_1$ , the size of the obtained interval (and consequently the computational cost of the subsequent optimization of the target function in that interval) will depend on the choice of  $t_1$ , as it is evident, for example, at the sight of (45), (50), or (51).

## 8 Sampling the search-interval

As it was already discussed, the main problem when dealing with the optimization of (5) is the presence of non-differentiable points. Nevertheless, the target function is convex between any two consecutive non-differentiable points; therefore, as a first approach to the optimization problem one could think of considering all those non-differentiable points that have a non-neglectable probability and optimizing the target function into the intervals defined by each two consecutive points. Doing so, the convergence to the value minimizing  $L(t, \mathbf{z})$  can be ensured.

The first question to be answered about this approach is its feasibility. In other words, how does the number of non-differentiable points to be considered increases with the dimensionality of the problem? Obviously, if this number were not bounded, this would imply a serious implementation problem to this strategy, as the required resources would be also unlimited.

In order to answer this question, experiments were performed where the variance-based scaling estimator  $\hat{t}_{\text{var}}(\mathbf{z})$  was used to define an interval of radius 5 times the square root of the CRB of that estimator around the estimated value; this interval determines the non-differentiable points that can not be neglected. As the estimation variance decreases with  $1/n$ , the width of that interval will decrease with  $1/\sqrt{n}$ . On the other hand, the density of non-differentiable points increases with  $n$ . Consequently, the number of points that one must take into account in the proposed strategy increases in average with  $\sqrt{n}$ . Plots illustrating these results can be found in Figs. 14, 15, and 16.

Given that the approach of considering all the non-differential points has been shown to be computationally unfeasible, other strategies must be proposed in order to explore the search interval seeking  $L(t, \mathbf{z})$  minimum.

Our proposals are based on the study of  $L(t, \mathbf{Z})$  main lobe width. Basically, the width of that lobe depends on the behavior with  $t$  of the quantization error Euclidean norm in the first term of (5). The value of the target function is minimum at a point close to  $t_0$  (check Sect. 11 for further details), as the variance of the quantization error is minimized in the neighborhood of that point. When  $t$  deviates from  $t_0$ , but it is still close to  $t_0$  (following the conditions introduced at the first part of Sect. 3.4), the modulo- $\Lambda$  reduction has not to be considered and the quantization error variance can be written as  $(t_0 - t)^2 \sigma_X^2 + (t - \alpha t_0)^2 \sigma_\Lambda^2 + \sigma_N^2$ . As  $t$  deviates from  $t_0$ , and due to the presence of the modulo operation, this variance is finally upper-bounded by  $t^2 \sigma_\Lambda^2$ ; from a statistical point of view, the target function main lobe ends when the variance of the modulo-reduced quantization error approaches this upper-bound. Based on these ideas, we will determine a set of points in the search interval trying to ensure that at least one of them is in the target function main lobe. When the

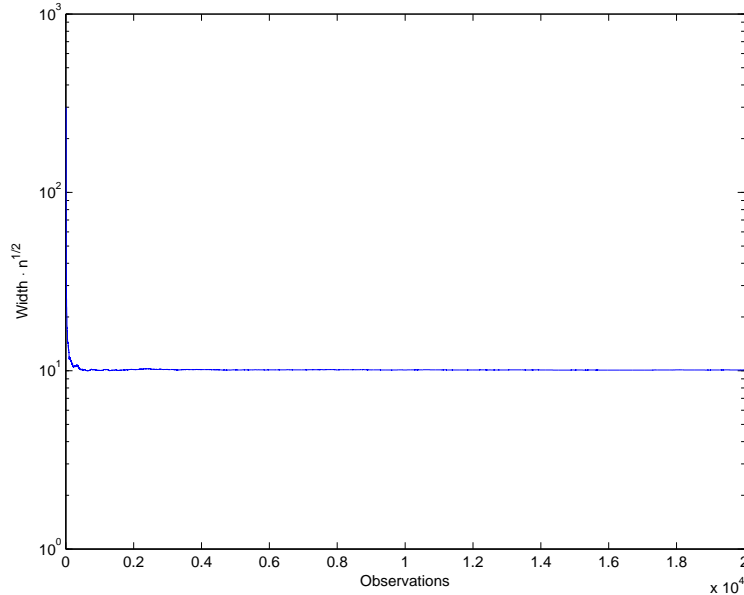


Figure 14: Width of the interval (obtained by using the variance-based methodology described above) multiplied by  $\sqrt{n}$  versus the dimensionality of the problem  $n$ . HLR  $\approx 25.5630$  dB, SCR  $\approx -6.6199$  dB, TNL  $\approx -0.4833$  dB,  $\alpha = 0.6$ ,  $t_0 = 0.7$ .

number of observations is large,  $L(t, \mathbf{z})$  will tend to be convex in its main lobe, as it will asymptotically follow the characterization introduced in Sect. 3.4; thus, conventional or ad-hoc optimization algorithms could be used to minimize that function, taking as starting points those mentioned above. As long as one of those points indeed belongs to the target function main lobe, it will lead us to the minimum of  $L(t, \mathbf{z})$  (based on the asymptotic convexity of the target function for  $n \rightarrow \infty$ ).

Therefore, the question to be solved is how we can define a minimum set of points (as the final optimization algorithm considers as starting points all the elements in that set, its computational cost is linearly increased with the cardinality of the set, so we are interested in defining a minimum size set) in order to be reasonably sure that one of them will lie on the main lobe of the target function. We will define our *candidate point set* (hereafter, *candidate set*) by exploiting that the boundary of the target function main lobe depends on the quantization error variance approaching  $t^2\sigma_\Lambda^2$ .

## 8.1 First approach. Scalar quantizer case

The reasoning behind this approach is that for the scalar quantizer case, and similarly for the low-dimensional lattice case, the effect of the modulo-reduction on the variance of the modularized random vector is rather smooth, in the sense that for achieving the mentioned upper-bound  $t^2\sigma_\Lambda^2$ , the variance of the input random vector should be much larger than that value. This is not the



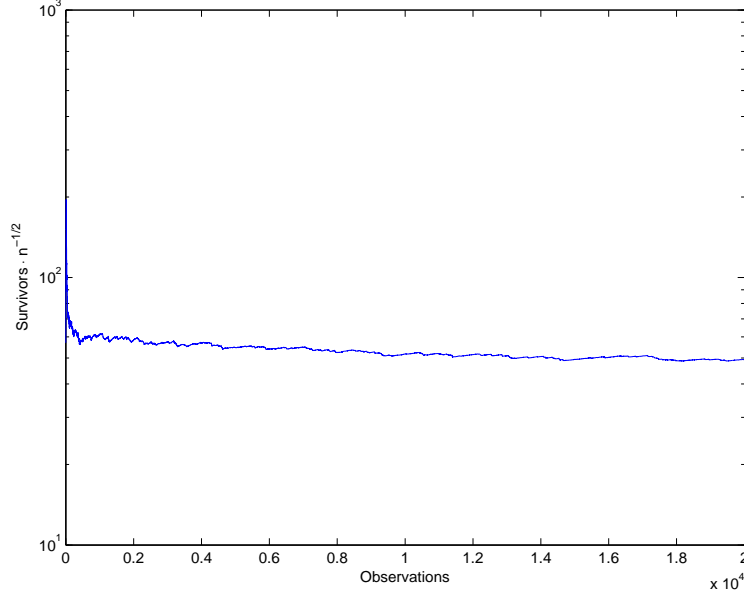


Figure 15: Number of non-differentiable points in the intervals described above divided by  $\sqrt{n}$  versus the dimensionality of the problem  $n$ . HLR  $\approx 25.5630$  dB, SCR  $\approx -6.6199$  dB, TNLN  $\approx -0.4833$  dB,  $\alpha = 0.6$ ,  $t_0 = 0.7$ .

case for the high-dimensional lattice case, where the input variance needed for saturating the output variance is just  $t^2\sigma_\Lambda^2$ ; that is why a specific interval search sampling method is proposed for the high-dimensional good lattice case (please refer to the next section). Coming back to the scalar quantizer scenario, as the input vs. output variance function is smooth, one has some margin for considering values of  $(t_0 - t)^2\sigma_X^2 + (t - \alpha t_0)^2\sigma_\Lambda^2 + \sigma_N^2$  larger than  $t^2\sigma_\Lambda^2$ , and consequently this threshold will not be considered by the current search interval sampling method.

Instead, the approach proposed for the low-dimensional lattice case is based on assuming that the current point, let us denote it as  $t(i)$ , is indeed  $t_0$ ; if we want its nearest points in the candidate set to also belong to its main lobe, upper and lower-bounds can be defined to those nearest point values in order to the resulting quantization error variance be close enough to the quantization error variance at the current point (calculated assuming that it is indeed the real scaling factor), as otherwise we will probably be outside the main lobe. Mathematically, the variance of the quantization error at  $t(i)$ , assuming that it is the real scaling factor, is given by

$$t^2(i)(1 - \alpha)^2\sigma_\Lambda^2 + \sigma_N^2,$$

while that at the nearest point in the candidate set, denoted as  $t(i + 1)$ , can be calculated as

$$[t(i + 1) - t(i)]^2 + [t(i + 1) - \alpha t(i)]^2\sigma_\Lambda^2 + \sigma_N^2.$$

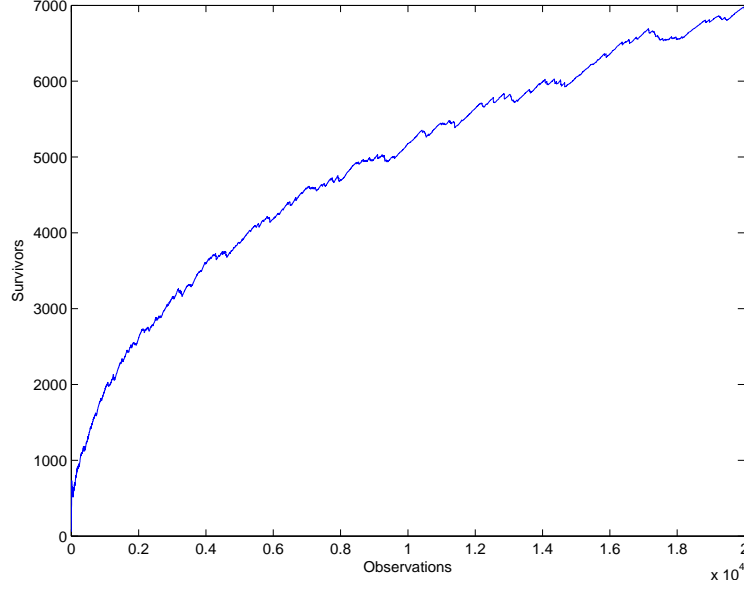


Figure 16: Number of non-differentiable points in the intervals described above versus the dimensionality of the problem  $n$ . HLR  $\approx 25.5630$  dB, SCR  $\approx -6.6199$  dB, TNLR  $\approx -0.4833$  dB,  $\alpha = 0.6$ ,  $t_0 = 0.7$ .

Constraining the latter variance to be smaller than or equal to the former one plus  $K_1 t^2(i+1)\sigma_\Lambda^2$  in order to ensure that  $t(i+1)$  is still in the main lobe of the target function, the two following constraints on  $t(i+1)$  are obtained:

$$t(i+1) \geq t_{l,\text{id}} \triangleq \frac{t(i) \left[ \alpha \sigma_\Lambda^2 + \sigma_X^2 - \sigma_\Lambda \sqrt{\sigma_\Lambda^2 [(1-\alpha)^2 + K_1(2\alpha-1)] + K_1 \sigma_X^2} \right]}{\sigma_X^2 + \sigma_\Lambda^2 (1-K_1)} \quad (56)$$

$$t(i+1) \leq t_{u,\text{id}} \triangleq \frac{t(i) \left[ \alpha \sigma_\Lambda^2 + \sigma_X^2 + \sigma_\Lambda \sqrt{\sigma_\Lambda^2 [(1-\alpha)^2 + K_1(2\alpha-1)] + K_1 \sigma_X^2} \right]}{\sigma_X^2 + \sigma_\Lambda^2 (1-K_1)} \quad (57)$$

Obviously  $K_1$  plays a trade-off role: the smaller  $K_1$ , the more confident we can be that our candidate set will contain at least one point at the main lobe, but also the larger the cardinality of that set, and consequently the larger the computational cost of the subsequent optimization algorithm.

Whenever explicit reference to other method defining the candidate set is not provided, we will assume that the procedure used for defining that set is initialized with the search interval lower-bound  $t_{\text{lower}}$  and successive points are computed based on (57), until the computed point being larger than or equal to the search interval upper-bound  $t_{\text{upper}}$ .

Note that other criteria could be defined based on this variance-based idea for setting the candidate set, as for example: 1) starting the sampling at  $t_{\text{upper}}$ , and use (56) for computing  $t(i+1)$ , or 2) starting at  $t_1$ , and use both (56) and (57) for computing the next candidate points (the latter is indeed used in Sect. 9.3).

## 8.2 Second approach. High-dimensional good lattices

Contrarily to the low-dimensional lattice case, in the high-dimensional good lattice case the variance of the modulo-reduced random vector is equal to the variance of the non-reduced random vector as long as this value is smaller than or equal to  $t^2\sigma_\Lambda^2$ ; once the input variance is larger than this threshold, the output variance stalls at  $t^2\sigma_\Lambda^2$ . Therefore, in this scenario it will be specially critical to consider points in the candidate set such that the variance of the quantization error is smaller than  $t^2\sigma_\Lambda^2$ ; otherwise, the main lobe will not be longer detectable.

Taking into account the previous discussion, the method proposed for sampling the search interval will look for those  $t$  such that

$$(t_0 - t)^2\sigma_X^2 + (t - \alpha t_0)^2\sigma_\Lambda^2 + \sigma_N^2 = t^2\sigma_\Lambda^2. \quad (58)$$

This equation has two solutions with  $t$ , namely

$$t_{l,\text{hd}} = \frac{t_0 (\sigma_X^2 + \alpha\sigma_\Lambda^2) - \sqrt{t_0^2\alpha\sigma_\Lambda^2 [\sigma_X^2 (2 - \alpha) + \alpha\sigma_\Lambda^2] - \sigma_N^2\sigma_X^2}}{\sigma_X^2}, \quad (59)$$

$$t_{u,\text{hd}} = \frac{t_0 (\sigma_X^2 + \alpha\sigma_\Lambda^2) + \sqrt{t_0^2\alpha\sigma_\Lambda^2 [\sigma_X^2 (2 - \alpha) + \alpha\sigma_\Lambda^2] - \sigma_N^2\sigma_X^2}}{\sigma_X^2}. \quad (60)$$

Be aware that both of them go to  $t_0$  when  $\text{HLR} \rightarrow \infty$ , and  $\text{TNLR} < 1$ . These solutions will be real, consequently defining the real roots of (58) we are interested in, when

$$|t_0| \geq \sqrt{\frac{\sigma_X^2\sigma_N^2}{\alpha\sigma_\Lambda^2 [\sigma_X^2 (2 - \alpha) + \alpha\sigma_\Lambda^2]}}; \quad (61)$$

otherwise,  $t^2\sigma_\Lambda^2$  will be smaller than the left term in (58) for any  $t$ , indicating that the main lobe just does not exist. Be aware that when  $\text{HLR} \rightarrow \infty$ , the last condition is equivalent to

$$t_0^2\sigma_\Lambda^2\alpha(2 - \alpha) \geq \sigma_N^2,$$

which is nothing but  $\text{TNLR} \leq 1$ .

Note that if (61) is verified, then  $t_{u,\text{hd}} \geq t_0$  holds. Furthermore,  $t_{l,\text{hd}} \leq t_0$  if and only if

$$\sigma_\Lambda^2 \geq \frac{\sigma_N^2}{\alpha(2 - \alpha)t_0^2},$$

or equivalently,  $\text{TNLR} \leq 1$  (independently of  $\text{HLR}$ ).

Consequently, the algorithm we propose in this scenario for sampling the search interval is the following:

- $t(1) = t_{\text{lower}}$ .
- $i = 1$ .

- While  $(t(i) < t_{\text{upper}})$

– If  $|t(i)| \geq \sqrt{\frac{\sigma_X^2 \sigma_N^2}{\alpha \sigma_\Lambda^2 [\sigma_X^2 (2-\alpha) + \alpha \sigma_\Lambda^2]}}$ , then

$$* t(i+1) = \frac{t(i)(\sigma_X^2 + \alpha \sigma_\Lambda^2) + \sqrt{t(i)^2 \alpha \sigma_\Lambda^2 [\sigma_X^2 (2-\alpha) + \alpha \sigma_\Lambda^2] - \sigma_N^2 \sigma_X^2}}{\sigma_X^2}.$$

else

$$* t(i+1) = \frac{t(i) [\alpha \sigma_\Lambda^2 + \sigma_X^2 + \sigma_\Lambda \sqrt{\sigma_\Lambda^2 [(1-\alpha)^2 + K_1(2\alpha-1)] + K_1 \sigma_X^2}}{\sigma_X^2 + \sigma_\Lambda^2 (1-K_1)}$$

–  $i = i + 1$ .

It is important to note that for the case where the value of  $t(i)$  is so small that if it were the real scaling factor, then no real solution exists to (58), i.e., the quantization error will be uniformly distributed over the considered Voronoi region for any value of  $t$ , we have chosen an alternative strategy for computing  $t(i+1)$  based on the procedure proposed in the last section. Another possible strategy dealing with the case where  $t_{\text{lower}} < \sqrt{\frac{\sigma_X^2 \sigma_N^2}{\alpha \sigma_\Lambda^2 [\sigma_X^2 (2-\alpha) + \alpha \sigma_\Lambda^2]}}$  is setting

$t(1) = t_{\text{lower}}$ , and  $t(2) = \sqrt{\frac{\sigma_X^2 \sigma_N^2}{\alpha \sigma_\Lambda^2 [\sigma_X^2 (2-\alpha) + \alpha \sigma_\Lambda^2]}}$ , since as long as  $t_0$  (or  $t(i+1)$ ) were smaller than the right term in (61), the target function will not have main lobe, making impossible the search of  $\hat{t}(\mathbf{z})$ .

Similarly to the previous method, alternative criteria could be developed for computing the candidate set based on this idea.

### 8.3 Future work

It would be interesting to study the cardinality of the candidate set (and consequently the computational cost of the subsequent optimization algorithm) as a function of:

- $\sigma_X^2$
- $\sigma_N^2$
- $\sigma_W^2$
- $K_1$
- $n$
- $P_{e1}$

## 9 Optimization algorithms

Once the candidate set has been determined, we will look for the minimum of  $L(t, \mathbf{z})$ , using as starting points of the optimization algorithm each point in that set; as it was mentioned above, for large values of  $n$  the considered target function will be convex in the main lobe, so for a large number of observations

one can ensure the global minimum of the target function to be found. Several choices can be proposed for this optimization algorithm; next, some of them are detailed.

## 9.1 Derivative-based optimization

This method determines for each point in the candidate set a point where the derivative of the target function is null, providing as final estimation of  $t_0$  that null-derivative point where the target function is minimized. Namely:

- For each  $t(i)$  in the candidate set:
  - $s_0 = \text{sign} [L(t(i) + \epsilon_1, \mathbf{z}) - L(t(i), \mathbf{z})]$ . In the reported experiments  $\epsilon_1 = 10^{-5}$ .
  - $s_1 = s_0$ .
  - $\text{step} = 10^{-3}$ .
  - While ( $s_1 == s_0$ )
    - \*  $\text{step} = 2\text{step}$ .
    - \*  $t_{\text{aux}} = |t(i) - s_0\text{step}|$ .
    - \*  $s_1 = \text{sign} [L(t_{\text{aux}} + \epsilon_1, \mathbf{z}) - L(t_{\text{aux}}, \mathbf{z})]$ .
  - $t_l = \min(t(i), t_{\text{aux}})$ .
  - $t_u = \max(t(i), t_{\text{aux}})$ .
  - While ( $(t_u - t_l) > \epsilon_2$ ) (in the reported experiments  $\epsilon_2 = 10^{-5}$ )
    - \*  $t_{\text{aux}} = (t_u + t_l)/2$ .
    - \*  $s_1 = \text{sign} [L(t_{\text{aux}} + \epsilon_1, \mathbf{z}) - L(t_{\text{aux}}, \mathbf{z})]$ .
    - \* If ( $s_1 > 0$ ) then
      - $t_u = t_{\text{aux}}$ .
    - \* else
      - $t_l = t_{\text{aux}}$ .
  - $L\_value(i) = L(t_{\text{aux}}, \mathbf{z})$ .
  - $\text{null\_der}(i) = t_{\text{aux}}$ .
- $i^* = \text{argmin}_i L\_value(i)$ .
- If  $L(\text{null\_der}(i^*), \mathbf{z}) < L(t_1, \mathbf{z})$  then
  - $\hat{t}(\mathbf{z}) = \text{null\_der}(i^*)$ .
- else
  - $\hat{t}(\mathbf{z}) = t_1$ .

### Advantages:

- The provided estimate is ensured to be at least a local minimum.

- Almost exclusively based on evaluating the target function. Additional logic is very simple.

**Drawbacks:**

- Very high computational cost. The target function must be evaluated at a large number of points for each initial candidate.
- As it is based on the derivative of the target function, the target function must be evaluated twice for each point that is really tested.
- The computational cost will depend on the precision one wants to achieve ( $\epsilon_2$ ).

## 9.2 Decision-Aided optimization

The next method we proposed to estimate  $t_0$  from the candidate set decodes the received sequence assuming that the initial considered point is a good approximation to  $t_0$ , so the decoded centroid will be indeed the one used at the embedder. From that estimate of the centroid used at the embedder, the scaling factor minimizing the distance from the scaled centroid to the received signal is computed.

It comprises the following steps:

- For each  $t(i)$  in the candidate set:

- centroid =  $Q_\Lambda \left( \frac{\mathbf{z}}{t(i)} - \mathbf{d} \right) + \mathbf{d}$ .
- $t_{\text{aux}} = \frac{\|\mathbf{z}\|^2}{\mathbf{z}^T \cdot \text{centroid}}$ .
- $L\_value(i) = L(t_{\text{aux}}, \mathbf{z})$ .
- $t_{\text{dfe}}(i) = t_{\text{aux}}$ .

- $i^* = \operatorname{argmin}_i L\_value(i)$ .
- If  $L(t_{\text{dfe}}(i^*), \mathbf{z}) < L(t_1, \mathbf{z})$  then
  - $\hat{t}(\mathbf{z}) = t_{\text{dfe}}(i^*)$ .

- else

- $\hat{t}(\mathbf{z}) = t_1$ .

**Advantages:**

- Reduced computational cost. The target function is only evaluated once per initial candidate point.
- Additional computational cost, beyond the target function evaluation, is cheap.
- The computational cost does not depend on the desired precision.

**Drawbacks:**

- The resulting estimate is not guaranteed to be a local minimum of the target function. The target function used for updating  $t(i)$ , i.e., the distance from the scaled estimated centroid to the received signal, is not the target function of our optimization problem (although under the proposed hypotheses it will be a good approximation).

**9.3 Progressively widened DA**

The two methods proposed so far verify that their computational cost is proportional to the number of points in the candidate set. Nevertheless, most of those points will be far from  $t_0$ , as the search interval will be usually pessimistic, since the probability of the real scaling factor being out of that interval will be set to a very small value. Therefore, a way for reducing the computational cost of the previous schemes would be to perform the optimization algorithm first at those points that one assumes to be most likely close to  $t_0$ , and check if one can trust on them for being a good estimate of  $t_0$ ; if one can, the search can be stopped. In order to do this suitability check, we will need some kind of test or measure informing us about the goodness of that point. Given that we have a statistical characterization of the target function both for  $t = t_0$  (provided in Sect. 3.1) and for  $t$  not being close to  $t_0$  (following the description provided in Sect.3.2), we will exploit these characterizations for proposing statistical tests that can help us to determine if a given point  $t$  is likely to be  $t_0$  or not.

Therefore, departing from a initial point that we think that could be a good estimate of  $t_0$ , e.g.  $t_1$ , we will perform an optimization in order to minimize the value of the target function, obtaining a value  $t_2$ . If the new point  $t_2$  passes the mentioned statistical test, then the search will be stopped and that point will be provided as our estimation of  $t_0$ . Otherwise, we will evaluate the statistical test for a larger and a smaller value of  $t$ . Consequently we will progressively widen the search interval taking as initial point  $t_1$  (or any other point that is assumed to be a good approximation to  $t_0$ ), so in most cases it will not be necessary to perform an optimization algorithm for all the points in the candidate set, but just in those that are considered to be more likely, allowing to reduce the computational cost of the resulting scheme.

Several choices can be proposed for the computation of  $t_2$ ; given that our final target is to have a good estimate of  $t_0$ , we could use the two optimization algorithms proposed in the last sections in order to compute that point. Indeed, in the subsequent description of the current method we will focus on the case where the DA-based scheme is used for computing the mentioned point. In that case, the current optimization method can be described for the scalar quantizer case as:

- $t_u = t_1$
- $t_l = t_1$
- $i = 1$

- found= 0
- While ((( $t_u \leq t_{\text{upper}}$ ) or ( $t_l \geq t_{\text{lower}}$ )) and (found= 0))
  - If ( $t_u \leq t_{\text{upper}}$ ) then
    - \* centroid =  $Q_{\Lambda} \left( \frac{\mathbf{z}}{t_u} - \mathbf{d} \right) + \mathbf{d}$ .
    - \*  $t_{\text{aux}} = \frac{\|\mathbf{z}\|^2}{\mathbf{z}^T \cdot \text{centroid}}$ .
    - \* L\_value( $i$ ) =  $L(t_{\text{aux}}, \mathbf{z})$ .
    - \*  $t_{\text{dfe}}(i) = t_{\text{aux}}$ .
    - \*  $i = i + 1$ .
    - \*
$$t_u = \frac{t_u \left[ \alpha \sigma_{\Lambda}^2 + \sigma_X^2 + \sigma_{\Lambda} \sqrt{\sigma_{\Lambda}^2 [(1 - \alpha)^2 + K_1(2\alpha - 1)] + K_1 \sigma_X^2} \right]}{\sigma_X^2 + \sigma_{\Lambda}^2 (1 - K_1)}.$$
  - If ( $t_l \geq t_{\text{lower}}$ ) then
    - \* If ( $i \neq 2$ ) then
      - centroid =  $Q_{\Lambda} \left( \frac{\mathbf{z}}{t_l} - \mathbf{d} \right) + \mathbf{d}$ .
      - $t_{\text{aux}} = \frac{\|\mathbf{z}\|^2}{\mathbf{z}^T \cdot \text{centroid}}$ .
      - L\_value( $i$ ) =  $L(t_{\text{aux}}, \mathbf{z})$ .
      - $t_{\text{dfe}}(i) = t_{\text{aux}}$ .
      - $i = i + 1$ .
    - \*
$$t_l = \frac{t_l \left[ \alpha \sigma_{\Lambda}^2 + 12\sigma_X^2 - \sigma_{\Lambda} \sqrt{\sigma_{\Lambda}^2 [(1 - \alpha)^2 + K_1(2\alpha - 1)] + K_1 \sigma_X^2} \right]}{\sigma_X^2 + \sigma_{\Lambda}^2 (1 - K_1)},$$
  - $i^* = \text{argmin}_i \text{L\_value}(i)$ .
  - If ( $(L(t_{\text{dfe}}(i^*), \mathbf{z}) < \tau_{t=t_0}(t_{\text{dfe}}(i^*), P_{e2}))$  and ( $L(t_{\text{dfe}}(i^*), \mathbf{z}) < \tau_{t \neq t_0}(t_{\text{dfe}}(i^*), P_{e3}))$ ) then
    - \* found = 1
- $i^* = \text{argmin}_i \text{L\_value}(i)$ .
- If  $L(t_{\text{dfe}}(i^*), \mathbf{z}) < L(t_1, \mathbf{z})$  then
  - $\hat{t}(\mathbf{z}) = t_{\text{dfe}}(i^*)$ .
- else
  - $\hat{t}(\mathbf{z}) = t_1$ .

where, assuming that the Gaussian approximation can be used,

$$\tau_{t=t_0}(t, P_{e2}) = \text{E}[L(t, \mathbf{Z})|t = t_0] + \sqrt{\text{Var}[L(t, \mathbf{Z})|t = t_0]} Q^{-1}(P_{e2}),$$



and

$$\tau_{t \neq t_0}(t, P_{e3}) = \mathbb{E}[L(t, \mathbf{Z})|t \neq t_0] + \sqrt{\text{Var}[L(t, \mathbf{Z})|t \neq t_0]}Q^{-1}(1 - P_{e3}),$$

with  $\mathbb{E}[L(t, \mathbf{Z})|t = t_0]$  taking the value in (8), and  $\text{Var}[L(t, \mathbf{Z})|t = t_0]$  by (9) for the scalar quantizer case and (10) for the high-dimensional good lattice case; for  $\mathbb{E}[L(t, \mathbf{Z})|t \neq t_0]$  and  $\text{Var}[L(t, \mathbf{Z})|t \neq t_0]$  we use

$$\mathbb{E}[L(t, \mathbf{Z})|t \neq t_0] = \frac{nt^2\sigma_\Lambda^2}{\sigma_N^2 + (1 - \alpha)^2t^2\sigma_\Lambda^2} + n \log [2\pi (\sigma_N^2 + (1 - \alpha)^2t^2\sigma_\Lambda^2)] + \frac{\|\mathbf{z}\|^2}{\sigma_X^2t^2},$$

and

$$\text{Var}[L(t, \mathbf{Z})|t \neq t_0] = \frac{n144t^4\sigma_\Lambda^4/180}{(\sigma_N^2 + (1 - \alpha)^2t^2\sigma_\Lambda^2)^2},$$

for the scalar quantizer case, while for the high-dimensional good lattice case

$$\text{Var}[L(t, \mathbf{Z})|t \neq t_0] = \frac{2nt^4\sigma_\Lambda^4}{(\sigma_N^2 + (1 - \alpha)^2t^2\sigma_\Lambda^2)^2};$$

note that the mean and variance used for the case  $t \neq t_0$  are not those at (11), as the values there depend on  $t_0$ , which is not available when running the optimization algorithm; therefore, we have preferred to consider the last term in the target function to be deterministic, as it was also done in Sect. 6.3.

Furthermore, when high-dimensional good lattices are used, one could replace the computation of  $t_u$  and  $t_l$  in the previous description of the algorithm, which is based on  $t_{u,\text{ld}}$  and  $t_{l,\text{ld}}$ , by its counterpart respectively based on  $t_{u,\text{hd}}$  and  $t_{l,\text{hd}}$ , defined in Sect. 8.2, or on some of its variants depending on the verification of (61).

**Advantages:**

- The number of points used for initializing the optimization algorithm is reduced in comparison with those used by the previously proposed algorithms.

**Drawbacks:**

- The statistical tests performed for checking the suitability of the studied points increase the computational cost per initial point.

## 9.4 On-line DA

All the methods presented so far are designed for working with blocks of  $n$  samples of the received signal. Nevertheless, practical communications schemes usually require on-line algorithms, where an algorithm output is generated each time a sample of the received signal is input. With this target in mind, an on-line version of the DA-based algorithm presented above was developed. Denoting by  $\mathbf{z}^{(j)} = (z_1, \dots, z_j)$ , the proposed scheme can be summarized as follows:

- locked = 0

- When the  $j$ -th sample is available:
    - If (locked= 0) then
      - \* Compute  $t_1$  using  $\mathbf{z}^{(j)}$  and a scheme of those introduced in Sect. 5.
    - else
      - \*  $t_1 = t_{\text{on-line}}$
    - centroid =  $Q_\Lambda \left( \frac{\mathbf{z}^{(j)}}{t_1} - \mathbf{d}^{(j)} \right) + \mathbf{d}^{(j)}$ .
    - $t_3 = \frac{\|\mathbf{z}^{(j)}\|^2}{(\mathbf{z}^{(j)})^T \cdot \text{centroid}}$ .
    - If  $((L(t_3, \mathbf{z}^{(j)}) < \tau_{t=t_0}(t_3, P_{e2}))$  and  $(L(t_3, \mathbf{z}^{(j)}) < \tau_{t \neq t_0}(t_3, P_{e3}))$ ) then
      - \* locked = 1
      - \*  $t_{\text{on-line}} = t_3$
    - else
      - \* Compute the interval search from  $t_3$  and  $\mathbf{z}^{(j)}$ , for  $P_{e1}$ .
      - \* Compute the candidate set from the interval search.
      - \* For each  $t(i)$  in the candidate set:
        - centroid =  $Q_\Lambda \left( \frac{\mathbf{z}^{(j)}}{t(i)} - \mathbf{d}^{(j)} \right) + \mathbf{d}^{(j)}$ .
        - $t_{\text{aux}} = \frac{\|\mathbf{z}^{(j)}\|^2}{(\mathbf{z}^{(j)})^T \cdot \text{centroid}}$ .
        - $L\_value(i) = L(t_{\text{aux}}, \mathbf{z}^{(j)})$ .
        - $t_{\text{dfe}}(i) = t_{\text{aux}}$ .
      - \*  $i^* = \text{argmin}_i L\_value(i)$ .
      - \* If  $L(t_{\text{dfe}}(i^*), \mathbf{z}^{(j)}) < L(t_1, \mathbf{z}^{(j)})$  then
        - $t_1 = t_{\text{dfe}}(i^*)$ .
      - \* If  $((L(t_1, \mathbf{z}^{(j)}) < \tau_{t=t_0}(t_1, P_{e4}))$  and  $(L(t_1, \mathbf{z}^{(j)}) < \tau_{t \neq t_0}(t_1, P_{e5}))$ ) then
        - locked = 1.
        - $t_{\text{on-line}} = t_1$ .
      - \* else
        - locked = 0.
- The output estimation is  $t_{\text{on-line}}$ .

#### Advantages:

- Once the system is locked, a very reduced computational cost is required.
- Due to the statistical characterization of  $L(t, \mathbf{z})$ , one knows when  $t_{\text{on-line}}$  is a good estimate.
- It allows to establish different threshold probabilities depending on the system being initially locked or not ( $P_{e2}$  and  $P_{e3}$ , versus  $P_{e4}$  and  $P_{e5}$ , respectively).

**Drawbacks:**

- If the system unlocks, one must define a search interval and run the optimization algorithm considering each point in the candidate set as initial point (although a strategy similar to *Progressively Widened DA* might be also adopted); this could make difficult a real-time implementation where all the received samples were processed.

## 9.5 General remark

Finally, we would like to remark that there is a series of parameters involved in all the proposed schemes that allow to achieve a trade-off between computational cost and estimation algorithm performance. Some of these parameters are  $P_{e1}$ ,  $P_{e2}$ ,  $P_{e3}$ ,  $P_{e4}$ ,  $P_{e5}$ , and  $K_1$ . Setting these parameters to different values, one can range from the basic variance-based estimator to more sophisticated and accurate estimates. Therefore, the choice of those parameters values will depend on the considered application scenario.

Furthermore, one could also think of other optimization algorithms specially designed for working in strongly computationally constrained scenarios. For example, one could envisage the case where only a fixed number of candidates can be considered as initial points of the optimization algorithm, due to real-time computation restrictions; in that case, a possible choice could be to take as initial point of the search interval sampling method  $t_1$ , and then calculate the two sequences of both larger and smaller candidates, obtained by applying the formulas derived in Sect. 8, until the upper-bounded number of initial points being achieved.

## 10 Fisher information analysis

For calculating the Fisher information of the proposed scheme, we will use the pdf approximation in (6), whose minus logarithm is

$$\frac{1}{2} \left[ \frac{\|(\mathbf{z}-t\mathbf{d})\bmod(t\Lambda)\|^2}{\sigma_N^2+(1-\alpha)^2t^2\sigma_\Lambda^2} + n \log (2\pi (\sigma_N^2 + (1-\alpha)^2t^2\sigma_\Lambda^2)) + \frac{\|\mathbf{z}\|^2}{\sigma_X^2t^2} + n \log (2\pi\sigma_X^2) \right]; \quad (62)$$

in order to statistically characterize the first term, we will consider that, as it was shown above,  $(\mathbf{z} - t\mathbf{d})\bmod(t\Lambda) = [(t_0 - t)\mathbf{x} + (t - \alpha t_0)[(\mathbf{x} - \mathbf{d})\bmod\Lambda] + n]\bmod(t\Lambda)$ , so (62) can be rewritten as

$$\frac{1}{2} \left[ \frac{\|[(t_0-t)\mathbf{x}+(t-\alpha t_0)[(\mathbf{x}-\mathbf{d})\bmod\Lambda]+\mathbf{n}]\bmod(t\Lambda)\|^2}{\sigma_N^2+(1-\alpha)^2t^2\sigma_\Lambda^2} + n \log (2\pi (\sigma_N^2 + (1-\alpha)^2t^2\sigma_\Lambda^2)) + \frac{\|(\mathbf{x}+\mathbf{w})_{t_0}+\mathbf{n}\|^2}{\sigma_X^2t^2} + n \log (2\pi\sigma_X^2) \right]. \quad (63)$$

In order to calculate the Fisher information we will evaluate the second derivative of (63) with respect to  $t$  at  $t_0$ ; consequently, we will be only interested in

those values of  $t$  in an arbitrarily small neighborhood around  $t_0$ . Thus, as far as  $(1 - \alpha)t_0^2\sigma_\Lambda^2 + \sigma_N^2 \ll t_0^2\sigma_\Lambda^2$ , i.e., as far as  $\text{TNLR} \rightarrow 0$  for the low-dimensional lattice case, or  $(1 - \alpha)t_0^2\sigma_\Lambda^2 + \sigma_N^2 < t_0^2\sigma_\Lambda^2$ , i.e., as far as  $\text{TNLR} < 1$  for the high-dimensional good lattice case, we can neglect the modulo- $\Lambda$  reduction in the first term, and (63) can be rewritten as

$$\frac{1}{2} \left[ \frac{\| (t_0 - t)\mathbf{x} + (t - \alpha t_0)[(\mathbf{x} - \mathbf{d}) \bmod \Lambda] + \mathbf{n} \|^2}{\sigma_N^2 + (1 - \alpha)^2 t^2 \sigma_\Lambda^2} + n \log (2\pi (\sigma_N^2 + (1 - \alpha)^2 t^2 \sigma_\Lambda^2)) \right. \\ \left. + \frac{\| (\mathbf{x} + \mathbf{w})t_0 + \mathbf{n} \|^2}{\sigma_X^2 t^2} + n \log (2\pi \sigma_X^2) \right]. \quad (64)$$

Calculating the first derivative of the last expression with respect to  $t$ , one obtains

$$\frac{1}{2} \sum_{j=1}^n \left[ - \frac{2((t_0 - t)x_j + (t - \alpha t_0)w_j + n_j)(\sigma_N^2(x_j - w_j) + (1 - \alpha)^2 \sigma_\Lambda^2 t(n_j + t_0(x_j - \alpha w_j)))}{(\sigma_N^2 + (1 - \alpha)^2 t^2 \sigma_\Lambda^2)^2} \right. \\ \left. + \frac{2(1 - \alpha)^2 \sigma_\Lambda^2 t}{\sigma_N^2 + (1 - \alpha)^2 t^2 \sigma_\Lambda^2} - \frac{2((x_j + w_j)t_0 + n_j)^2}{\sigma_X^2 t^3} \right], \quad (65)$$

and the second derivative is

$$\frac{1}{2} \sum_{j=1}^n \left[ 2 \left( \sigma_N^4 (w_j - x_j)^2 + (1 - \alpha)^4 \sigma_\Lambda^4 t^2 ((x_j - \alpha w_j)t_0 + n_j) ((3t_0 - 2t)x_j - (3t_0\alpha - 2t)w_j + 3n_j) \right. \right. \\ \left. \left. - (1 - \alpha)^2 \sigma_\Lambda^2 \sigma_N^2 \left[ 3t^2 (w_j - x_j)^2 + n_j^2 - 6tt_0 (w_j - x_j)(\alpha w_j - x_j) + t_0^2 (x_j - \alpha w_j)^2 \right. \right. \right. \\ \left. \left. + 2n_j (3t(w_j - x_j) + t_0(x_j - \alpha w_j)) \right] \right) (\sigma_N^2 + (1 - \alpha)^2 \sigma_\Lambda^2 t^2)^{-3} \\ \left. + \frac{2(1 - \alpha)^2 \sigma_\Lambda^2 \sigma_N^2 - 2(1 - \alpha)^4 \sigma_\Lambda^4 t^2}{(\sigma_N^2 + (1 - \alpha)^2 \sigma_\Lambda^2 t^2)^2} + \frac{6((x_j + w_j)t_0 + n_j)^2}{\sigma_X^2 t^4} \right].$$

Calculating the mean with respect to  $\mathbf{X}$ ,  $\mathbf{W}$ , and  $\mathbf{N}$ , one obtains

$$n \left( \sigma_N^4 (\sigma_X^2 + \alpha^2 \sigma_\Lambda^2) + (1 - \alpha)^4 \sigma_\Lambda^4 t^2 (t_0(3t_0 - 2t)\sigma_X^2 + t_0(3\alpha t_0 - 2t)\alpha^3 \sigma_\Lambda^2 + 3\sigma_N^2) \right. \\ \left. - (1 - \alpha)^2 \sigma_\Lambda^2 \sigma_N^2 \left[ 3t^2 (\sigma_X^2 + \alpha^2 \sigma_\Lambda^2) + \sigma_N^2 - 6tt_0 (\sigma_X^2 + \alpha^3 \sigma_\Lambda^2) + t_0^2 (\sigma_X^2 + \alpha^4 \sigma_\Lambda^2) \right] \right) \\ (\sigma_N^2 + (1 - \alpha)^2 \sigma_\Lambda^2 t^2)^{-3} + n \frac{(1 - \alpha)^2 \sigma_\Lambda^2 \sigma_N^2 - (1 - \alpha)^4 \sigma_\Lambda^4 t^2}{(\sigma_N^2 + (1 - \alpha)^2 \sigma_\Lambda^2 t^2)^2} + \frac{3n ((\sigma_X^2 + \alpha^2 \sigma_\Lambda^2)t_0^2 + \sigma_N^2)}{\sigma_X^2 t^4};$$

evaluating that expression at  $t = t_0$ , the result is the Fisher information

$$I(t_0) = n \left( \sigma_N^4 (\sigma_X^2 + \alpha^2 \sigma_\Lambda^2) + (1 - \alpha)^4 \sigma_\Lambda^4 t_0^2 (t_0^2 \sigma_X^2 + t_0^2 (3\alpha - 2)\alpha^3 \sigma_\Lambda^2 + 3\sigma_N^2) \right. \\ \left. - (1 - \alpha)^2 \sigma_\Lambda^2 \sigma_N^2 \left[ 3t_0^2 (\sigma_X^2 + \alpha^2 \sigma_\Lambda^2) + \sigma_N^2 - 6t_0^2 (\sigma_X^2 + \alpha^3 \sigma_\Lambda^2) + t_0^2 (\sigma_X^2 + \alpha^4 \sigma_\Lambda^2) \right] \right) \\ (\sigma_N^2 + (1 - \alpha)^2 t_0^2 \sigma_\Lambda^2)^{-3} + n \frac{(1 - \alpha)^2 \sigma_\Lambda^2 \sigma_N^2 - (1 - \alpha)^4 \sigma_\Lambda^4 t_0^2}{(\sigma_N^2 + (1 - \alpha)^2 \sigma_\Lambda^2 t_0^2)^2} + \frac{3n ((\sigma_X^2 + \alpha^2 \sigma_\Lambda^2)t_0^2 + \sigma_N^2)}{\sigma_X^2 t_0^4}.$$

In order to get a larger insight into the last formula, and be able to use it for further theoretical derivations, we will approximate the first term taking into account that  $\text{HLR} \rightarrow \infty$ , and  $\text{TNLR} < 1$ , so it will asymptotically converge to

$$\frac{n \left( \sigma_X^2 (\sigma_N^4 + (1-\alpha)^4 \sigma_\Lambda^4 t_0^4 + 2(1-\alpha)^2 \sigma_\Lambda^2 \sigma_N^2 t_0^2) \right)}{(\sigma_N^2 + (1-\alpha)^2 \sigma_\Lambda^2 t_0^2)^3} = \frac{n \left( \sigma_X^2 (\sigma_N^2 + (1-\alpha)^2 \sigma_\Lambda^2 t_0^2)^2 \right)}{(\sigma_N^2 + (1-\alpha)^2 \sigma_\Lambda^2 t_0^2)^3} = \frac{n \sigma_X^2}{\sigma_N^2 + (1-\alpha)^2 \sigma_\Lambda^2 t_0^2}, \quad (66)$$

going to infinity under the aforementioned conditions. Concerning the second term, it can be lower-bounded as

$$n \frac{(1-\alpha)^2 \sigma_\Lambda^2 \sigma_N^2 - (1-\alpha)^4 \sigma_\Lambda^4 t_0^2}{(\sigma_N^2 + (1-\alpha)^2 \sigma_\Lambda^2 t_0^2)^2} \geq n \frac{-(1-\alpha)^4 \sigma_\Lambda^4 t_0^2}{(\sigma_N^2 + (1-\alpha)^2 \sigma_\Lambda^2 t_0^2)^2} \geq n \frac{-(1-\alpha)^4 \sigma_\Lambda^4 t_0^2}{((1-\alpha)^2 \sigma_\Lambda^2 t_0^2)^2} = \frac{-n}{t_0^2};$$

similarly, it can be upper-bounded as

$$n \frac{(1-\alpha)^2 \sigma_\Lambda^2 \sigma_N^2 - (1-\alpha)^4 \sigma_\Lambda^4 t_0^2}{(\sigma_N^2 + (1-\alpha)^2 \sigma_\Lambda^2 t_0^2)^2} \leq n \frac{(1-\alpha)^2 \sigma_\Lambda^2 \sigma_N^2}{(\sigma_N^2 + (1-\alpha)^2 \sigma_\Lambda^2 t_0^2)^2} \leq n \frac{(1-\alpha)^2 \sigma_\Lambda^2 \sigma_N^2}{2(1-\alpha)^2 \sigma_\Lambda^2 \sigma_N^2 t_0^2} = \frac{n}{2t_0^2}.$$

Finally, based on  $\text{HLR} \rightarrow \infty$ , and  $\text{TNLR} < 1$ , the last term will go to  $\frac{3n}{t_0^2}$ . Therefore, as long as  $t_0 > 0$ ,  $\text{HLR} \rightarrow \infty$ , and  $\text{TNLR} < 1$ , the Fisher information will asymptotically converge to (66). In terms of  $\sigma_X^2$ ,  $\sigma_W^2$ ,  $\sigma_N^2$ ,  $t_0$ , and  $\alpha$  (66) can be written as

$$I(t_0) = \frac{n \sigma_X^2}{\sigma_N^2 + \frac{(1-\alpha)^2}{\alpha^2} \sigma_W^2 t_0^2}. \quad (67)$$

It is interesting to note that the last function is monotonically increasing with  $\alpha$ . Nevertheless, in order to  $\text{TNLR} < 1$  (the relaxed condition on **Hypothesis 3** corresponding to high-dimensional good lattices), the following upper-bound on the feasible value of  $\alpha$  can be established

$$\alpha \leq \min \left( \frac{2\sigma_W^2 t_0^2}{\sigma_N^2 + \sigma_W^2 t_0^2} - \epsilon, 1 \right) \triangleq \alpha_{\text{sup-FI}},$$

where  $\epsilon > 0$  is arbitrarily small, and the left term in the min function is nothing but twice the  $\alpha$  proposed by Costa, after replacing the embedded signal power by its effective value at the receiver;  $\alpha_{\text{sup-FI}}$  stands for the supremum of  $\alpha$  values such that  $\text{TNLR} < 1$ , which at the same time is arbitrarily close to the value of  $\alpha$  maximizing the Fisher information.

Remember that for the low-dimensional lattice case, the condition on  $\text{TNLR}$  is  $\text{TNLR} \rightarrow 0$ , being much more strict, and constraining  $\alpha$  to be smaller than  $\alpha_{\text{sup-FI}}$ . Consequently, the value of the Fisher information for the scalar/low-dimensional lattice quantizer case will be smaller than that achieved for high-dimensional good lattices, proving the goodness of the latter for this application.

In any case, the difference between the value of  $\alpha$  maximizing the Fisher information for low-dimensional lattices and  $\alpha_{\text{sup-FI}}$  will verify:

- The larger the shaping-gain of the considered lattice, the closer both values will be, as the fundamental Voronoi region of that lattice will be more similar to a hypersphere, reducing the probability that the total noise is modulo- $\Lambda$  reduced.
- The smaller the effective WNR,  $\sigma_W^2 t_0^2 / \sigma_N^2$ , the closer both values will be. Indeed, the smaller the effective WNR, the smaller will be the importance of the AWGN introduced by the channel in the total noise, and the more important the role of the self-noise; nevertheless, the self-noise has the same shape that the fundamental Voronoi region of the considered lattice, so it does not produce modulo- $\Lambda$  reduction.

From a geometric point of view, one can see the links between the Fisher information and the curvature (usually defined as the second derivative of the considered function) of the target function at  $t = t_0$ .

### 10.1 Fisher information based on Erez's approach

In order to show that the obtained result could be also achieved by using Erez's lattice-quantization approach, instead of the one followed in the last sections (more related to Chen and Wornell's interpretation), in this section we summarize what would happen if Erez's quantizing strategy were followed. For the sake of avoiding unnecessary repetition, we will focus on those aspects that differ from the approach introduced above.

In Erez's approach, the watermarked signal would be calculated as

$$\mathbf{y} = \mathbf{x} - [(\alpha \mathbf{x} - \mathbf{d}) \bmod \Lambda],$$

so

$$f_{\mathbf{Z}|T,K}(\mathbf{z}|t, \mathbf{d}) \approx \frac{|\mathcal{V}(\Lambda)| e^{-\frac{\|\mathbf{z}\|^2}{2\sigma_X^2 t^2}} e^{-\frac{\|(\alpha \mathbf{z} - t \mathbf{d}) \bmod (t\Lambda)\|^2}{2(\alpha^2 \sigma_N^2 + (1-\alpha)^2 t^2 \sigma_\Lambda^2)}}}{(2\pi\sigma_X^2)^{n/2} \left[ 2\pi (\alpha^2 \sigma_N^2 + (1-\alpha)^2 t^2 \sigma_\Lambda^2) \right]^{n/2}}, \quad (68)$$

and

$$\begin{aligned}
(\alpha \mathbf{z} - t \mathbf{d}) \bmod(t\Lambda) &= \left[ \alpha t_0 \left( \mathbf{x} - [(\alpha \mathbf{x} - \mathbf{d}) \bmod \Lambda] \right) + \alpha \mathbf{n} - t \mathbf{d} \right] \bmod(t\Lambda) \\
&= \left[ t_0 \left( \alpha \mathbf{x} - \alpha [(\alpha \mathbf{x} - \mathbf{d}) \bmod \Lambda] \right) + \alpha \mathbf{n} - t \mathbf{d} \right] \bmod(t\Lambda) \\
&= \left[ (t_0 - t) \alpha \mathbf{x} - (t_0 - t) \alpha [(\alpha \mathbf{x} - \mathbf{d}) \bmod \Lambda] + \alpha \mathbf{n} \right. \\
&\quad \left. + t \left( \alpha \mathbf{x} - \mathbf{d} - \alpha [(\alpha \mathbf{x} - \mathbf{d}) \bmod \Lambda] \right) \right] \bmod(t\Lambda) \\
&= \left[ (t_0 - t) \alpha \mathbf{x} - (t_0 - t) \alpha [(\alpha \mathbf{x} - \mathbf{d}) \bmod \Lambda] + \alpha \mathbf{n} \right. \\
&\quad \left. + t \left( (\alpha \mathbf{x} - \mathbf{d}) \bmod \Lambda - \alpha [(\alpha \mathbf{x} - \mathbf{d}) \bmod \Lambda] \right) \right] \bmod(t\Lambda) \\
&= \left[ (t_0 - t) \alpha \mathbf{x} - (t_0 - t) \alpha [(\alpha \mathbf{x} - \mathbf{d}) \bmod \Lambda] + \alpha \mathbf{n} \right. \\
&\quad \left. + t(1 - \alpha) \left( (\alpha \mathbf{x} - \mathbf{d}) \bmod \Lambda \right) \right] \bmod(t\Lambda) \\
&= \left[ (t_0 - t) \alpha \mathbf{x} + (t - \alpha t_0) [(\alpha \mathbf{x} - \mathbf{d}) \bmod \Lambda] + \alpha \mathbf{n} \right] \bmod(t\Lambda).
\end{aligned}$$

As it was shown in Sect. 10, when computing the derivatives of the logarithm of the pdf the dominant term will be the that corresponding to  $[(t_0 - t) \alpha \mathbf{x}] \bmod(t\Lambda)$ , so we will approximate the first derivative of minus the logarithm of (68) with respect to  $t$  by

$$\sum_{j=1}^n \frac{\alpha^2 (t - t_0) (\alpha^2 \sigma_N^2 + (1 - \alpha)^2 t t_0 \sigma_\Lambda^2) x_j^2}{(\alpha^2 \sigma_N^2 + (1 - \alpha)^2 t^2 \sigma_\Lambda^2)^2},$$

and the second derivative by

$$\begin{aligned}
&\sum_{j=1}^n \left( 2\alpha^2 \left[ \sigma_N^2 (\alpha^4 \sigma_N^2 - 3(1 - \alpha)^2 \alpha^2 t^2 \sigma_\Lambda^2) - 2(1 - \alpha)^2 \sigma_\Lambda^2 t (-3\alpha^2 \sigma_N^2 + (1 - \alpha)^2 t^2 \sigma_\Lambda^2) t_0 \right. \right. \\
&\quad \left. \left. + (1 - \alpha)^2 \sigma_\Lambda^2 (-\alpha^2 \sigma_N^2 + 3(1 - \alpha)^2 t^2 \sigma_\Lambda^2) t_0^2 \right] x_j^2 \right) (\alpha^2 \sigma_N^2 + (1 - \alpha)^2 t^2 \sigma_\Lambda^2)^{-3}.
\end{aligned}$$

Taking the mean of the last expression and replacing  $t$  by  $t_0$ , one obtains

$$\begin{aligned}
&n \left( 2\alpha^2 \left[ \sigma_N^2 (\alpha^4 \sigma_N^2 - 3(1 - \alpha)^2 \alpha^2 \sigma_\Lambda^2 t_0^2) - 2(1 - \alpha)^2 \sigma_\Lambda^2 t_0 (-3\alpha^2 \sigma_N^2 + (1 - \alpha)^2 t_0^2 \sigma_\Lambda^2) t_0 \right. \right. \\
&\quad \left. \left. + (1 - \alpha)^2 \sigma_\Lambda^2 (-\alpha^2 \sigma_N^2 + 3(1 - \alpha)^2 t_0^2 \sigma_\Lambda^2) t_0^2 \right] \sigma_X^2 \right) (\alpha^2 \sigma_N^2 + (1 - \alpha)^2 t_0^2 \sigma_\Lambda^2)^{-3} = \\
&\quad \frac{n \alpha^2 \sigma_X^2}{\alpha^2 \sigma_N^2 + (1 - \alpha)^2 t_0^2 \sigma_\Lambda^2};
\end{aligned}$$

therefore, the Fisher information in terms of  $\sigma_X^2$ ,  $\sigma_W^2$ ,  $\sigma_N^2$ ,  $t_0$ , and  $\alpha$  is given by

$$I(t_0) = \frac{n\alpha^2\sigma_X^2}{\alpha^2\sigma_N^2 + (1-\alpha)^2\sigma_W^2 t_0^2}, \quad (69)$$

providing the same result that was previously described in (67).

## 11 Bias analysis

At the sight of (65), it is evident that the derivation of  $\hat{t}(\mathbf{z})$ , even when one just considers a small neighborhood around  $t_0$ , is a tough question. Indeed, one must find the roots of a six-order polynomial. Furthermore, in order to compute the bias, one should average over the pdfs of  $\mathbf{X}$ ,  $\mathbf{W}$ , and  $\mathbf{N}$  those cumbersome expressions. Therefore, some simplifications will be required in order to be able to derive insightful results. In this report, the bias analysis will be based on the following assumptions:

- $n \rightarrow \infty$ : this will allow us to replace the square Euclidean norm of a random vector by its variance.
- We will constrain our analysis to the high-dimensional good lattice case, as in that case, as long as  $\text{TNLR} < 1$  the modulo-lattice reduction can be neglected.
- As it was mentioned before in this report, we will assume that the variance of the modulo-reduced version of the total noise vector is equal to the variance the total noise vector as long as the latter is smaller than or equal to  $\sigma_\Lambda^2 t^2$ , i.e.,  $\text{TNLR} < 1$ , and equal to  $\sigma_\Lambda^2 t^2$  otherwise.

Therefore, based on  $\sigma_E^2(t) \triangleq (t_0 - t)^2\sigma_X^2 + (t - \alpha t_0)^2\sigma_\Lambda^2 + \sigma_N^2$ , our study of the bias will be splitted into two different scenarios:

- $\sigma_E^2(t) < \sigma_\Lambda^2 t^2$ , or equivalently,  $t \in (t_{l,\text{hd}}, t_{u,\text{hd}})$ , based on the results derived in Sect. 8.2 (formulas (59) and (60)).
- $\sigma_E^2(t) \geq \sigma_\Lambda^2 t^2$ , or equivalently  $t \leq t_{l,\text{hd}}$ , or  $t \geq t_{u,\text{hd}}$ .

Obviously,

$$\min_{t \in (t_{l,\text{hd}}, t_{u,\text{hd}})} \frac{L(t, \mathbf{z})}{n} \leq \frac{L(t_0, \mathbf{z})}{n},$$

since, as it was proved in Sect. 8.2, whenever  $\text{TNLR} \leq 1$ ,  $t_0 \in (t_{l,\text{hd}}, t_{u,\text{hd}})$ . Therefore, if

$$\frac{L(t_0, \mathbf{z})}{n} \leq \min_{t \in (0, t_{l,\text{hd}}] \cup [t_{u,\text{hd}}, \infty)} \frac{L(t, \mathbf{z})}{n},$$

it would be clear that the minimum of the target function would be achieved in  $(t_{l,\text{hd}}, t_{u,\text{hd}})$ , and we could focus our analysis in that interval.



We base our comparison on  $\text{HLR} \rightarrow \infty$ , and  $\text{TNLR} < 1$ , so

$$\frac{L(t_0, \mathbf{z})}{n} = 2 + \log [2\pi (\sigma_N^2 + (1 - \alpha)^2 \sigma_\Lambda^2 t_0^2)],$$

and, for  $t \in (0, t_{l,\text{hd}}] \cup [t_{u,\text{hd}}, \infty)$ ,

$$\frac{L(t, \mathbf{z})}{n} \approx \frac{\sigma_\Lambda^2 t^2}{\sigma_N^2 + (1 - \alpha)^2 \sigma_\Lambda^2 t^2} + \log [2\pi (\sigma_N^2 + (1 - \alpha)^2 \sigma_\Lambda^2 t^2)] + \frac{t_0^2}{t^2};$$

it is straightforward to see that the result of subtracting the first formula to the second one is

$$\frac{t_0^2}{t^2} - 2 + \frac{\sigma_\Lambda^2 t^2}{\sigma_N^2 + (1 - \alpha)^2 \sigma_\Lambda^2 t^2} + \log \left( \frac{\sigma_N^2 + (1 - \alpha)^2 t^2 \sigma_\Lambda^2}{\sigma_N^2 + (1 - \alpha)^2 t_0^2 \sigma_\Lambda^2} \right),$$

which is nothing but  $f(t, \sigma_\Lambda^2)$ , defined in (37). In Sect. 6.3.1 we have already proved that this function is non-negative for any  $t$ , confirming that the minimum of the target function will be achieved in  $(t_{l,\text{hd}}, t_{u,\text{hd}})$

Therefore, we will focus our analysis on the interval  $t \in (t_{l,\text{hd}}, t_{u,\text{hd}})$ . Based on the assumptions mentioned at the beginning of this section,  $L(t, \mathbf{z})/n$  can be approximated by

$$\frac{L(t, \mathbf{z})}{n} \approx \frac{(t_0 - t)^2 \sigma_X^2 + (t - \alpha t_0)^2 \sigma_\Lambda^2 + \sigma_N^2}{\sigma_N^2 + (1 - \alpha)^2 \sigma_\Lambda^2 t^2} + \log [2\pi (\sigma_N^2 + (1 - \alpha)^2 \sigma_\Lambda^2 t^2)] + \frac{(\sigma_X^2 + \alpha^2 \sigma_\Lambda^2) t_0^2 + \sigma_N^2}{\sigma_X^2 t^2} \quad (70)$$

whose derivative with respect to  $t$  is

$$\begin{aligned} & \frac{2\sigma_N^2 [(2 - \alpha) \alpha \sigma_\Lambda^2 + \sigma_X^2] t + 2(\alpha \sigma_\Lambda^2 + \sigma_X^2) ((1 - \alpha)^2 \sigma_\Lambda^2 t^2 - \sigma_N^2) t_0 - 2(1 - \alpha)^2 \sigma_\Lambda^2 (\sigma_X^2 + \alpha^2 \sigma_\Lambda^2) t t_0^2}{(\sigma_N^2 + (1 - \alpha)^2 \sigma_\Lambda^2 t^2)^2} \\ & + \frac{2(1 - \alpha)^2 \sigma_\Lambda^2 t}{\sigma_N^2 + (1 - \alpha)^2 \sigma_\Lambda^2 t^2} + \frac{2[(\sigma_X^2 + \alpha^2 \sigma_\Lambda^2) t_0^2 + \sigma_N^2]}{\sigma_X^2 t^3}. \end{aligned}$$

In order to find the points where the derivative is null, we can multiply the last formula by  $\sigma_X^2 t^3 (\sigma_N^2 + (1 - \alpha)^2 \sigma_\Lambda^2 t^2)^2$ , obtaining a polynomial that can be written as  $a_0 + a_1 t + a_2 t^2 + a_3 t^3 + a_4 t^4 + a_5 t^5 + a_6 t^6$ , where

$$\begin{aligned} a_0 &= -2\sigma_N^4 [(\sigma_X^2 + \alpha^2 \sigma_\Lambda^2) t_0^2 + \sigma_N^2], \\ a_1 &= 0, \\ a_2 &= -4(1 - \alpha)^2 \sigma_\Lambda^2 \sigma_N^2 [(\sigma_X^2 + \alpha^2 \sigma_\Lambda^2) t_0^2 + \sigma_N^2], \\ a_3 &= -2\sigma_N^2 \sigma_X^2 (\sigma_X^2 + \alpha \sigma_\Lambda^2) t_0, \\ a_4 &= -2 \left( -\sigma_N^2 \sigma_X^4 + (1 - \alpha)^4 \alpha^2 \sigma_\Lambda^6 t_0^2 + \sigma_\Lambda^2 \sigma_X^2 [(1 - \alpha)^2 \sigma_X^2 t_0^2 - \sigma_N^2] \right. \\ & \quad \left. + (1 - \alpha)^2 \sigma_\Lambda^4 [(1 - \alpha)^2 \sigma_N^2 + (1 - 2\alpha + 2\alpha^2) \sigma_X^2 t_0^2] \right), \\ a_5 &= 2(1 - \alpha)^2 \sigma_\Lambda^2 \sigma_X^2 (\alpha \sigma_\Lambda^2 + \sigma_X^2) t_0, \\ a_6 &= 2(1 - \alpha)^4 \sigma_\Lambda^4 \sigma_X^2; \end{aligned}$$

therefore, using Descartes' sign rule, the mentioned derivative will be null at most at one positive  $t$ .

As the solution of the previous polynomial is indeed pretty cumbersome, for any  $t_0 > \epsilon$ , with  $\epsilon > 0$ , we will calculate the order 2 Taylor series expansion around  $t_0$ , i.e.,  $b_0 + b_1(t - t_0) + b_2(t - t_0)^2/2$ , based on the reasonable assumption that the minimum of  $L(t, \mathbf{z})$  will be close to  $t_0$ . Take into account that this assumption is based on  $t \in (t_{l,\text{hd}}, t_{u,\text{hd}})$ ,  $\text{HLR} \rightarrow \infty$ , and  $\text{TNLR} < 1$ ; as it was mentioned in Sect. 8.2, under those conditions both  $t_{l,\text{hd}}$ , and  $t_{u,\text{hd}}$  go to  $t_0$ . The resulting Taylor series expansion will be optimized. Consequently, we will evaluate  $L(t, \mathbf{z})/n$  and (71) at  $t = t_0$ , yielding

$$b_0 = 2 + \frac{\sigma_N^2 + \alpha^2 \sigma_\Lambda^2 t_0^2}{\sigma_X^2 t_0^2} + \log [2\pi (\sigma_N^2 + (1 - \alpha)^2 \sigma_\Lambda^2 t_0^2)],$$

$$b_1 = \frac{2(1 - \alpha) \sigma_\Lambda^2 t_0}{\sigma_N^2 + (1 - \alpha)^2 \sigma_\Lambda^2 t_0^2} - \frac{2 [(\sigma_X^2 + \alpha^2 \sigma_\Lambda^2) t_0^2 + \sigma_N^2]}{\sigma_X^2 t_0^3}.$$

Concerning the order two coefficient, we will calculate the second derivative of (70), yielding

$$2 \left( \sigma_N^4 \sigma_X^2 - (1 - \alpha)^4 \sigma_\Lambda^6 t^2 \left[ (1 - \alpha)^2 t^2 + 2\alpha t t_0 - 3\alpha^2 t_0^2 \right] \right. \\ \left. + (1 - \alpha)^2 \sigma_\Lambda^4 \left( 3(-2\alpha) \alpha \sigma_N^2 t^2 - 2t \left[ (1 - \alpha)^2 \sigma_X^2 t^2 - 3\alpha \sigma_N^2 \right] t_0 + \left[ 3(1 - \alpha)^2 \sigma_X^2 t^2 - \alpha^2 \sigma_N^2 \right] t_0^2 \right) \right. \\ \left. + \sigma_\Lambda^2 \sigma_N^2 \left[ \sigma_N^2 - (1 - \alpha)^2 \sigma_X^2 (3t^2 - 6t t_0 + t_0^2) \right] \right) \left( \sigma_N^2 + (1 - \alpha)^2 \sigma_\Lambda^2 t^2 \right)^{-3} + \frac{6 [(\sigma_X^2 + \alpha^2 \sigma_\Lambda^2) t_0^2 + \sigma_N^2]}{\sigma_X^2 t^4},$$

that evaluated at  $t = t_0$  gives

$$b_2 = \frac{4(1 - \alpha)^2 \sigma_\Lambda^2 \sigma_N^2 + 2 [(2\alpha^2 - 1) \sigma_\Lambda^2 + \sigma_X^2] (\sigma_N^2 + (1 - \alpha)^2 \sigma_\Lambda^2 t_0^2)}{(\sigma_N^2 + (1 - \alpha)^2 \sigma_\Lambda^2 t_0^2)^2} + \frac{6 [(\sigma_X^2 + \alpha^2 \sigma_\Lambda^2) t_0^2 + \sigma_N^2]}{\sigma_X^2 t_0^4}.$$

An example of the resulting approximation can be found in Fig. 17.

Obviously, the minimum will be achieved at  $t_{\min} = t_0 - \frac{b_1}{b_2}$ . In order to gain theoretical insight, we will use that  $\text{HLR} \rightarrow \infty$ , and  $\text{TNLR} < 1$ , or equivalently for fixed  $\sigma_\Lambda^2$  and  $\sigma_N^2$ ,  $\sigma_X^2 \rightarrow \infty$ , for calculating

$$\lim_{\sigma_X^2 \rightarrow \infty} -\frac{\sigma_X^2 b_1}{b_2} = \frac{\sigma_N^2 + (\alpha^2 - \alpha) \sigma_\Lambda^2 t_0^2}{t_0} = \frac{\sigma_N^2}{t_0} - \frac{(1 - \alpha) \sigma_W^2 t_0}{\alpha}.$$

Therefore, the bias in that asymptotic case has been shown to converge to

$$b(t_0) = \frac{1}{\sigma_X^2} \left[ \frac{\sigma_N^2}{t_0} - \frac{(1 - \alpha) \sigma_W^2 t_0}{\alpha} \right]. \quad (71)$$

It is easy to see that under the assumptions of  $\text{HLR} \rightarrow \infty$ , and  $\text{TNLR} < 1$ , the bias nullifies for

$$\alpha_{\text{no-bias}} \triangleq \frac{\sigma_W^2 t_0^2}{\sigma_N^2 + \sigma_W^2 t_0^2},$$

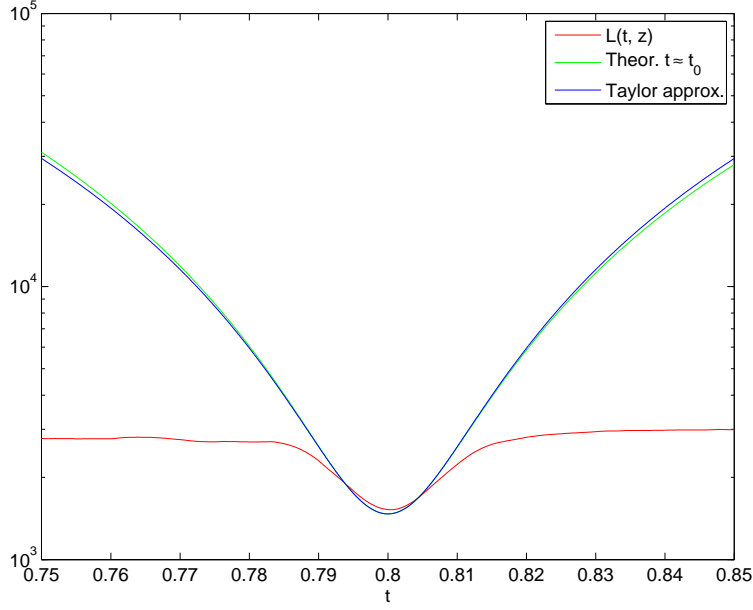


Figure 17: Comparison between  $L(t, \mathbf{z})$ , (70) and the order 2 Taylor series expansion. HLR  $\approx 34.9765$  dB, SCR  $\approx -1.0618$  dB, TNLR  $\approx -3.5736$  dB,  $t_0 = 0.8$ ,  $\alpha = \alpha_{\text{Costa}} \approx 0.5608$ ,  $n = 1000$ , scalar quantizer.

which is nothing but the  $\alpha$  derived by Costa, after replacing the embedded signal power by its effective value at the receiver.

In the case where  $t_0 \rightarrow 0$  the Taylor series expansion of order 2 can not be performed, as there does not exist a neighborhood of  $t_0$  where the target function is differentiable. In any case, it is easy to see that the derivative of (70) evaluated at  $t_0 = 0$  is

$$\frac{2 \left( t^2 - \frac{\sigma_N^2}{\sigma_X^2} \right)}{t^3};$$

therefore, in that case the bias will be

$$b(t_0) = \sqrt{\frac{\sigma_N^2}{\sigma_X^2}}.$$

## 12 Total MSE lower-bound and $\alpha$ optimization

In the previous sections we have studied both the Fisher information and the bias of our estimator, obtaining close formulas in both cases for the high-dimensional good lattice case, when HLR  $\rightarrow \infty$ , and TNLR  $< 1$ . Combining both expressions, the MSE of the proposed estimator can be lower-bounded by

$$\mathbb{E} \left\{ (t_0 - \hat{t}(\mathbf{z}))^2 \right\} \geq \frac{\left[ 1 + \frac{\partial b(t_0)}{\partial t_0} \right]^2}{I(t_0)} + b(t_0)^2. \quad (72)$$

We will focus our analysis on the non-degenerated case where  $t_0$  does not go to 0. In this scenario,  $I(t_0)$  is given by (67), and  $b(t_0)$  by (71); thus, the derivative of  $b(t_0)$  with respect to  $t_0$  is

$$\frac{\partial b(t_0)}{\partial t_0} = \frac{-1}{\sigma_X^2 t_0^2} [(1 - \alpha) \alpha \sigma_N^2 t_0^2 + \sigma_N^2];$$

if  $\text{TNLR} < 1$  and  $\text{HLR} \rightarrow \infty$ , then the last expression goes to 0, so it can be neglected in (72).

Therefore, we will write

$$\mathbb{E} \left\{ (t_0 - \hat{t}(\mathbf{z}))^2 \right\} \geq \frac{1}{I(t_0)} + b(t_0)^2 = \frac{\sigma_N^2 + \frac{(1-\alpha)^2}{\alpha^2} \sigma_W^2 t_0^2}{n \sigma_X^2} + \left( \frac{1}{\sigma_X^2} \left[ \frac{\sigma_N^2}{t_0} - \frac{(1-\alpha) \sigma_W^2 t_0}{\alpha} \right] \right)^2 \quad (73)$$

It is worth pointing out that the Fisher information contribution decreases with  $n \sigma_X^2$ , while the bias one decreases with  $\sigma_X^4$ . Therefore, the dominant effect will depend on the ratio  $\frac{\sigma_X^2}{n}$ : the larger it is, the more dominant the Fisher information will be; the smaller it is, the more important the bias contribution.

## 12.1 $\alpha$ optimization

In the previous sections we also derived the value of  $\alpha$  maximizing the Fisher information  $\alpha_{\text{sup-FI}}$ , and minimizing the bias effect  $\alpha_{\text{no-bias}}$ ; given that both values are different, when trying to optimize both functions simultaneously, i.e. when minimizing (73), a trade-off between the optimal  $\alpha$  corresponding to both contributions must be achieved. In that sense, and taking into account the discussion in the previous paragraph, one would expect the obtained  $\alpha$  to be closer to  $\alpha_{\text{sup-FI}}$  when  $\frac{\sigma_X^2}{n}$  is large, and closer to  $\alpha_{\text{no-bias}}$  when that ratio is small.

Indeed, the derivative of the total MSE lower-bound with respect to  $\alpha$  is

$$\frac{\partial \left( \frac{1}{I(t_0)} + b(t_0)^2 \right)}{\partial \alpha} = \frac{2 \sigma_W^2 [n \alpha \sigma_N^2 - (1 - \alpha) (n \sigma_W^2 + \sigma_X^2) t_0^2]}{n \alpha^3 \sigma_X^4},$$

which is null at

$$\alpha = \frac{n \sigma_W^2 t_0^2 + \sigma_X^2 t_0^2}{n \sigma_N^2 + n \sigma_W^2 t_0^2 + \sigma_X^2 t_0^2}, \quad (74)$$

where the target function has its only local (and consequently global) minimum. Be aware that when  $\frac{\sigma_X^2}{n} \rightarrow \infty$  (and based on  $\text{HLR} \rightarrow \infty$ , and  $\text{TNLR} < 1$ ), (74) goes to 1, while if  $\frac{\sigma_X^2}{n} \rightarrow 0$ , (74) goes to  $\alpha_{\text{no-bias}}$  (i.e.,  $\alpha_{\text{Costa}}$ ). Taking into account that  $\alpha$  must be smaller than  $\alpha_{\text{sup-FI}}$  in order to  $\text{TNLR} < 1$ , the feasible value of  $\alpha$  minimizing the total MSE lower-bound is finally given by

$$\alpha_{\text{opt}} \triangleq \min \left( \frac{n \sigma_W^2 t_0^2 + \sigma_X^2 t_0^2}{n \sigma_N^2 + n \sigma_W^2 t_0^2 + \sigma_X^2 t_0^2}, \frac{2 \sigma_W^2 t_0^2}{\sigma_N^2 + \sigma_W^2 t_0^2} - \epsilon \right), \quad (75)$$

for  $\epsilon > 0$  arbitrarily small.

As expected, when  $\frac{\sigma_X^2}{n} \rightarrow 0$ ,  $\alpha_{\text{opt}} \rightarrow \alpha_{\text{no-bias}}$ , while when  $\frac{\sigma_X^2}{n} \rightarrow \infty$ ,  $\alpha_{\text{opt}} \rightarrow \alpha_{\text{sup-FI}}$ . In the intermediate cases,  $\alpha_{\text{opt}}$  will balance the effect of both contributions. Although obvious at the sight of (75), it is interesting to mention that the optimal  $\alpha$  value depends on this scenario both on  $\sigma_X^2$  and  $n$ , contrarily to Costa's original proposal.

Finally, when  $\alpha_{\text{opt}}$  is used, if the left argument of the min function is active in (75), one has that

$$\mathbb{E} \left\{ (t_0 - \hat{t}(\mathbf{z}))^2 \right\} \geq \frac{\sigma_N^2 \left( \frac{1}{n} + \frac{\sigma_N^2}{(n\sigma_W^2 + \sigma_X^2)t_0^2} \right)}{\sigma_X^2};$$

if  $\text{HLR} \gg 1$  and  $\text{TNLR} < 1$ , then we can approximate the right term by

$$\frac{\sigma_N^2}{n\sigma_X^2}. \quad (76)$$

On the other hand, if the active argument is the second one, then

$$\mathbb{E} \left\{ (t_0 - \hat{t}(\mathbf{z}))^2 \right\} \geq \frac{(n\sigma_W^2 + \sigma_X^2) (\sigma_N^2 + \sigma_W^2 t_0^2)^2}{4n\sigma_W^2 \sigma_X^4 t_0^2}.$$

Finally, for further comparison we also find useful to derive the total MSE lower-bound when  $\alpha = \alpha_{\text{no-bias}}$ , which is

$$\mathbb{E} \left\{ (t_0 - \hat{t}(\mathbf{z}))^2 \right\} \geq \frac{\sigma_N^2 (\sigma_N^2 + \sigma_W^2 t_0^2)}{n\sigma_W^2 \sigma_X^2 t_0^2},$$

based on  $\text{TNLR} < 1$ , the right term is smaller than

$$\frac{\sigma_N^2/\alpha^2}{n\sigma_X^2}. \quad (77)$$

### 13 Fundamental bounds

The bounds derived in this section will not depend on the particular estimation scheme that one is considering. Therefore, we will obtain an estimation error variance lower-bound to any estimation scheme where

- the channel state  $\mathbf{X}$ , follows a  $\mathcal{N}(\mathbf{0}, \sigma_X^2 I_{n \times n})$ .
- the transmitter, who anticausally knows  $\mathbf{X}$  but can not choose it, can produce a signal  $\mathbf{W}$  of power  $\sigma_W^2 \ll \sigma_X^2$ , which is added to  $\mathbf{X}$ .
- the resulting signal is scaled by an unknown parameter  $t_0$ , and added AWGN  $\mathbf{N}$  independent of both  $\mathbf{X}$  and  $\mathbf{W}$ , with power  $\sigma_N^2$ .
- the decoder has not access to  $\mathbf{X}$ , but only to  $t_0(\mathbf{X} + \mathbf{W}) + \mathbf{N}$ .

In that scenario, and given that  $\frac{\sigma_W^2}{\sigma_X^2} \rightarrow 0$ , one can assume that  $\mathbf{Y} = \mathbf{X} + \mathbf{W}$  will be also asymptotically Gaussian, as  $\mathbf{W}$  will not significantly modify the distribution of  $\mathbf{X}$ . Additionally,  $(\sigma_X - \sigma_W)^2 \leq \sigma_Y^2 \leq (\sigma_X + \sigma_W)^2$ , and whenever  $\mathbf{W}$  is constrained to be independent of  $\mathbf{X}$ ,  $\sigma_Y^2 = \sigma_X^2 + \sigma_W^2$ .

Therefore, in the Gaussian framework we can bound the performance of such a scheme by that of a scheme where the transmitter can choose to his/her will  $\mathbf{X}$  (as long as the Gaussian constraint is respected), and then design  $\mathbf{W}$  accordingly, and the chosen value  $\mathbf{Y}$  is also known at the receiver side; this new scenario corresponds to the case where *pilot signals* are used. In that framework, the pdf of the received signal is

$$f_{Z|Y,t_0}(\mathbf{z}|\mathbf{y}, t) = \frac{e^{-\|\mathbf{z}-t\mathbf{y}\|^2 / 2\sigma_N^2}}{(2\pi\sigma_N^2)^{n/2}},$$

since, as it was mentioned before, the receiver will know what was the transmitted signal  $\mathbf{y}$ . It is straightforward to see that in this scenario the CRB equals to

$$\frac{\sigma_N^2}{n\sigma_Y^2}.$$

Having the last expression in mind, we will envisage two different scenarios providing different values of  $\sigma_Y^2$ ; first, if complete freedom on choosing  $\mathbf{W}$  is available, one has that

$$\mathbb{E}\{(t_0 - \hat{t}(\mathbf{Z}))^2\} \geq \sigma_{\text{bound1}}^2 \triangleq \frac{\sigma_N^2}{n(\sigma_X + \sigma_W)^2};$$

on the other hand, if  $\mathbf{W}$  is required to be independent of  $\mathbf{X}$ , then

$$\mathbb{E}\{(t_0 - \hat{t}(\mathbf{Z}))^2\} \geq \sigma_{\text{bound2}}^2 \triangleq \frac{\sigma_N^2}{n(\sigma_X^2 + \sigma_W^2)}.$$

Obviously  $\sigma_{\text{bound1}}^2 \leq \sigma_{\text{bound2}}^2$ ; nevertheless, when  $\frac{\sigma_W^2}{\sigma_X^2} \rightarrow 0$ , both expressions are asymptotically equivalent.

## 14 Intuitive insights

In this section we try to provide an intuitive insight on the total MSE lower-bound obtained in Sect. 12, and its comparison with the fundamental lower-bound derived in the previous section.

First, we would like to emphasize the similarities between (76) and (77), and the CRB obtained for the case where the transmitter can choose the state of the channel, i.e., when pilot signals are used,  $\frac{\sigma_N^2}{n(\sigma_X + \sigma_W)^2}$ . Based on HLR  $\rightarrow \infty$ ,  $(\sigma_X + \sigma_W)^2 \approx \sigma_X^2$ . Therefore, the lower-bound in (77), which is non-minimal, as the optimal value of  $\alpha$  is not used, differs from the fundamental bound just by the division by  $\alpha^2$ ; furthermore, (76) asymptotically converge to

that fundamental bound. Thus, the advantage of the proposed quantization-based scheme being able not only to reduce the host signal interference, but indeed to use it for helping in the estimation of the scalar multiplicative factor. Similarly, the signal variance term that appears at the denominator of both expressions is slightly reduced when quantization-based techniques are used in comparison with the pilot-based strategy. In any case, the variance used by the pilot-based strategy will be  $(\sigma_X + \sigma_W)^2$ , while the variance used by our quantization-based scheme is just  $\sigma_W^2$ ; the advantage of our scheme could be also studied in terms of the increased payload (as in pilot-based schemes the considered signals does not convey information).

But, how it is possible that similar performance is achieved by our quantization-based scaling estimation scheme and by the pilot-based strategies? If we assume that the estimator of the proposed quantization-based scheme were aided by a genie, who would say what was the centroid used at the embedder, both schemes would be equivalent, except for two facts already mentioned (the increase in the total noise variance, and the decrease of transmitted power). Although the scheme we are considering is obviously non-genie-based, it is indeed implicitly based on correctly estimating the centroid used at the embedder. This fact is reflected on the derivation of the total MSE lower-bound when assuming that the modulo- $\Lambda$  reduction can be neglected, which is only possible if the estimated centroid is that used at the embedder.

From the last discussion one can glimpse the importance of being able to find a  $t$  close enough to  $t_0$  so the total noise at  $t$ , i.e.,  $(t_0 - t)\mathbf{x} + (t - \alpha t_0)[(\mathbf{x} - \mathbf{d})\text{mod}\Lambda] + \mathbf{n}$  is not modulo-reduced, so the used centroid can be correctly estimated. It is easy to figure out that the closer  $\alpha$  to  $\frac{2\sigma_W^2 t_0^2}{\sigma_N^2 + \sigma_W^2 t_0^2}$ , the smaller the size of the interval of  $t$  around  $t_0$  for which the modulo reduction can be neglected. Indeed, this discussion is also related to our study of the search interval sampling. Therefore, if high-dimensional good lattices were used, and the value of  $\alpha$  approached  $\alpha_{\text{sup-FI}}$ , then the distance between consecutive candidate points should be arbitrarily small, in order to the variance of the total noise at the new location be still smaller than the second moment per dimension of the lattice. Consequently, the correct estimation of the centroid at the embedder is achieved at the cost of increasing the computational cost of the estimation algorithm. This comment also makes evident the trade-off that should be achieved between estimation algorithm performance, in terms of estimation error variance, and the required computational cost.

Finally, we would like to emphasize that the larger the HLR, the smaller the total MSE lower-bound, but the larger the computational cost, as the sampling of the search interval should be thinner.

## 15 Experimental results

In this section we summarize the main results obtained by considering multidimensional lattices. Specifically, we quantize the host signal by using the coarse lattice proposed in [4]; the reported results were obtained by considering constraint length 7, and the generator polynomial proposed in [3] (in octal

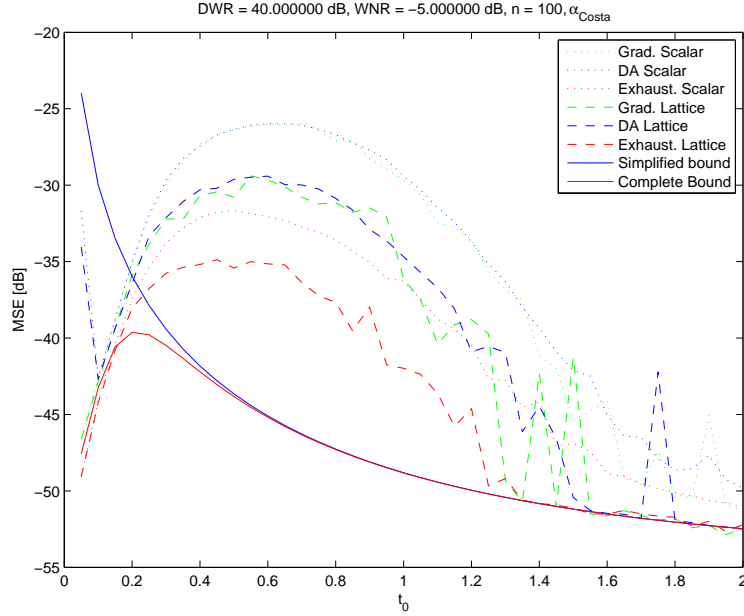


Figure 18: MSE obtained for different estimation algorithms, both for scalar quantizer and multidimensional lattices.  $DWR = 40$  dB,  $WNR = -5$  dB,  $n = 100$ ,  $\alpha_{Costa}$ .

notation,  $(133, 171)$ ), which yields a shaping gain of 1.26 dB. Note that other choices, for example based on the coarse lattice used in [2], are possible. In all the plots in this section *Simplified bound* stands for the value of (73).

First, in Figs. 18-25 we show the MSE results as a function of  $t_0$  for different estimation algorithms, for both scalar quantizers and the multidimensional lattice proposed in [4]. Note that in some cases the plots show an MSE obtained by exhaustive search which is smaller than the corresponding MSE bound; this is due to the fact that the dominant effect in those cases is the exhaustive search quantization.

In general, all those plots show the advantage of considering multidimensional lattices instead of scalar quantizers, specially for large values of  $n$ , where one can really take advantage of the shaping of the multidimensional lattices, as well as a very good agreement between the theoretical bounds and the experimental results.



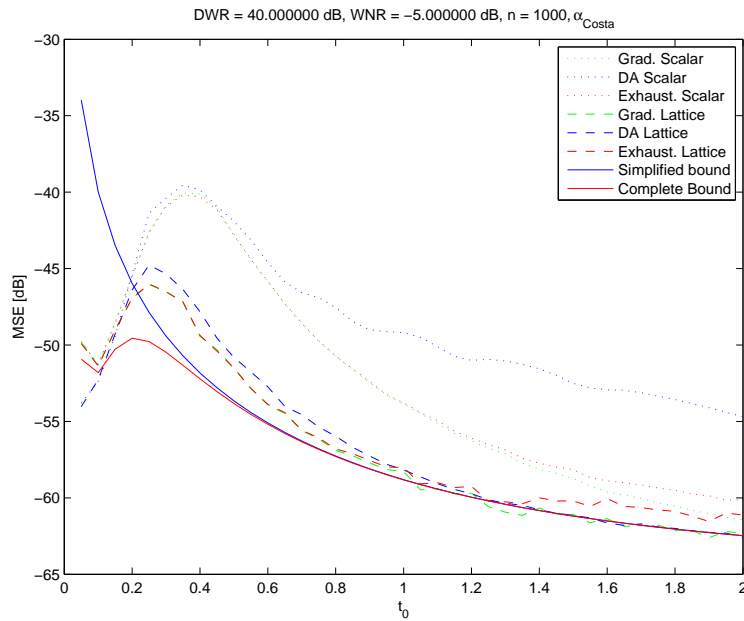


Figure 19: MSE obtained for different estimation algorithms, both for scalar quantizer and multidimensional lattices.  $DWR = 40$  dB,  $WNR = -5$  dB,  $n = 1000$ ,  $\alpha_{Costa}$ .

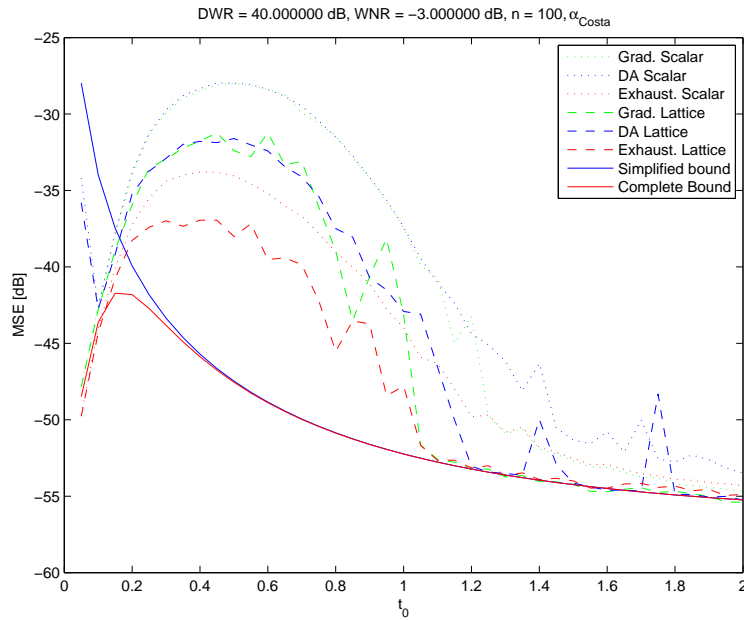


Figure 20: MSE obtained for different estimation algorithms, both for scalar quantizer and multidimensional lattices.  $DWR = 40$  dB,  $WNR = -3$  dB,  $n = 100$ ,  $\alpha_{Costa}$ .

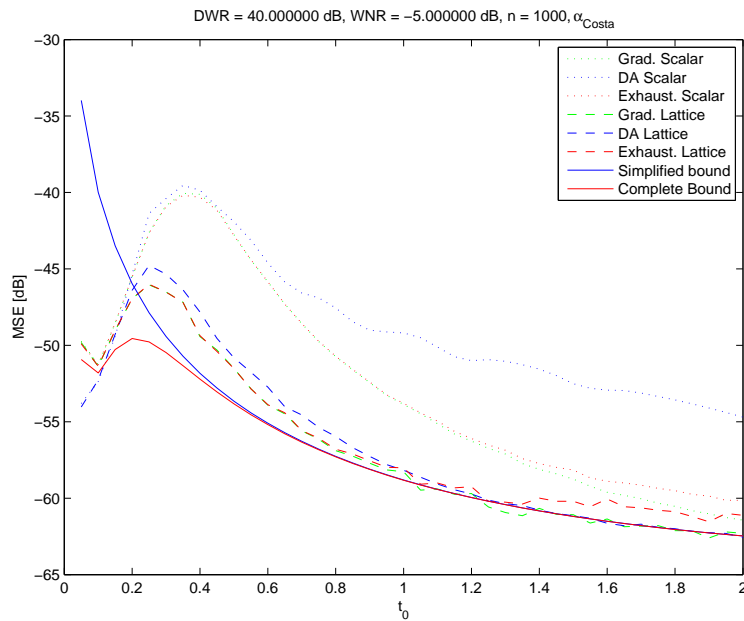


Figure 21: MSE obtained for different estimation algorithms, both for scalar quantizer and multidimensional lattices. DWR = 40 dB, WNR = -3 dB,  $n = 1000$ ,  $\alpha_{\text{Costa}}$ .

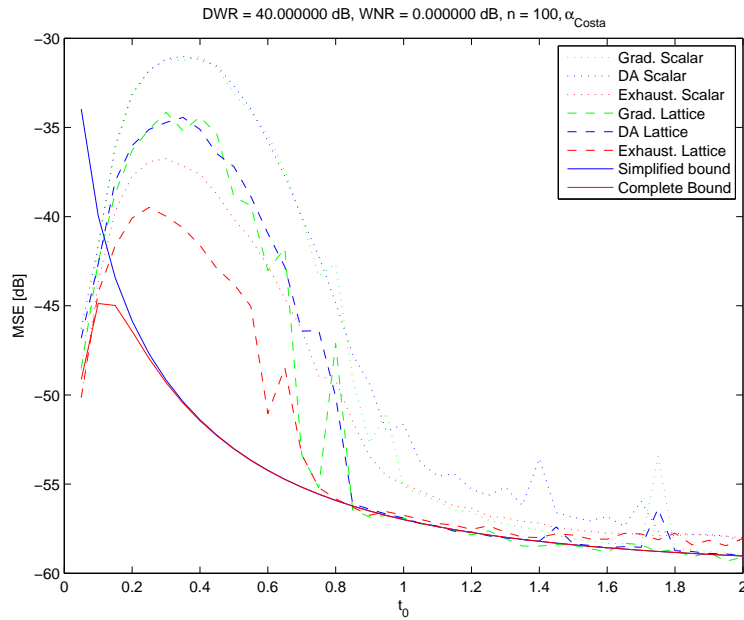


Figure 22: MSE obtained for different estimation algorithms, both for scalar quantizer and multidimensional lattices. DWR = 40 dB, WNR = 0 dB,  $n = 100$ ,  $\alpha_{\text{Costa}}$ .

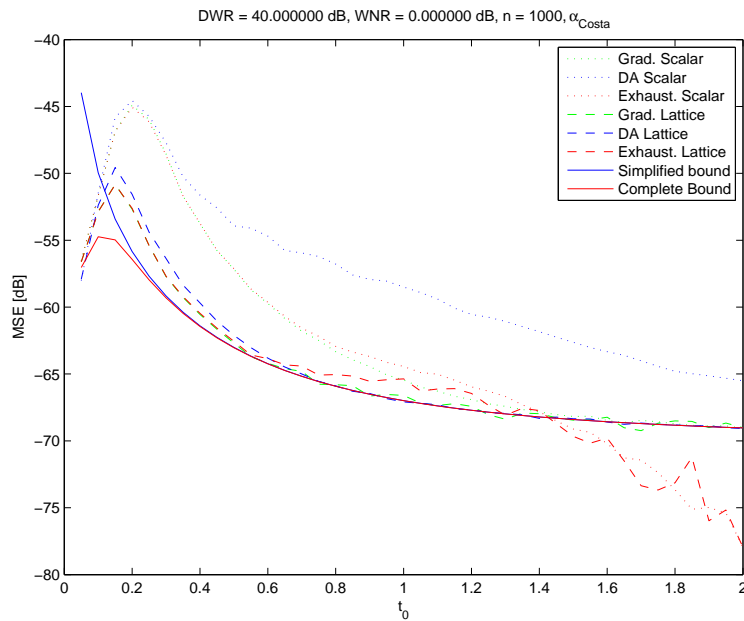


Figure 23: MSE obtained for different estimation algorithms, both for scalar quantizer and multidimensional lattices.  $DWR = 40$  dB,  $WNR = 0$  dB,  $n = 1000$ ,  $\alpha_{Costa}$ .

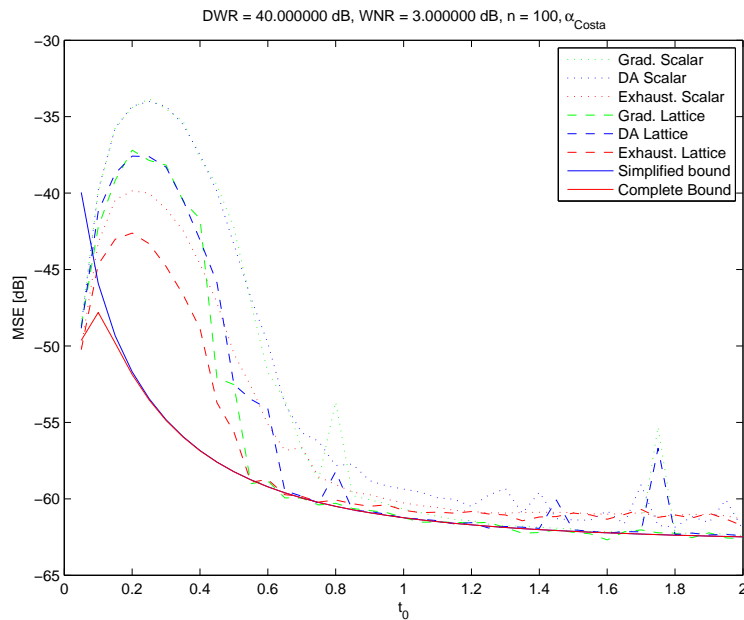


Figure 24: MSE obtained for different estimation algorithms, both for scalar quantizer and multidimensional lattices.  $DWR = 40$  dB,  $WNR = 3$  dB,  $n = 100$ ,  $\alpha_{Costa}$ .

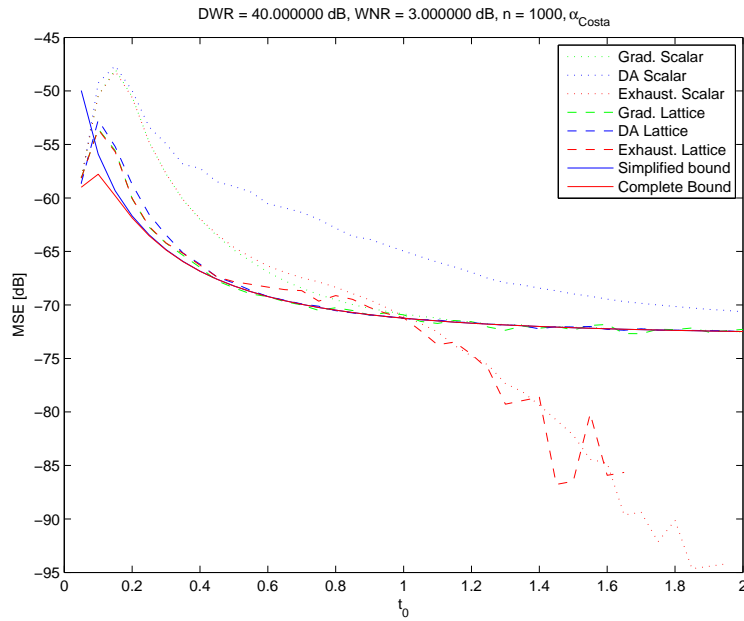


Figure 25: MSE obtained for different estimation algorithms, both for scalar quantizer and multidimensional lattices. DWR = 40 dB, WNR = 3 dB,  $n = 1000$ ,  $\alpha_{\text{Costa}}$ .

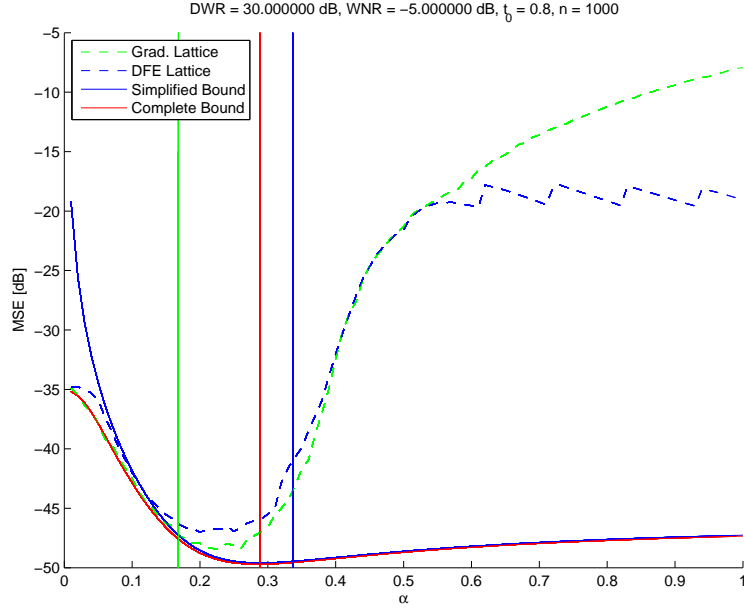


Figure 26: MSE as a function of  $\alpha$  obtained for different estimation algorithms and multidimensional lattices. DWR = 30 dB, WNR = -5 dB,  $n = 1000$ .

A second set of plots are those in Figs. 26-49, where we show the behavior of the MSE as a function of  $\alpha$ , in order to illustrate the correctness of the discussion in Sect. 12. In particular, we can see how the optimal value of  $\alpha$  depends on the ratio  $\sigma_X^2/n$ , as a trade-off between the CRB component of the MSE and the bias of the estimation must be achieved. These plots also show the  $\alpha_{\text{no-bias}}$  value (remember that this is the  $\alpha$  derived by Costa for the communications problem) as a solid green line,  $\alpha_{\text{sup-FI}}$  as a solid blue line, and  $\alpha_{\text{opt}}$  as a solid red line, illustrating that indeed the optimal value of  $\alpha$  is virtually  $\alpha_{\text{opt}}$ . Furthermore, and contrarily to what happens in the communications framework, the location of the optimal value of  $\alpha$  (i.e., approximately  $\alpha_{\text{opt}}$ ) depends on  $n$ . We would like to emphasize the outstanding agreement between theoretical and experimental results show in these plots, as well as the expected significant increase in the MSE for those values of  $\alpha$  larger than  $\alpha_{\text{sup-FI}}$ .

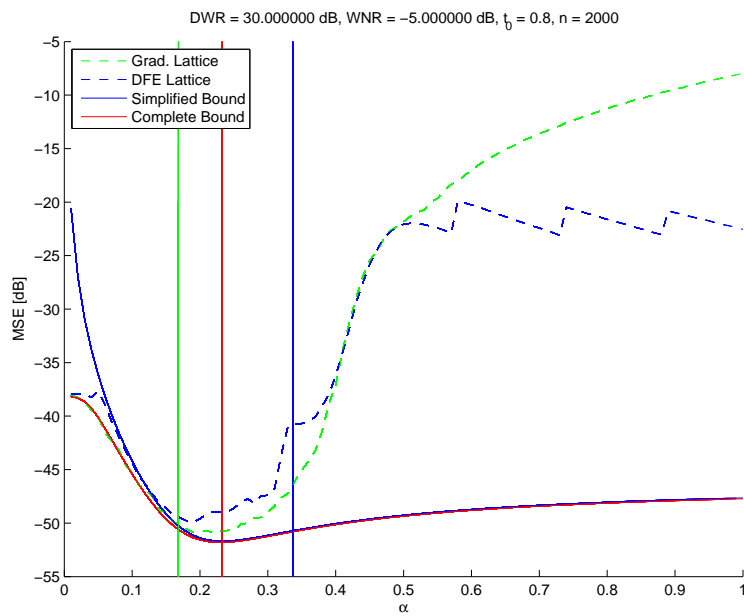


Figure 27: MSE as a function of  $\alpha$  obtained for different estimation algorithms and multidimensional lattices. DWR = 30 dB, WNR = -5 dB,  $n = 2000$ .

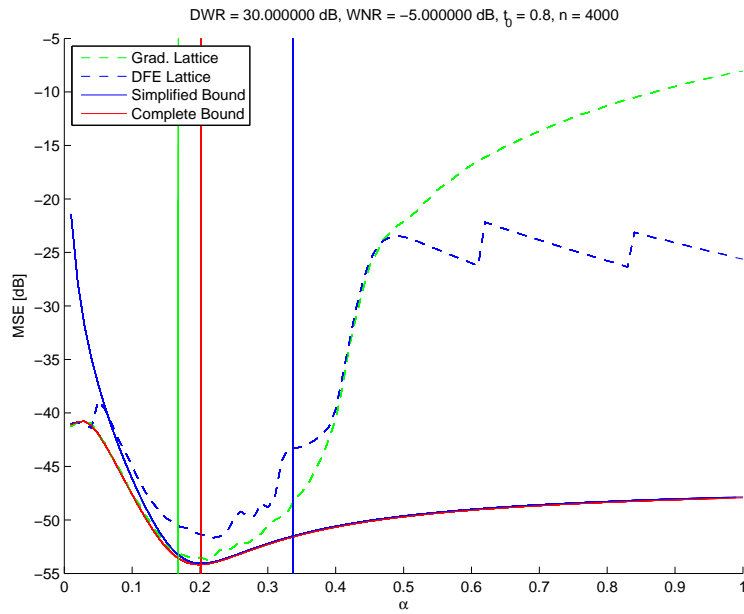


Figure 28: MSE as a function of  $\alpha$  obtained for different estimation algorithms and multidimensional lattices. DWR = 30 dB, WNR = -5 dB,  $n = 4000$ .

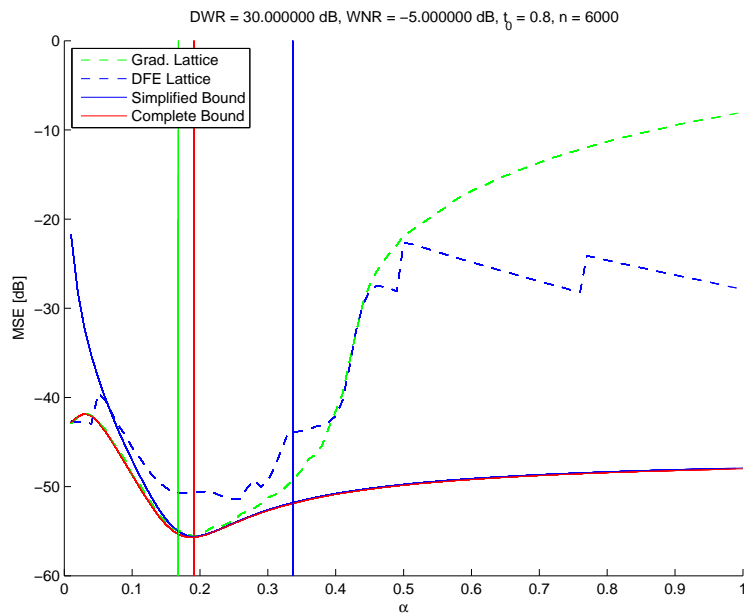


Figure 29: MSE as a function of  $\alpha$  obtained for different estimation algorithms and multidimensional lattices. DWR = 30 dB, WNR = -5 dB,  $n = 6000$ .

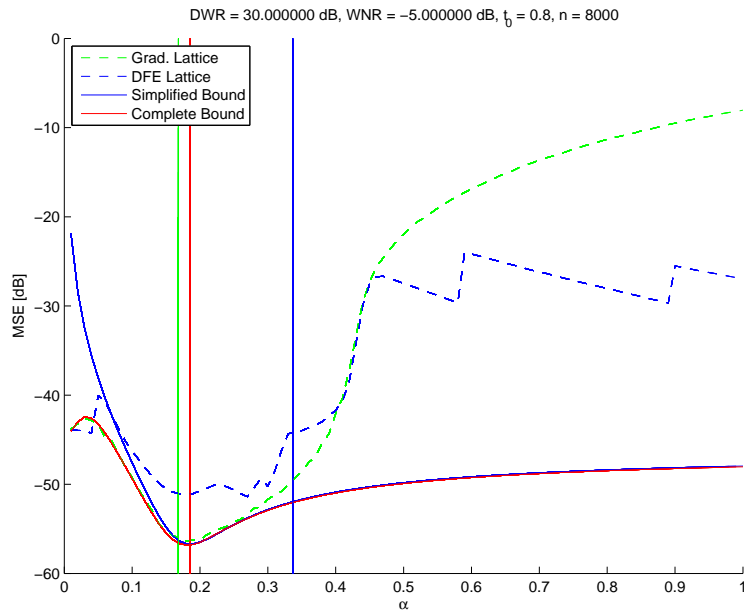


Figure 30: MSE as a function of  $\alpha$  obtained for different estimation algorithms and multidimensional lattices. DWR = 30 dB, WNR = -5 dB,  $n = 8000$ .

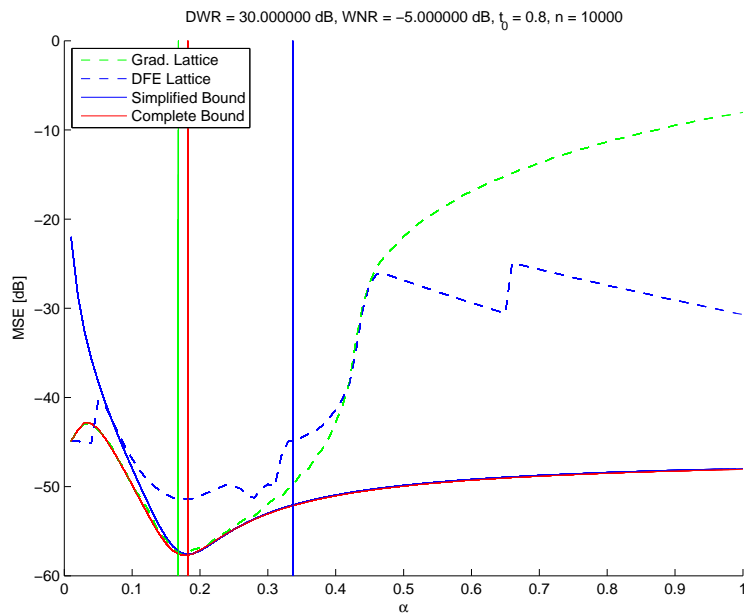


Figure 31: MSE as a function of  $\alpha$  obtained for different estimation algorithms and multidimensional lattices. DWR = 30 dB, WNR = -5 dB,  $n = 10000$ .



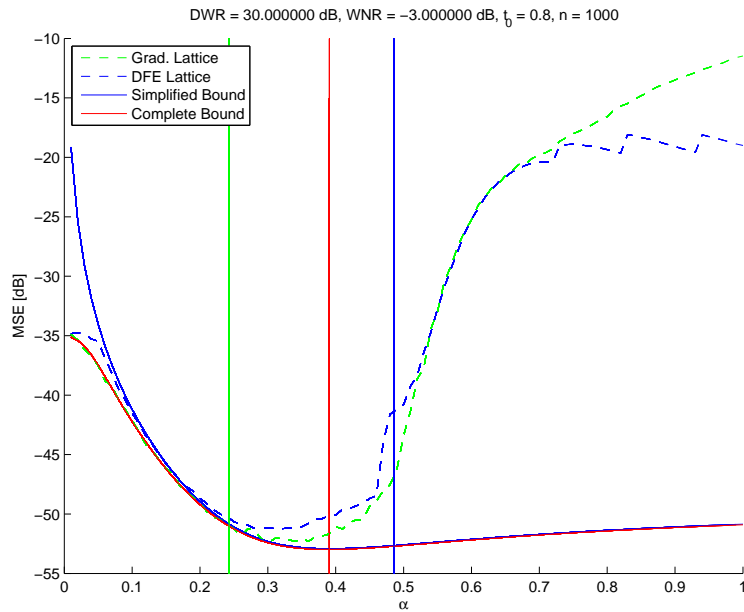


Figure 32: MSE as a function of  $\alpha$  obtained for different estimation algorithms and multidimensional lattices. DWR = 30 dB, WNR = -3 dB,  $n = 1000$ .

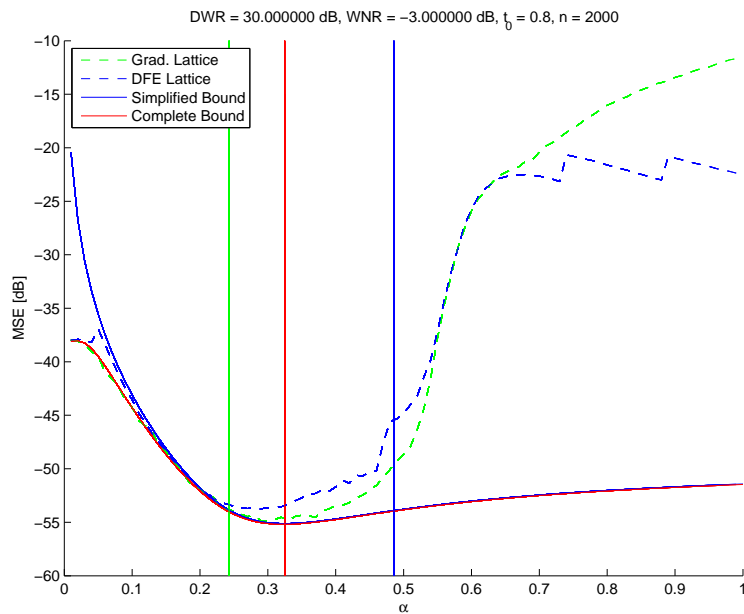


Figure 33: MSE as a function of  $\alpha$  obtained for different estimation algorithms and multidimensional lattices. DWR = 30 dB, WNR = -3 dB,  $n = 2000$ .

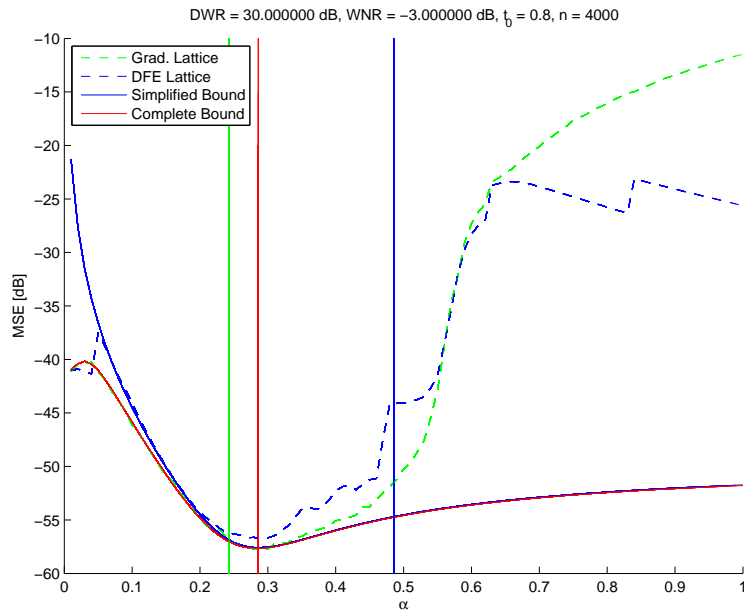


Figure 34: MSE as a function of  $\alpha$  obtained for different estimation algorithms and multidimensional lattices. DWR = 30 dB, WNR = -3 dB,  $n = 4000$ .

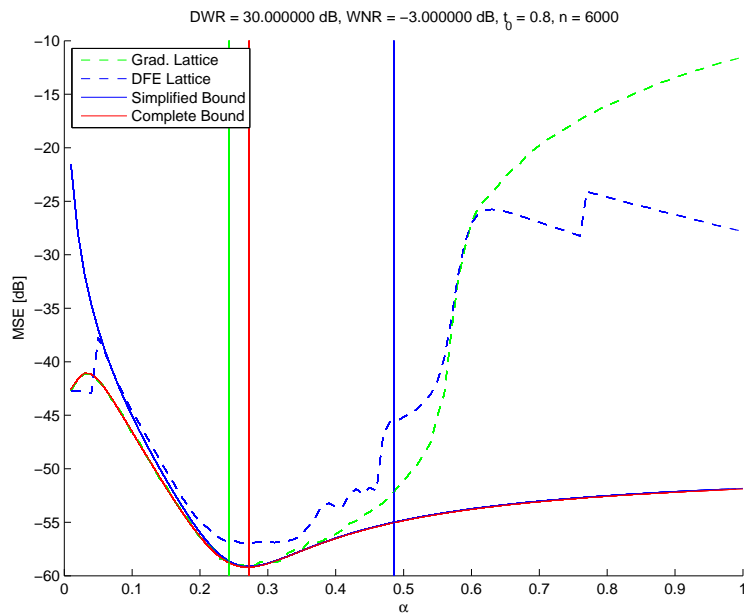


Figure 35: MSE as a function of  $\alpha$  obtained for different estimation algorithms and multidimensional lattices. DWR = 30 dB, WNR = -3 dB,  $n = 6000$ .

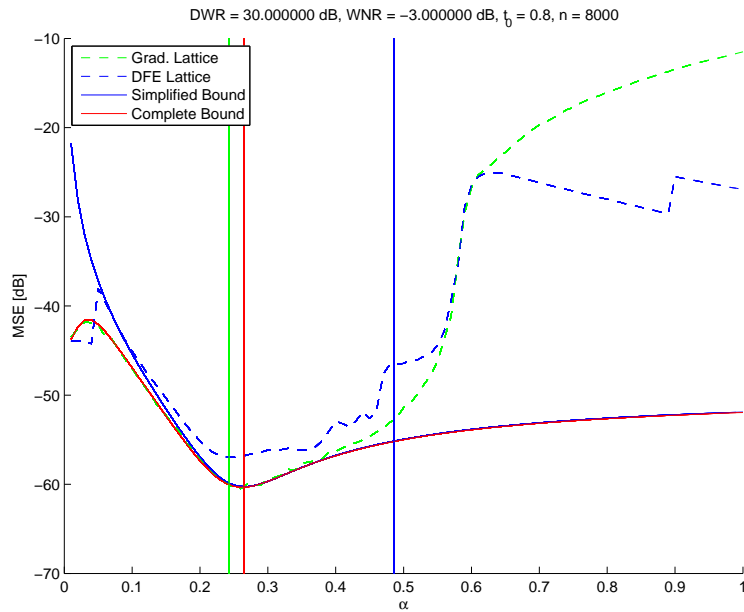


Figure 36: MSE as a function of  $\alpha$  obtained for different estimation algorithms and multidimensional lattices. DWR = 30 dB, WNR = -3 dB,  $n = 8000$ .

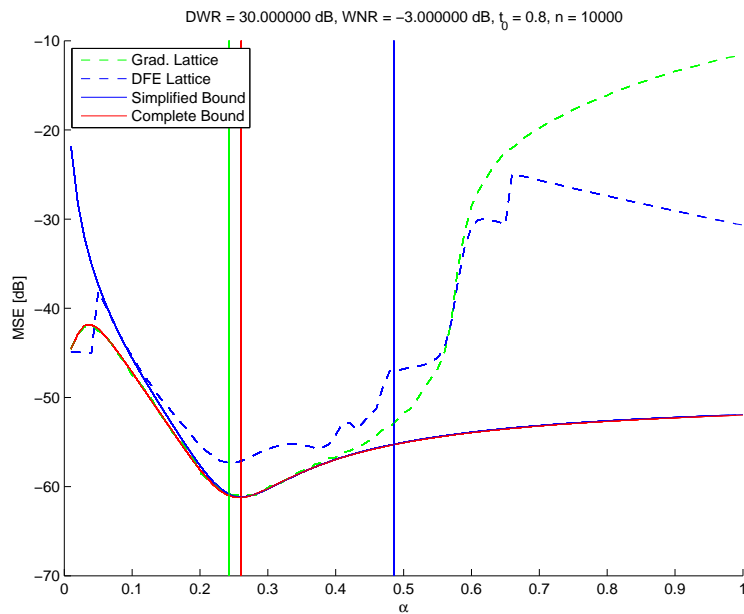


Figure 37: MSE as a function of  $\alpha$  obtained for different estimation algorithms and multidimensional lattices. DWR = 30 dB, WNR = -3 dB,  $n = 10000$ .

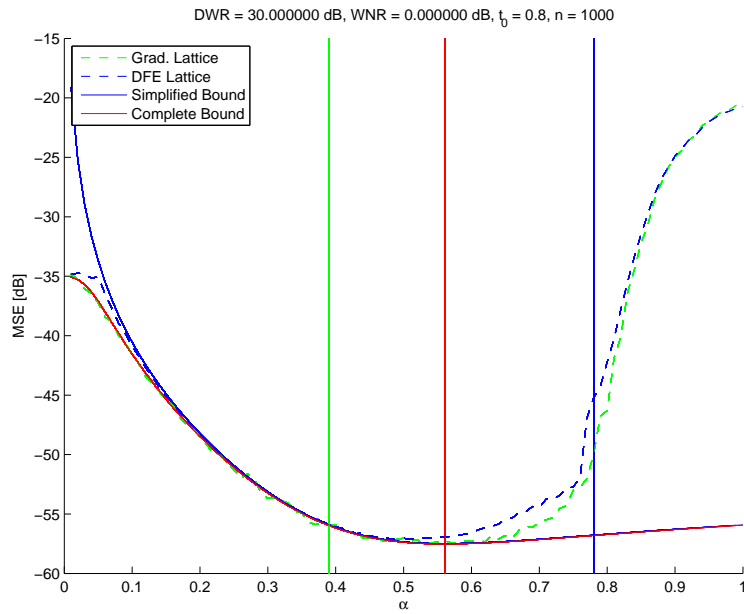


Figure 38: MSE as a function of  $\alpha$  obtained for different estimation algorithms and multidimensional lattices. DWR = 30 dB, WNR = 0 dB,  $n = 1000$ .

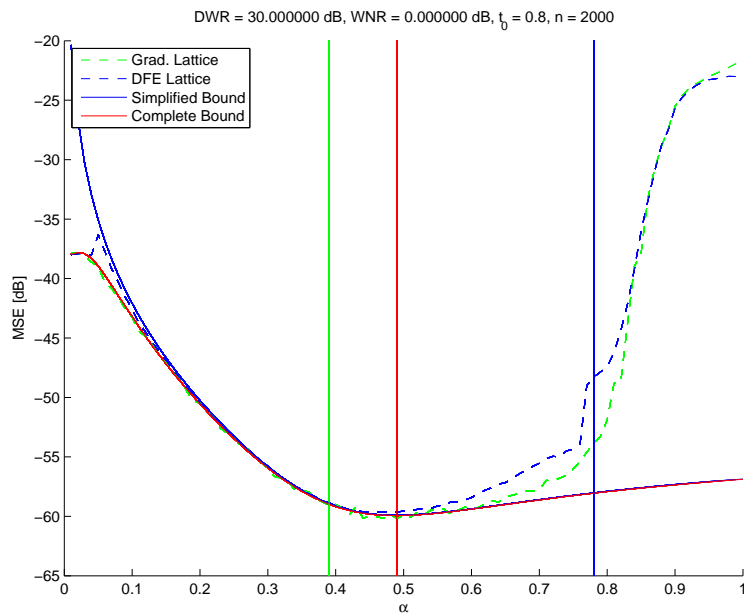


Figure 39: MSE as a function of  $\alpha$  obtained for different estimation algorithms and multidimensional lattices. DWR = 30 dB, WNR = 0 dB,  $n = 2000$ .

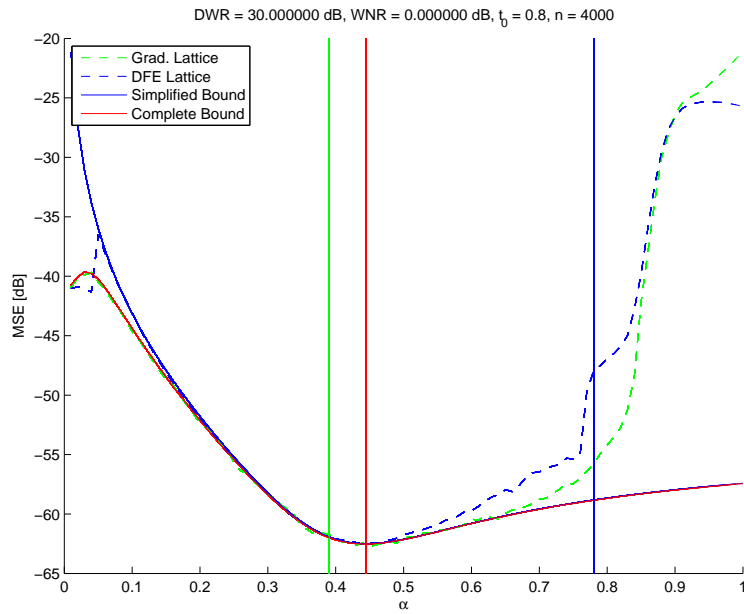


Figure 40: MSE as a function of  $\alpha$  obtained for different estimation algorithms and multidimensional lattices. DWR = 30 dB, WNR = 0 dB,  $n = 4000$ .

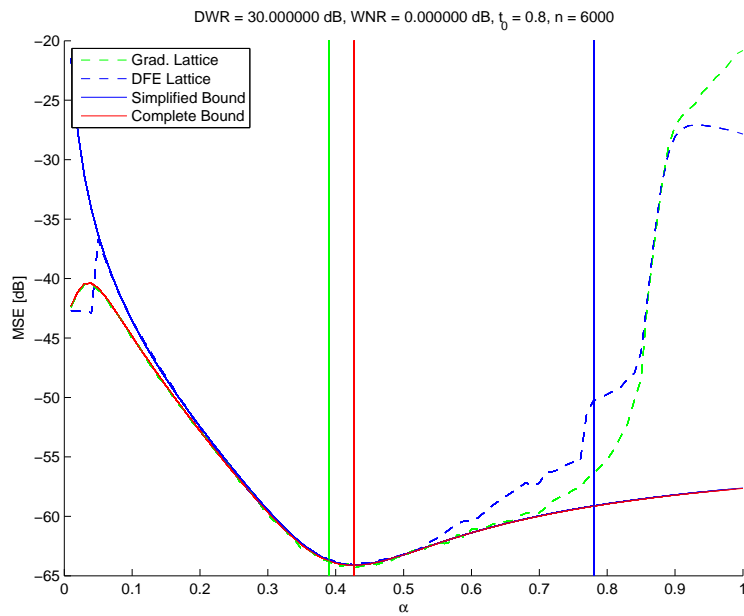


Figure 41: MSE as a function of  $\alpha$  obtained for different estimation algorithms and multidimensional lattices. DWR = 30 dB, WNR = 0 dB,  $n = 6000$ .

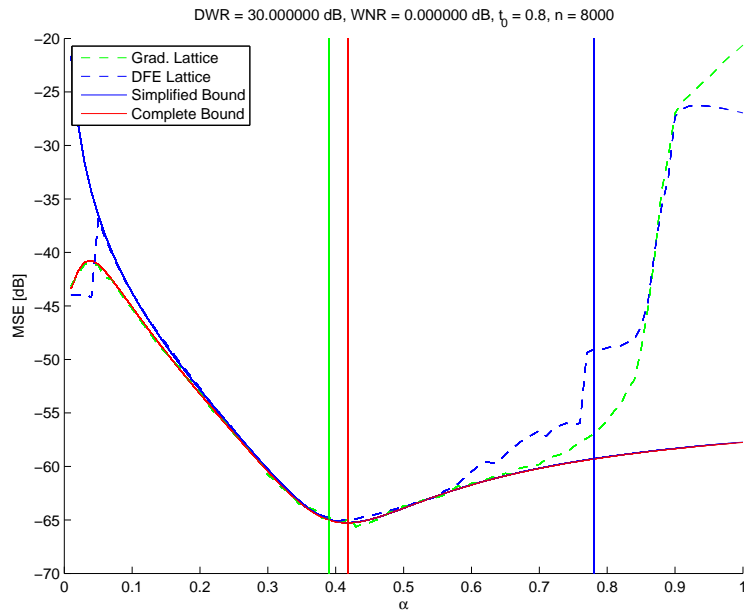


Figure 42: MSE as a function of  $\alpha$  obtained for different estimation algorithms and multidimensional lattices. DWR = 30 dB, WNR = 0 dB,  $n = 8000$ .

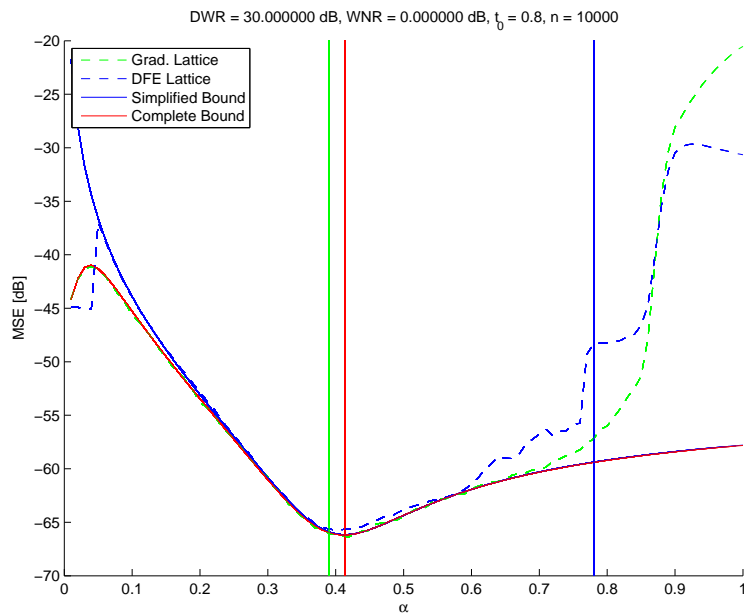


Figure 43: MSE as a function of  $\alpha$  obtained for different estimation algorithms and multidimensional lattices. DWR = 30 dB, WNR = 0 dB,  $n = 10000$ .

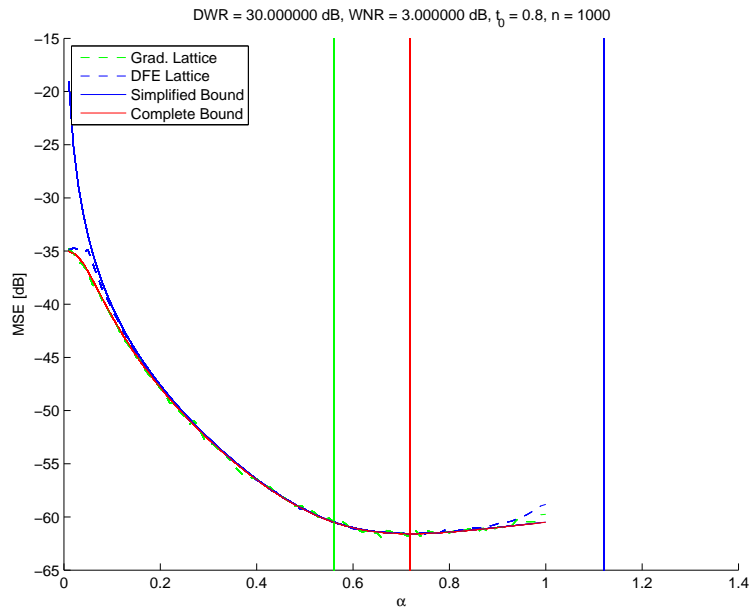


Figure 44: MSE as a function of  $\alpha$  obtained for different estimation algorithms and multidimensional lattices. DWR = 30 dB, WNR = 3 dB,  $n = 1000$ .

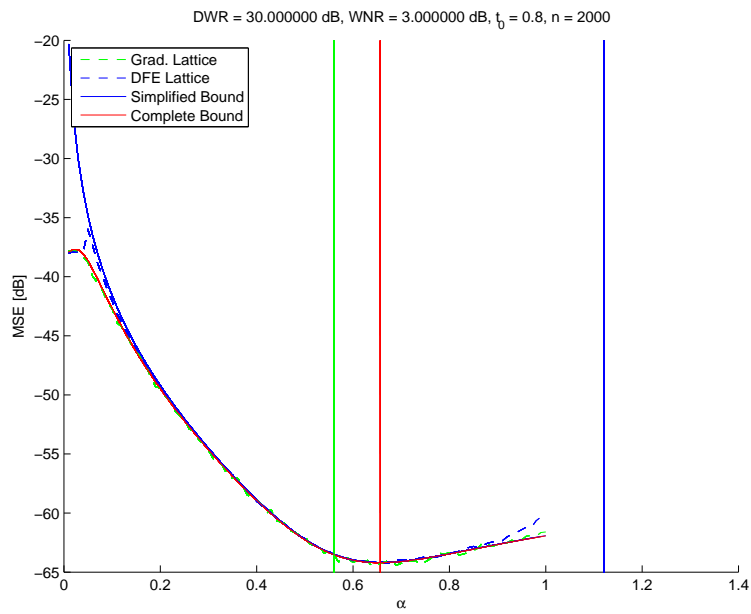


Figure 45: MSE as a function of  $\alpha$  obtained for different estimation algorithms and multidimensional lattices. DWR = 30 dB, WNR = 3 dB,  $n = 2000$ .

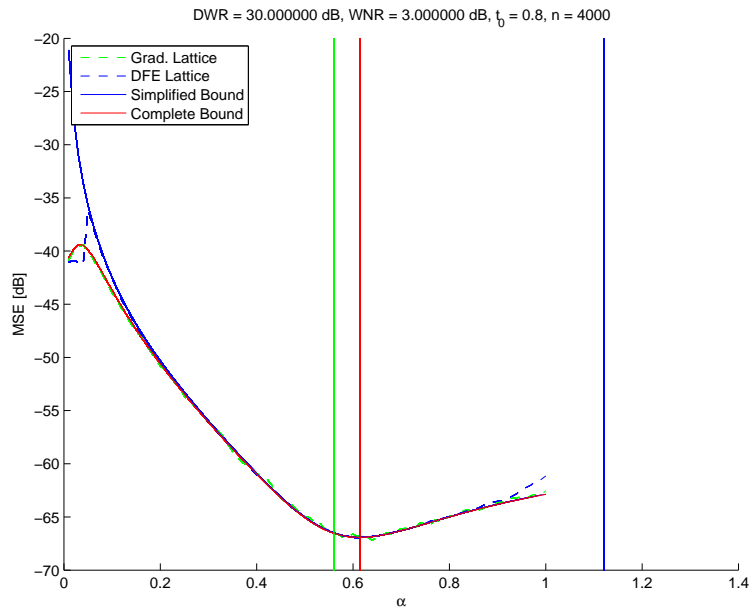


Figure 46: MSE as a function of  $\alpha$  obtained for different estimation algorithms and multidimensional lattices. DWR = 30 dB, WNR = 3 dB,  $n = 4000$ .

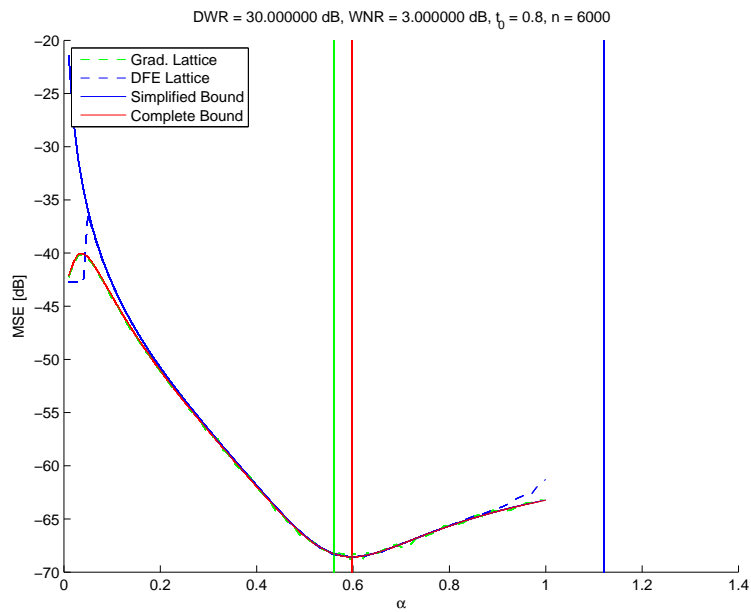


Figure 47: MSE as a function of  $\alpha$  obtained for different estimation algorithms and multidimensional lattices. DWR = 30 dB, WNR = 3 dB,  $n = 6000$ .



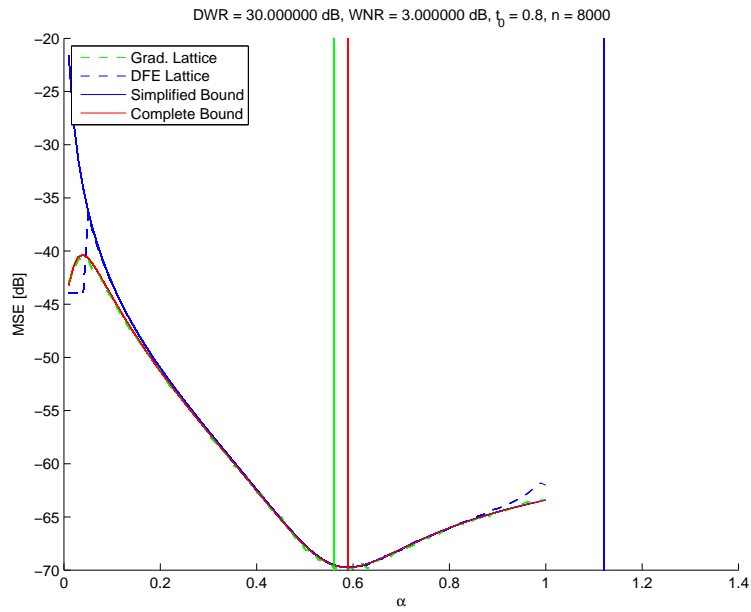


Figure 48: MSE as a function of  $\alpha$  obtained for different estimation algorithms and multidimensional lattices. DWR = 30 dB, WNR = 3 dB,  $n = 8000$ .

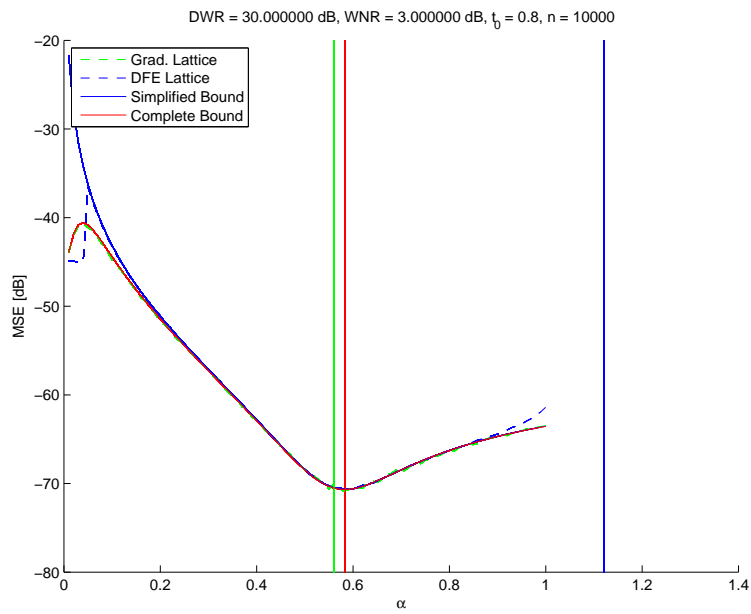


Figure 49: MSE as a function of  $\alpha$  obtained for different estimation algorithms and multidimensional lattices. DWR = 30 dB, WNR = 3 dB,  $n = 10000$ .

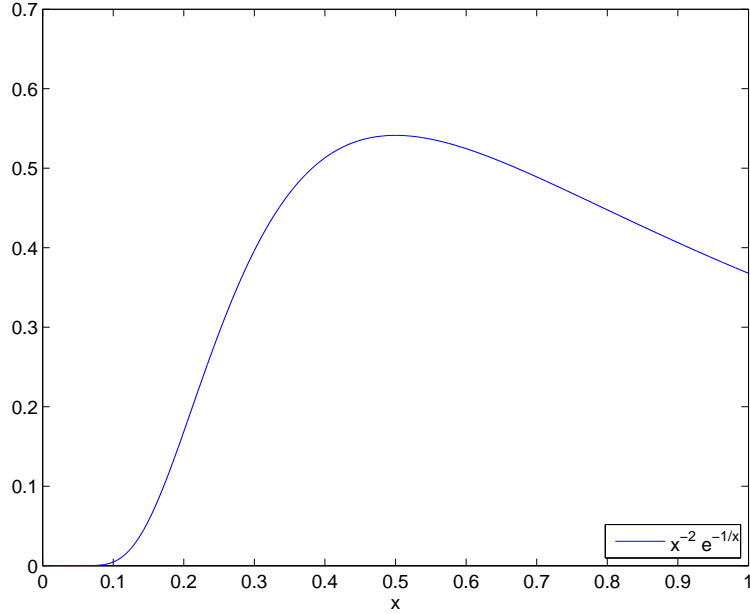


Figure 50:  $\frac{e^{-1/x}}{x^2}$ .

## A Proof of $\log(x) \geq -\frac{1}{x}$ for any $x \geq 0$

Due to the monotonically increasing nature with  $x$  of  $e^x$ , it is obvious that the target inequality can be rewritten as

$$x \geq e^{-\frac{1}{x}}, \text{ for any } x \geq 0. \quad (78)$$

Given that at  $x = 0$  both sides of the inequality take the same value, and that they are analytical functions, a sufficient condition for (78) to be verified is that the derivative with respect to  $x$  of the left side of (78) is larger than or equal to the right side for every  $x \geq 0$ , i.e.,

$$1 \geq \frac{e^{-\frac{1}{x}}}{x^2}, \text{ for every } x \geq 0. \quad (79)$$

Indeed, the derivative of the right side of (79) with respect to  $x$  is

$$\frac{e^{-\frac{1}{x}}(1-2x)}{x^4},$$

so the right side of (79) will have its global maximum located at  $x = 1/2$  (as it is shown in Fig. 50), where it will take the value  $4e^{-2} \approx 0.5413 < 1$ , proving the initial inequality.

## B A useful inequality

In this appendix we will prove that for any  $t_1 \geq t_0$ , or  $t_1 \in (\epsilon, t_0 - \epsilon)$ , with  $\epsilon > 0$  going to 0 for  $\text{HLR} \rightarrow \infty$  and  $\text{TNLR} < 1$ , the following inequality holds

$$t_1^2 e^{\frac{\sigma_X^2(t_0-t_1)^2}{\sigma_N^2+(1-\alpha)^2 t_1^2 \sigma_\Lambda^2}} \geq t_0^2,$$

or equivalently

$$\log \left( \frac{t_1^2}{t_0^2} \right) \geq \frac{-\sigma_X^2(t_0-t_1)^2}{\sigma_N^2+(1-\alpha)^2 t_1^2 \sigma_\Lambda^2}. \quad (80)$$

This inequality is obviously true for  $t_1 \geq t_0$ . For the case  $t_1 < t_0$  we will analyze the derivative with respect to  $t_1$  of

$$\log \left( \frac{t_1^2}{t_0^2} \right) + \frac{\sigma_X^2(t_0-t_1)^2}{\sigma_N^2+(1-\alpha)^2 t_1^2 \sigma_\Lambda^2}, \quad (81)$$

which is nothing but

$$\frac{2}{t_1} - \frac{2\sigma_X^2(t_0-t_1)(\sigma_N^2+(1-\alpha)^2 t_0 t_1 \sigma_\Lambda^2)}{(\sigma_N^2+(1-\alpha)^2 t_1^2 \sigma_\Lambda^2)^2}. \quad (82)$$

If we multiply the last expression by  $(\sigma_N^2+(1-\alpha)^2 t_1^2 \sigma_\Lambda^2)^2 t_1$ , then the result can be written like  $a_0 + a_1 t_1 + a_2 t_1^2 + a_3 t_1^3 + a_4 t_1^4$ , where

$$\begin{aligned} a_0 &= 2\sigma_N^4, \\ a_1 &= -2\sigma_N^2 \sigma_X^2 t_0, \\ a_2 &= 2\sigma_N^2 \sigma_X^2 + 2(1-\alpha)^2 \sigma_\Lambda^2 (2\sigma_N^2 - \sigma_X^2 t_0^2), \\ a_3 &= 2(1-\alpha)^2 \sigma_\Lambda^2 \sigma_X^2 t_0, \\ a_4 &= 2(1-\alpha)^4 \sigma_\Lambda^4; \end{aligned}$$

using Descartes' sign rule one gets that the number of points where the derivative of (81) is null for  $t_1 > 0$  is at most 2. Additionally, based on (81) evaluated at  $t_1 = t_0$  being null, and (82) evaluated at the same point being positive, it is obvious that there is an interval of points just to the left of  $t_1 = t_0$  where (81) is negative. Furthermore, (81) at  $t_1 \rightarrow 0$  is also negative. Taking into account that (82) is null at most at 2 points, it is clear that these two intervals (one on the left of  $t_0$ , and the other on the right of 0) will contain the only points  $t_1 > 0$  where (80) is not verified. Be aware that so far we have not proved that these intervals were disjoint, so it could be the case that (80) were indeed negative for  $t_1 \in [0, t_0)$ .

In order to bound the width of both intervals, we will take into account that

$$\log \left( \frac{t_1^2}{t_0^2} \right) + \frac{\sigma_X^2(t_0-t_1)^2}{\sigma_N^2+(1-\alpha)^2 t_1^2 \sigma_\Lambda^2} \geq \log \left( \frac{t_1^2}{t_0^2} \right) + \frac{\sigma_X^2(t_0-t_1)^2}{\sigma_N^2+(1-\alpha)^2 t_0^2 \sigma_\Lambda^2}, \quad (83)$$

for any  $t_1 < t_0$ , and will focus on the left term. If one considers the following two points

$$t_{1,u} = \frac{1}{2} \left( t_0 + \sqrt{\frac{t_0}{\sigma_X}} \sqrt{\sigma_X t_0 - 4\sqrt{\sigma_N^2 + (1-\alpha)^2 \sigma_\Lambda^2 t_0^2}} \right),$$

$$t_{1,l} = \frac{1}{2} \left( t_0 - \sqrt{\frac{t_0}{\sigma_X}} \sqrt{\sigma_X t_0 - 4\sqrt{\sigma_N^2 + (1-\alpha)^2 \sigma_\Lambda^2 t_0^2}} \right),$$

where  $t_{1,u} < t_0$ , and  $t_{1,l} > 0$ , then the evaluation of (83) at them can be written as  $\log(x_u) + \frac{1}{x_u}$  and  $\log(x_l) + \frac{1}{x_l}$ , respectively, where

$$x_u = \frac{\left( t_0 + \sqrt{\frac{t_0}{\sigma_X}} \sqrt{\sigma_X t_0 - 4\sqrt{\sigma_N^2 + (1-\alpha)^2 \sigma_\Lambda^2 t_0^2}} \right)^2}{4t_0^2},$$

$$x_l = \frac{\left( t_0 - \sqrt{\frac{t_0}{\sigma_X}} \sqrt{\sigma_X t_0 - 4\sqrt{\sigma_N^2 + (1-\alpha)^2 \sigma_\Lambda^2 t_0^2}} \right)^2}{4t_0^2}.$$

Given that both  $x_u$  and  $x_l$  are non-negative, by using App. A we have proved that (83) evaluated at  $t_{1,u}$  and at  $t_{1,l}$  is positive. Furthermore, for  $\text{TNLR} < 1$ ,

$$\lim_{\text{HLR} \rightarrow \infty} t_{1,u} = t_0,$$

$$\lim_{\text{HLR} \rightarrow \infty} t_{1,l} = 0,$$

proving the desired result.

Fig. 51 illustrates the behavior of the considered function for  $t_1$  smaller than but close to  $t_0$ . As expected, the larger the HLR, the closer to  $t_0$  the considered function takes positive values. Additionally, the corresponding values of  $t_{1,u}$  are plotted for the sake of completeness.

Similarly, Figs. 52 and 53 illustrate the behavior of the considered function for values of  $t_1$  close to 0. Again, the shown behavior is that predicted by the performed theoretical analysis. In that sense, the larger the HLR, the closer to 0 the considered function takes positive values. Additionally, the corresponding values of  $t_{1,l}$  are plotted for the sake of completeness.

## References

- [1] Richard Courant and Fritz John. *Introduction to Calculus and Analysis*. Springer, 1989.
- [2] Uri Erez and Stephan ten Brink. A close-to-capacity dirty paper coding scheme. *IEEE Transactions on Information Theory*, 51(10):3417–3432, October 2005.
- [3] Knud J. Larsen. Short convolutional codes with maximal free distance for rates  $\frac{1}{2}$ ,  $\frac{1}{3}$ , and  $\frac{1}{4}$ . *IEEE Transactions on Information Theory*, 19(3):371–372, May 1973.

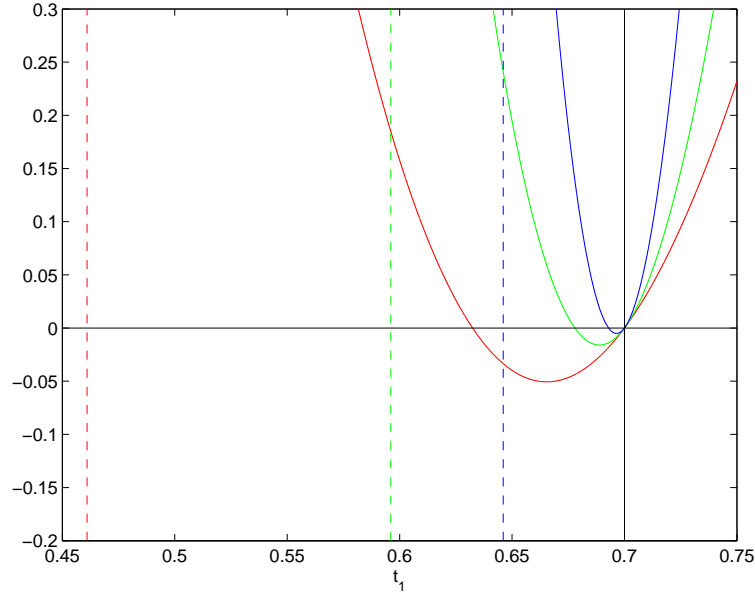


Figure 51: Comparison of (81) for different values of HLR (red 10 dB, green 15 dB, blue 20 dB).  $\text{SCR} \approx 0.0980$  dB,  $\text{TNLR} \approx -2.9616$  dB,  $t_0 = 0.7$ ,  $\alpha = \alpha_{\text{Costa}} \approx 0.4944$ . The vertical colored dashed lines stand for the values of  $t_{1,u}$  derived by using (35), showing that they converge to  $t_0$  (vertical black dashed line) as  $\text{HLR} \rightarrow \infty$ .

- [4] Yong Sun, Angelos D. Liveris, Vladimir Stankovic, and Zixiang Xiong. Near-capacity dirty-paper code designs based on TCQ and IRA codes. In *International Symposium on Information Theory*, pages 184–188, September 2005.
- [5] Ram Zamir and Meir Feder. On lattice quantization noise. *IEEE Transactions on Information Theory*, 42(4):1152–1159, July 1996.

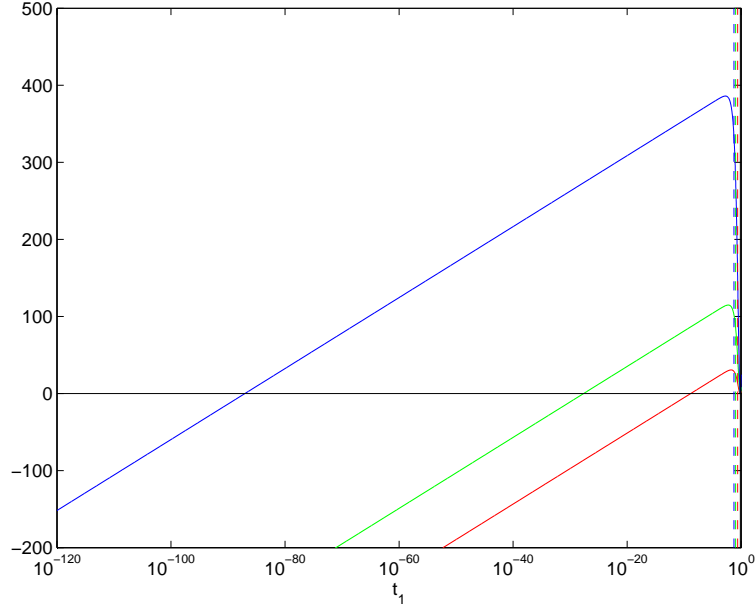


Figure 52: Comparison of (81) for different values of HLR (red 10 dB, green 15 dB, blue 20 dB).  $\text{SCR} \approx 0.0980$  dB,  $\text{TNLR} \approx -2.9616$  dB,  $t_0 = 0.7$ ,  $\alpha = \alpha_{\text{Costa}} \approx 0.4944$ . The vertical colored dashed lines stand for the values of  $t_{1,l}$  derived by using (35), showing that they converge to 0 as  $\text{HLR} \rightarrow \infty$ .

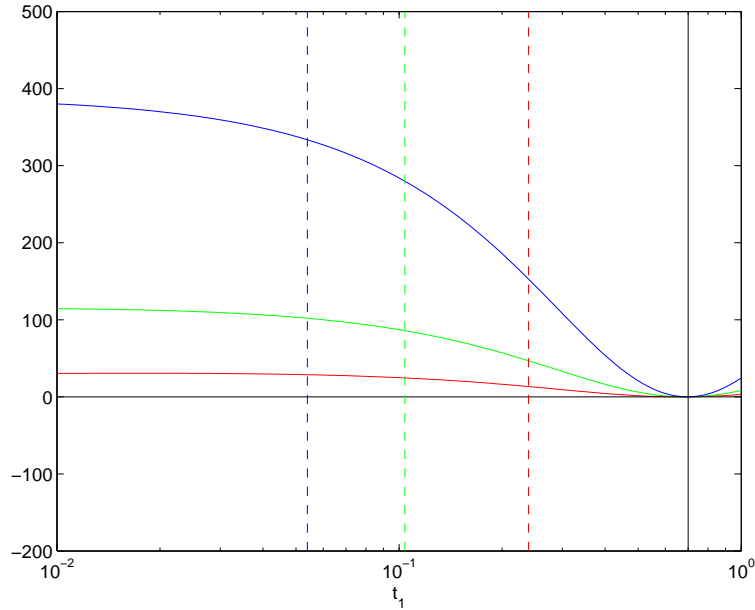


Figure 53: Comparison of (81) for different values of HLR (red 10 dB, green 15 dB, blue 20 dB).  $\text{SCR} \approx 0.0980$  dB,  $\text{TNLR} \approx -2.9616$  dB,  $t_0 = 0.7$ ,  $\alpha = \alpha_{\text{Costa}} \approx 0.4944$ . The vertical colored dashed lines stand for the values of  $t_{1,l}$  derived by using (35), showing that they converge to 0 as  $\text{HLR} \rightarrow \infty$ .